Effect of high pressure - low temperature phase transitions on model systems, foods and microorganisms

vorgelegt von
Diplom-Ingenieur
Cornelius Martin Luscher

Von der Fakultät III – Prozesswissenschaften
der Technischen Universität Berlin
zur Erlangung des akademischen Grades
Doktor der Ingenieurwissenschaften
- Dr.-Ing. -
genehmigte Dissertation

Promotionsausschuss:
Vorsitzender: Prof. Dr.-Ing. Frank-Jürgen Methner
1. Berichter: Prof. Dr. Dipl.-Ing. Dietrich Knorr
2. Berichter: Prof. Dr. Alain Le Bail

Tag der wissenschaftlichen Aussprache: 25.01.2008

Berlin 2008

D 83

Für Barbara, Lukas
und Jonathan

Acknowledgements

This dissertation is the final result of my studies at the Department of Food Biotechnology and Food Process Engineering, Technische Universität Berlin in Berlin-Dahlem from the years 2002 to 2007.

First of all my deepest gratitude goes to Prof. Dietrich Knorr, head of the department, for providing a pleasant place of research and work, for giving support, encouragement, discussions and guidance of the work. I also want to express my deep gratitude to Prof. Alain Le Bail from ENITIIA, Nantes, for his interest in my work and the willingness to come to Berlin to finish the graduation process. Merci beaucoup! A special thanks to Prof. Frank-Jürgen Methner for taking the time to supervise the graduation commission.

My sincere gratitude goes to the students that contributed to the work: Ana Balasa, Antje Fröhling, Jan Sunderhoff, Marcel Pohl and Ashkan Motahar. Without you, this would not be possible. Thank you to the "high pressure – low temperature group" in Dahlem over the years for encouragement and discussion, to Oliver Schlüter who taught me the first steps in this exciting field, to Gabriel Urrutia, Julia Schneider and Marcus Volkert. Thank you to the technical staff, Irene Hemmerich for flow cytometry, Stefan Boguslawski for high pressure assistance, Martin Bunzeit and Gisela Martens for microbiological assistance. Thanks to Sybille Candea and Sophie Uhlig for their administrative work. Thank you to everyone who had interest in my work and discussed it with me over the years, to Edwin Ananta, Volker Heinz only to mention the first two that come to my mind. Thank you for proof reading to Marcus, Barbara and Ana, who closed the circle from making the first experiments to eliminating the last English language problems.

A special thank has to be expressed to everyone who was part of the department over the years for making this place a special part of my life not only during working time. Besides the aforementioned this includes Stefan Töpfl, my office mate during most of the way, Roman Buckow, Alex Mathys, Marco Zenker, Adriano Ardia, Birgit Rumpold and all the other colleagues and students that are simply too numerous to be mentioned.

The last thank you goes to my family, my parents, grandparents and friends for supporting me in all ways! Thank you to Barbara, Lukas and the little boy waiting for sunlight that kept me motivated in the weeks of writing the text.

Table of contents

Zusammenfassung

Im Druckbereich über 210 MPa existieren Eis III und weitere Eismodifikationen, die eine größere Dichte als flüssiges Wasser aufweisen. Bei Entspannung auf atmosphärischen Druck (0,1 MPa) wandelt sich Eis III zu gewöhnlichem Eis I um und vergrößert dabei sein Volumen in einer schnellen Phasenumwandlung in Bruchteilen einer Sekunde. Dieser Effekt wurde ausgenutzt, um einen Prozess zu entwickeln, der es ermöglicht Mikroorganismen in gefrorenen Lebensmitteln durch Behandlung mit hohem hydrostatischem Druck zu inaktivieren.

Zunächst wurden Prozessbedingungen bis 500 MPa untersucht, indem Gefrier- und Schmelzpunkte konzentrierter Saccharose- und NaCl-Lösungen unter Beteiligung der Eisformen I, III und V ermittelt und mittels Simon-Gleichungen beschrieben wurden. Das Unterkühlungsverhalten und die konzentrationsabhängige Gefrierpunkterniedrigung wurden evaluiert und daraus gefolgert, dass die Phasengrenzlinien dieser Lösungen nicht durch Parallelverschiebung der Linien für reines Wasser zu tieferen Temperaturen ermittelt werden können. Eine Gleichung wurde aufgestellt, die es ermöglicht den Schmelzdruck von Saccharoselösungen in Abhängigkeit von Solvatkonzentration und Temperatur im Eis I – Bereich zu berechnen. Der Phasenübergang von Eis I zu Eis III während der Druckbehandlung von gefrorenen biologischen Materialien wurde auf der Grundlage dieser Erkenntnisse untersucht. Die verschiedenen Mechanismen von partiellem druckinduziertem Schmelzen und direktem Eiskristallphasenübergang in Abhängigkeit vom Temperaturniveau konnten voneinander abgegrenzt werden, so dass geeignete Behandlungsparameter definiert werden konnten.

Die Schädigung von Bakterien nach Gefrieren und Gefrierlagerung wurde mittels Durchflusszytometrie untersucht und die Stresswirkung von Gefrierkonzentrierung und kalter Temperatur von der Eiskristallschädigung abgegrenzt. Bakterien überdauerten Gefrieren und Lagerung bei -18 °C besser als bei -40 °C, da sich bei -18 °C kein intrazelluläres Eis bildet. Bei -40 °C erscheint es wahrscheinlich, dass sich intrazelluläres Eis während der Lagerung aber nicht direkt beim Gefrieren bildet.

Bei Druckbehandlung von *L. innocua* in gefrorener Pufferlösung bei -45 °C und 300 MPa wurden schon nach sehr kurzer Behandlungszeit (< 1 min) drei Zehnerpotenzen Inaktivierung erreicht, aufgrund des Zellaufschlusses, der auf den Eis III – Phasenübergang zurückgeführt wurde. Bei anderen vegetative Mikroorganismen wurde eine Reduzierung um etwa 3 bis 7 log – Stufen erzielt. In gefrorenem Hackfleisch konnte eine Inaktivierung von mindestens 2 log erreicht werden, wohingegen in Eiskrem nur weniger als 1 log Inaktivierung erreicht wurde. Der Einfluss verschiedener Behandlungsparameter wie Druck, Temperatur, Geschwindigkeit der Druckentspannung, Gefrierlagerung und andere weiterer Einflussgrößen wurde ebenfalls untersucht. Modelle, die den Mechanismus des Zellaufschlusses durch den Phasenübergang zu Eis III beschreiben wurden aufgestellt und diskutiert. Der Einfluss der Behandlung auf die Qualität von Lebensmitteln wurde am Beispiel von Schweinefleisch untersucht, doch waren die Auswirkungen auf Farbe, Textur, Abtropf- und Bratverlust nur gering.

Zusammenfassend ist die Druckbehandlung von gefrorenen Lebensmitteln bei 300 bis 400 MPa und Temperaturen von -30 bis -45 °C für kurze Zeitspannen von einer Minute und weniger ein technisch umsetzbarer Prozess, der die aktive Reduzierung der Zahl der Mikroorganismen ermöglicht.

Abstract

Under pressures of 210 MPa and above, ice III and other ice modifications exist, which have a higher density than liquid water. Phase transitions from ice III to ice I are going along with an increase in ice volume in parts of a second as the transition is very fast. This phenomenon was used to develop a process which makes the inactivation of microorganisms by pressure treatments in frozen food possible.

In the first part, processing criteria were examined by freezing and thawing of ices I, III and V in solutions of sucrose and NaCl at pressure to 500 MPa. Freezing and melting points were studied and parameters of Simon equations describing the phase transition lines were fitted. The supercooling behavior and the solute dependent freezing point depression were described and quantified. It was concluded that phase transition lines of solutions cannot be obtained by shifting transition lines of water parallel to lower temperatures. An equation was proposed for calculating the melting pressure of sucrose solution as a function of temperature and solute concentration in the ice I range. The phase transition of ice I to ice III during pressure cycles of frozen biomaterial was studied and mechanisms of partial thawing and direct crystal phase transition as a function of temperature were identified and suitable treatment parameters were proposed.

The freezing damage of bacteria was analyzed by flow cytometry after freezing and during frozen storage up to 100 days. The stress related to cold temperature and freeze concentration was separated from the effect of ice crystal damage on bacteria. It was found that bacteria survive freezing and frozen storage at -18 °C better than at -40 °C, because no intracellular ice forms at the higher temperature level. At -40 °C it is likely that intracellular ice forms during storage, but not immediately during freezing.

Pressure treatment of frozen model suspension of *L. innocua* at -45 C and 300 MPa revealed inactivation of 3 logs by cell disintegration after very short treatment times (< 1 min) due to ice III transitions. Other vegetative microorganisms were inactivated in a range of 3 to 7 logs. In frozen ground beef, *L. innocua* inactivation was about 2 logs, ice cream less than 1 log. Treatment parameters like pressure, temperature, pressure release, storage after treatment and others were examined. Models were discussed that describe the disintegrative effect of the transition on bacteria. Pork meat after such treatments was examined but only little effect on the quality was found.

It was concluded that treatment of frozen food by high pressure with parameters of 300 to 400 MPa, -30 to -45 °C and 1 min of pressure holding time is a technically feasible process that makes the active reduction of microbial counts possible.

Table of acronyms and symbols

Acronyms

ATP	Adenosine triphosphate
DMSO	Dimethyl sulfoxide
DSC	Differential scanning calorimetry
CF	Carboxyfluorescein
FPD	Freezing point depression
FSE	Fit standard error
IAPWS	International Association for the Properties of Water and Steam
IIF	Intracellular ice formation
IIR	International Institute of Refrigeration
LGG	*Lactobacillus rhamnosus* GG
NMR	Nuclear magnetic resonance
PBS	Phosphate buffer saline
PI	Propidium iodide

Symbols

a_w	Water activity	[-]
b	Molality	[mol kg^{-1}]
c_p	Specific heat capacity	[kJ kg^{-1} K^{-1}]
cfu	Colony forming units	[-]
g_N	Standard earth gravity	= 9.80665 m s^{-2}
G	Gibb's free energy	[J]
h	Specific enthalpy	[kJ kg^{-1}]
i	van'Hoff factor	[-]
k	Reaction rate constant	
K_f	Cryoscopic constant (coefficient)	[K kg mol^{-1}]
l	Length	[mm]
m	Mass	[kg]
p	Pressure	[Pa]
R	Universal gas constant	= 8.314472 J K^{-1} mol^{-1}
S	Entropy	[J K^{-1}]
t	Time	[s]
T	(Thermodynamic) Temperature	[K]
v	Specific volume	[cm^3 kg^{-1}]
V_a	Activation volume	[m^3]
w_ϑ	Local freezing rate	[K min^{-1}]
w_n	Nominal freezing rate	[cm h^{-1}]
w/w	Weight per weight	[%]
w/v	Weight per volume	[%]
x	Mass fraction	[-]
X	Mole fraction	[-]

Greek symbols

α	Thermal expansion factor	[K^{-1}]
α'	Solution factor	[K]
β	Compressibility factor	[Pa^{-1}]
α,β,χ,δ	Fitting parameters in Simon equations	[-]
γ	Activity coefficient	[-]

ϑ	(Celsius -) Temperature	[°C]
θ	Normalized temperature	[-]
π	Normalized pressure	[-]
Δh_f	Heat of fusion	[kJ kg^{-1}]
Δt_f	Duration of freezing	[s]
ΔT_f	Freezing point depression	[K]

Subscripts

a	Ash content
b	Bound water
ice	Idem
f	Freezing
m	Melting (in combination with number of the ice I/III/V)
n	Normalizing (reference point conditions)
o	Other solutes than ash
sv	Solvent
su	Solution
w	Water
x	Any substance

Superscripts

0	At reference conditions

1 Introduction

Frozen food is a commodity that is well accepted by the consumer and it is not possible to imagine the food market without it. By freezing, a lot of perishable foods can be preserved for months and longer in a fresh-like state and brought to the consumer far from their origin and throughout the year, like e.g. fish or vegetables. The retention of valuable chemical compounds of nutritive or organoleptic interest is among the highest of all preservation techniques, therefore they contribute to health and high-quality nutrition, despite the fact that frozen food is often regarded as heavily processed food. Moreover, a lot of convenience foods can only be provided in the frozen state, as other methods fail to preserve them with acceptable quality (e.g. pizza).

Major challenges to the preservation of food by freezing are the prevention of freezing damages. Depending on the nature and composition of the object, these quality problems are texture loss, color changes, drip loss and water binding loss, resulting in protein aggregation and hardening of meat. Some foods are severely impaired in one or more of their properties by freezing, while others are preserved without major quality loss. Other common problems in frozen food like freezer burn or the occurrence of ice flakes in frozen food bags are caused by storage problems in distribution or at home. They are attributed to inappropriate packaging and storage at fluctuating or too high temperatures.

The preservative effect in terms of microbiological spoilage arises from two mechanisms. The storage temperature is lower than the proliferation threshold of any microorganism and the reduction of liquid water by ice crystallization makes frozen food essentially a dry food. However, microbial counts are not enough reduced to characterize freezing as a pasteurization process, as a lot of microorganisms are able to recover after freezing. They even come across quite optimal growing conditions due to nutrient liquids that are leaking from food during thawing. Microbial problems associated with frozen food can be controlled effectively by freezing high quality produce, maintenance of the cold chain and appropriate thawing conditions with fast consumption. The targeted and effective pasteurization of frozen food without thawing is only possible by irradiation which is hardly accepted by the consumer.

A new technology arising on the food market since the 1990's is high pressure processing, which makes the production of fresh like foods possible. Hydrostatic pressure is applied technically to packaged foods that are immersed in pressure vessels filled with a pressure transmitting liquid. Commercial pasteurization regimes use pressure in a range of roughly 500 to

700 MPa (5 to 7 kbar) which leads to inactivation of microorganisms without requiring thermal impact of the product that would lead to changes in nutritive or organoleptic properties. Some examples of pressure treated foods on the market are high quality jams and juices in Japan, guacamole and oyster products in the USA and sliced ham products in Spain and Germany. Despite continuously growing interest in the technology, high pressure processing is still a niche process employed for non-frozen products which cannot be pasteurized in a package thermally with acceptable results.

High pressure food research has widened the scope widely beyond the pure pasteurization effect. Other pressure processes under research are the extension of microbial inactivation to sterilization conditions, structure and functionality modifications, like starch gelatinization or protein modification and the application of pressure to living organisms in order to make use of their stress response. Another process that can be modified by pressure is freezing and related to it the thawing process.

Water possesses the quite unusual property that it expands during solidification. While other liquids can be forced to the solid state by pressure, the freezing expansion leads to the behavior that the water freezing point is lowered if pressure is applied. A temperature of -22 °C in liquid water can be obtained at 210 MPa. Besides the common ice, which is referred to as ice I, other ice modifications exist with a more compact crystal structure making them denser then liquid water. In the temperature range of practical interest which can be defined as -50 °C to 100 °C, all other ices are stable only at pressures higher than 210 MPa (2.1 kbar).

One possibility to optimize freezing by high pressure is freezing to ice III which is the ice modification adjacent to ice I and the liquid in the pressure range from 210 to 350 MPa. Hence, it is possible, to freeze water to ice III at a pressure of 300 MPa, resulting in a slight shrinkage during freezing due to the dense crystal structure of this ice. Food frozen from this process has superior quality due to very limited ice crystal damage. Like discussed earlier, ice III is not stable at ambient pressure. Food frozen at 300 MPa and then decompressed suffers severely from the phase transition of ice III to ice I that runs very fast and results in a volume increase of 22 %, breaking up all structures that contain ice crystals due to expansion.

The underlying hypothesis that will be examined in this study, is the assumption that this transition from ice III to ice I should also affect microorganisms in frozen foods. It shall be examined, if pressure treatments of frozen food at temperatures below -22 °C with a transition to ice III during pressurization are a possible method to achieve inactivation of microorganisms in frozen food without thawing.

For that purpose the thesis comprises the following studies with different approaches that make the evaluation of such a process possible:

- *Phase transition studies.* The freezing and thawing of food under pressure is already well examined. During freezing however, solutes concentrate leaving some water as unfrozen concentrated solution. Systematic examination of concentrated model solutions of sucrose and sodium chloride during freezing and thawing should give new insights in the behavior of such liquids under pressure. Freezing point calculations under pressure shall be derived to obtain predictable values for the state of water in such systems. In a second step the phase transition of ice I to ice III upon pressurization is examined in detail in order to define treatment conditions suitable for examination.
- *Freeze stress of microorganisms.* The survival of bacteria during freezing and frozen storage is well established and was mainly studied in the 1950's and 60's when freezing became more and more important. Mechanisms of freezing injury are already identified and can be related to the state of water which can be frozen or liquid inside the cells. However, it is often difficult to identify the occurring freeze damage effects in bacteria by traditional microbiological methods. It shall be examined by flow cytometry, which is a method relatively new to food microbiology, which are the damaging effects of freezing and frozen storage on bacteria in conditions relevant to this study.
- *Pressure treatment of frozen food and food models.* The main part of this study is the investigation of microbial inactivation in food models and subsequently in real food pressure treated after freezing. The ice in these systems is subjected to a transition to ice III and thereby possibly inactivating microorganisms. Treatment parameters shall be identified for suitable processing and mechanisms of inactivation shall be explored as far as possible.
- *Quality of food subjected to such treatments.* It will be examined with pork meat which serves as an example what the effect of such ice III pressure treatments are on real food quality parameters besides microbial values.

The different topics associated with the multi-disciplinary approach will be presented in the following literature review. The state of the art of the different technologies associated with the approach will be described and the insights that lead to the hypothesis of this study are outlined.

2 Literature review

2.1 Food freezing

2.1.1 Definition and importance

In general use, the term *freezing* is used to describe the action of congealment by cold. From a thermodynamic point of view, freezing of water is the solidification of liquid, disordered water molecules to an ordered crystal structure. It is an exothermic reaction, thus latent heat is released. At ambient pressure the water crystallization results in an volume increase of 9 %, due to the spacious ice hexagonal structure.

The freezing of food with an aqueous basis is a well established method in food preservation. By definition of German and EU law, *frozen food is food which is subjected to a suitable freezing process, during which the zone of maximum crystallization is crossed as quick as necessary according to the constitution of the food. The temperature at all points of the food shall be at a minimum of -18 °C* (Bundesgesetzblatt 2007). Ice cream is often not included when talking about frozen food, as it is not always stored at -18 °C. Frozen food is a commodity well accepted by the consumers. In a saturated food market like Germany production increment was still possible over the last decade (Figure 2.1).

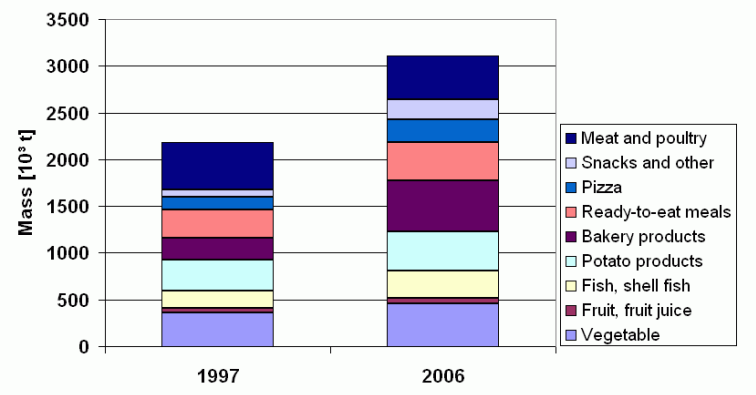

Figure 2.1 Frozen food production in Germany in 1997 and 2006. Ice cream is not included. (Deutsches Tiefkühlinstitut, 2007).

It is generally possible to provide food with a fresh-like character after thawing, despite freeze damages in structured foods. These freeze damages are related to the freezing rate and can be minimized by appropriate processing. Hence, it is a necessity to establish fast freezing procedures after harvest or production and a cold chain throughout shipment, sale and consumer. Along the supply chain, refrigeration units and appropriate storage facilities as well as electri-

cal energy are necessary. The overall technical complexity is therefore among the highest of all foodstuffs.

2.1.2 Freezing temperature and freezing rates

During freezing the temperature of the food product has to be lowered to at least -18 °C, the minimum storage temperature required. This cooling process is governed by the removal of the latent heat of the phase transition, or in other words, the heat of crystallization. A typical temperature profile of a freezing curve is shown in Figure 2.2. After cooling to the freezing temperature, the crystallization plateau visualizes the large amount of heat which has to be removed. At the same time, from the surface temperature curve the freezing process cannot be concluded directly, as no temperature plateau is visible.

The freezing temperature (initial freezing point) is usually defined as the plateau temperature or the temperature peak after supercooling, if a peak is visible and especially if no steady plateau temperature is available. However, various influences like cooling rate, sample size, position of the measuring device etc. can influence the peak temperature (Chen & Chen 1996). In the special case shown in Figure 2.2, the sample is sufficiently big and the heat transfer is sufficiently slow, to allow the development of a pronounced temperature plateau. Hence, it is more useful to select the plateau temperature as freezing temperature as it reflects the main temperature of the phase transition better than the peak temperature. It has to be concluded from this simple example, that the definition of freezing temperatures requires some experience and might lead to differing results, so the method used to derive a freezing point from a temperature curve should definitely be indicated.

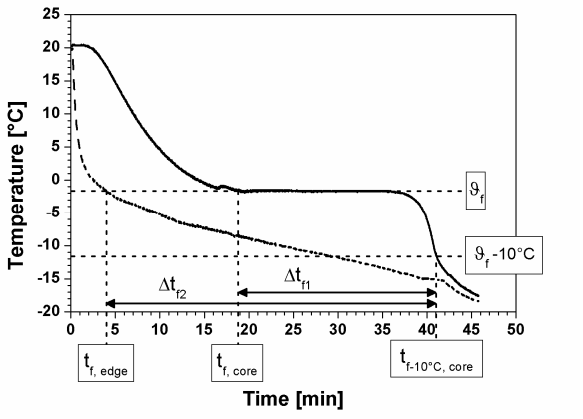

Figure 2.2 Typical freezing curve, in this example freezing of a potato cylinder (d=38 mm, l=50 mm) immersed in silicone oil (-20 °C). ━ core temperature; ╍ edge temperature.

The initial freezing point of an ideal binary solution is lowered depending on the molality of the solution (Debye & Hückel 1923). During freezing the solvent is freeze concentrated and consequently the plateau temperature sinks further. In complex systems like food, in principle the same is true; however, pure molalities cannot be calculated. With empirical equations the freezing temperature ϑ_f can be estimated from the food composition, given by the mass fractions x of water (w), ash (a), i.e. minerals, and other solutes (o), i.e. mainly protein and carbohydrates (Pham 1996).

$$\vartheta_f = -4.66 \cdot \frac{x_o}{x_w} - 46.4 \cdot \frac{x_a}{x_w}$$

Equation 1

Most of the ice crystallizes during the plateau phase of the temperature. The relative fraction of ice x_{ice} related to water content at a given temperature ϑ can be approximated as follows (Pham & Willix 1989).

$$x_{ice} = (1 - \frac{x_b}{x_w}) \cdot (1 - \frac{\vartheta_f}{\vartheta})$$

Equation 2

The mass fraction of bound water x_b can be derived from the following equation using the mass fractions of protein x_p and carbohydrates x_c (Miles 1991).

$$x_b = 0.3x_p + 0.1x_c$$

Equation 3

These equations were used to calculate freezing points and bound water of some typical foods relevant for freezing processes as presented in Table 2.1. The results are in good agreement with the typical freezing temperatures of food which usually vary between -1 °C and -2 °C. However biological variation of the composition is common and consequently the freezing temperatures are differing. More complex and more precise models have been proposed (see for example Boonsupthip & Heldman 2007), however, the accuracy of the aforementioned simple equations (Equation 1 to 3) is good enough for the purposes of this illustration.

Table 2.1 Composition data of some foods with calculated freezing points and bound water fraction.

[%]	Potato	Spinach	Lean pork	Cod	Apple	Ice cream
Water	77.8	91.6	73	82	85.3	65
Protein	2.1	2.5	19	17	0.3	5
Carbohydrates	17.9	2.4	0	0	14.2	21
Fat	0.1	0.3	7	0.3	0.4	13
Minerals	1	1.5	1	1	0.5	0.5
Freezing point (Eq.1) [°C]	-1.8	-1.0	-1.8	-1.5	-1.1	-2.2
Fraction of bound water (Eq.3) [%]	2.4	1.0	5.7	5.1	1.5	3.6

Compilation based on (Wirths 1985; Baltes 1989).

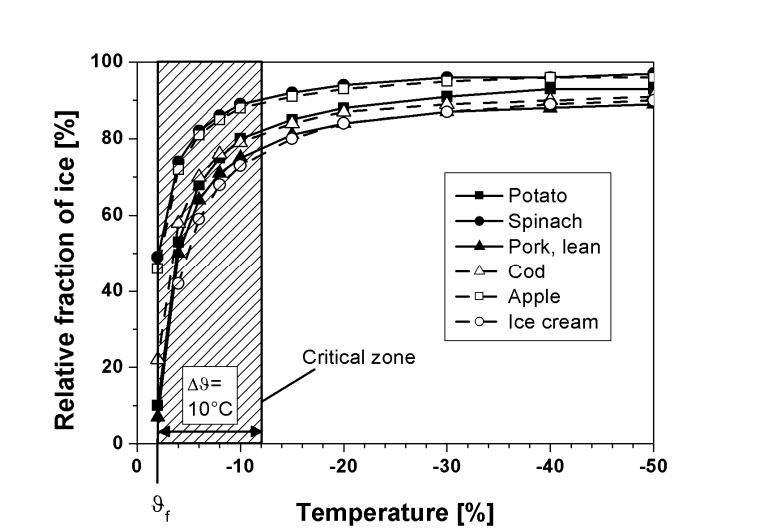

Figure 2.3 Relative ice fraction formed during freezing of water available in selected foods. The absolute water content of these foods ranges from 65 % to 92 % (Table 2.1).

These values were used to plot typical relations of ice versus freezing temperature according to equation 2. It can be observed in Figure 2.3 that 75 % or more of the water in all foods considered is frozen when the temperature reaches -12 °C, which is about 10 K below their respective freezing points. Dough products like bread usually have an even higher fraction of unfrozen water. A zone with a width of 10 K below the freezing point is therefore defined as the critical zone for freezing. As the ice crystal distribution after freezing of 75 % of water is largely set, the following freezing process is not decisive for the quality of the product.

Freezing rates are necessary to quantify the reaction rate of freezing. However, in literature the differing terms *freezing rate* and *cooling rate* are used but often not clearly defined. The lack of precise definitions can sometimes be overcome by consideration of the unit of the freezing rate; nevertheless the reference points and temperature span used for calculation of freezing rates remain unclear quite often. The term *cooling rate* is often used in cryobiology, which implies that simply the temperature difference from beginning to end of the cooling is divided by the cooling time. Often the cooling rate is not measured precisely but only estimated, which might be feasible for freezing applications, where the crystallization time is not governing the processing time like dripping droplets in liquid nitrogen. However, in food engineering, this is usually not suitable, as the processing time of freezing as well as the deterioration of freezing goods is related to the velocity at which the critical zone is crossed. Hence, it is useful to define the freezing rate related to the time necessary to reach 10 K below the freezing point where most of the crystallization is completed.

Two different definitions of freezing rates are in use, the local freezing rate and the nominal freezing rate. The *local freezing rate*, as it is commonly used in science, is usually defined as follows.

$$w_{\vartheta} = \frac{\vartheta_f - (\vartheta_f - 10K)}{\Delta t_{f1}} [K \cdot \min^{-1}]$$

Equation 4

It describes the rate of temperature decrease at one spot from freezing temperature to the temperature 10 K below the freezing point, thus covering the area of maximum crystallization. Δt_{f1} can be derived from the temperature curve at that point, e.g. the core, between the beginning of the temperature plateau and the point in time when the temperature is 10 K lower, as shown in Figure 2.2. The local freezing rate is usually given in [K min^{-1}]. It is of importance where accurate differences of freezing rates in different spots of one piece subjected to freezing need to be quantified. It is also convenient, if samples are small enough that no significant spatial distribution of freezing rates occurs.

The second definition of freezing rate will be referred to as the *nominal freezing rate*. It was defined by the International Institute of Refrigeration (IIR 1972).

$$w_n = \frac{l}{\Delta t_{f2}} [cm \cdot h^{-1}]$$

Equation 5

The geometrical distance from surface of the piece to be frozen to the thermal centre is denoted as l. The freezing time Δt_{f2} denotes the time from the start of freezing at the surface until completion of freezing at the centre (10 K below freezing point). This definition is of industrial importance as it shows at a glance the time necessary for a whole piece to freeze completely. However, it is consequently only an average for the whole piece as every piece freezes slower in the centre. The unit [cm h^{-1}] can be interpreted as the velocity of the ice front moving from the surface to the core.

2.1.3 Damage of cellular food during freezing

During ice formation a number of processes occur, which are detrimental to the structure of the product resulting in texture and drip losses. Foods which consist of cellular tissue like vegetables, fruit or meat have the most complex structure and are often the biggest challenge to freezing. The following considerations will therefore focus on such systems, nevertheless other highly structured systems like gels similar considerations can be made as well. Systems without rigid networks or cell walls like ice cream or juice concentrates usually do not suffer much damage from freezing.

Several effects of freezing on cellular structure have been discussed mainly focusing on mass transport due to water rearrangement and mechanical influences due to ice formation. The following microstructure model has evolved which includes all major considerations (Sahagian & Goff 1996). The weighting of the respective processes for foods of course varies due to considerable differences in composition.

During cooling, the temperature reaches freezing point, however, this freezing point on a microstructural level is not constant. The concentration in extracellular cavities, like veins, is usually not as high as inside the cells. Regardless of freezing rate, as shown in Figure 2.4, in the first moment water therefore crystallizes outside the cells (No.1 in both rows, all references to Figure 2.4). During subsequent freezing, an ice-rich matrix at low temperature will form around the cells. As slow freezing is close to equilibrium the osmolality of the extracellular space rises. This creates an osmotic gradient between the interior of the cell and the extracellular remaining liquid (No.2, slow freezing), which facilitates water diffusion through the cell membrane to minimize concentration differences (Reid 1990; 1993). This causes the growth of large extracellular ice crystals that break up considerable cavities and leave dehydrated cells behind (No.3, slow freezing) (Urrutia Benet 2006; Van Buggenhout, Lille et al. 2006a). Cell membranes can rupture due to phase transitions and solidification of the lipid bilayer (Steponkus 1984). After thawing, tissue softening due to cavities, broken cells, loss of

turgor and extensive drip loss due to unfavorable water distribution is the consequence (Anon & Calvelo 1980).

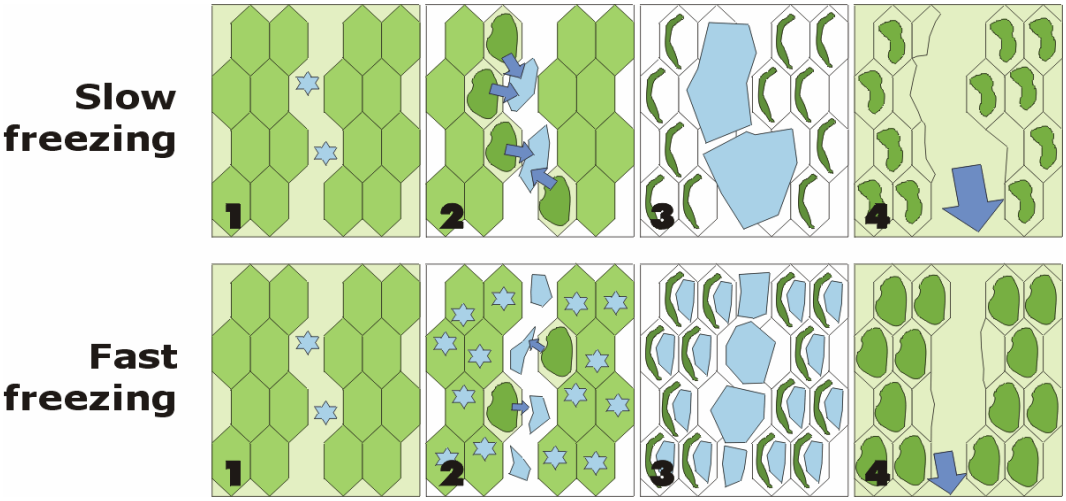

Figure 2.4 Effects of fast and slow freezing on cellular food.

However, if heat removal is rapid compared to water diffusion, small ice crystals are formed inside and outside the cells (No.2, fast freezing), leading to an even ice distribution with less cavities (No.3, fast freezing). This results in less tissue damage and drip loss (No.4, fast freezing) (Anon & Calvelo 1980). Depending on the cooling rate and a reduced permittivity for water of the cell membranes and cell walls increases the benefits of fast freezing. A very high permittivity allows cells to dehydrate even at high cooling rates (Reid 1993).

The effect of the freezing rate on the quality of frozen food in terms of food structure make it possible to differentiate groups of food according to their responses to freezing (Spieß 1981):

- Group 1 – freezing rate has no influence on frozen food quality. This includes products with high dry matter content (peas), meat with high fat content, some ready-to-eat products.
- Group 2 – freezing rate should not fall below a minimum of 0.5 to 1 K/min, however, faster freezing does not ameliorate the quality. Mainly lean meat, fish and starch-based ready-to-eat foods are arranged in this group.
- Group 3 – the rate of freezing is correlated to frozen food quality over a wide range. In this group, most fruit and vegetable (low dry matter, but rigid tissue structure) and gel-like products are comprised.
- Group 4 – like group 3, but too fast freezing may cause destruction of the tissue due to strains caused by low temperature (low dry matter, loose tissue – raspberry, cucumber).

2.1.4 Freezing effect on fish and meat

Both groups of animal tissue, fish and meat, have a common structural composition. In contrast to plant tissue, the purpose of the structure is to permit movement of the organism. The tissue is organized in bundles of fibrils, each fibril consist of filamentous proteins, myosin and actin, which are linked in a complex structure to form the actin-myosin complex. This complex contracts when triggered by neurons using ATP. It can be stated form a macroscopic point of view that freezing affects animal tissue less than foods from plant tissue, as animal muscle flesh is more flexible than immobile plant tissue (Goff 1992). Animal cell walls are less effective against ice propagation and hence favorable intracellular ice is more prevalent (Reid 1993). Intracellular ice formation may be promoted by the presence of ice on the external side of the membrane, so called surface catalyzed nucleation, or by intercellular particles called volume catalyzed nucleation (Karlsson, Cravalho & Toner 1993).

The freezing damage occurring in flesh proteins and therefore in the protein-rich animal tissue as a whole is related to the physical changes during freezing. A lot of water in its frozen form, ice, is removed from the protein, leaving the proteins in a concentrated solution of salts, which is subject to changes of pH, ionic strength, surface tension, viscosity and the presence of dissolved gases. At the same time, diffusion of reactants and catalysts is still possible (Mackie 1993). Figure 2.3 contains data of unfrozen water ratio in some frozen food, indicating the extreme loss of liquid water from the protein during freezing. The actin-myosin is therefore exposed to severe dehydration and exposed to a reactive concentrated solution which leads to complete or partial denaturation.

The effect of this exposure of proteins to the concentrated solution in animal tissue throughout freezing is of course related to the amount of frozen water and the length of exposure, i.e. the frozen storage time (Ngapo, Babare, Reynolds & Mawson 1999). For protein denaturation itself, the freezing rate does not have major influence on the frozen food quality. However, the freezing rate causes macroscopic physical changes like the “gaping” in fish flesh, which is the frequently observed separation of fish flesh fibers (Mackie 1993; Schubring, Meyer, Schlüter, Boguslawski & Knorr 2003). The freezing rate should not fall below a critical value of 0.5 to 1 K/min, which is reflected in the arrangement in groups 1 and 2 in the section above (Spieß 1981).

Myosin was identified as the major protein responsible for deteriorative effects in meat during freezing, which was related to extractability loss, loss in ATPase activity and reduced actin binding. These combined data suggest that changes in myosin are mainly responsible for the

changes in functional properties of the musle, such as reduced water-holding capacity and development of toughness. Although, the denaturation is not restricted to myosin, it seems that the major changes occur in it. The aggregation nature of myosin is presumably based on hydrogen bonds not including many sulfhydryl groups (-S-S-). However, formaldehyde which is produced by enzymatic activity might also be involved in myosin cross-links (Mackie 1993).

Besides drip loss and toughness of the tissue structure, the natural meat color is of interest in freezing preservation. Slowly frozen meat is excessively dark, whilst meat frozen in liquid nitrogen is unnaturally pale. The large variation in lightness is a result of differences in rate of ice crystal growth. Small crystals, formed by fast freezing, scatter more light than large crystals formed by slow freezing, and hence fast frozen meat is opaque and pale, and slow frozen is translucent and dark (MacDougall 1982). Most of the red meat color can be attributed to myoglobin with consideration of its biochemical state (more in chapter 2.3.1). During freezing and frozen storage the color is influenced by storage temperature and storage time, like in the case of other meat proteins. Additional factors like pH and oxygen availability that influence meat color must also be taken into account (Ranken 2000).

2.1.5 Survival of cells during freezing

From a food preservation perspective, freezing is not a method of destroying microorganisms purposively. Even though a large percentage of cells is inactivated during freezing, a high number of cells, depending on species and strain, are surviving, making freezing and freeze-drying also a method for storage of microorganisms, e.g. food starter cultures. A great deal of knowledge about the freezing survival of foodborne microorganisms was collected in the 1950's and 1960's when food freezing became a rising technology of food preservation, complemented by later examinations including newer techniques of microbial analysis. Valuable insights can also be gained from the present research in cryobiology on the freezing survival of higher mammal cells such as oocytes, stem cells or even embryos. However, regarding freezing rate, freezing volume as well as cell size and structure of the object, cryobiology differs considerably from food freezing and its spoilage and pathogenic microorganisms, which are mainly bacteria. In this section, some points shall be highlighted which are relevant for the understanding of freeze damage in bacteria.

Ingram (1951) summarized early the effect of freezing to microorganisms in general:

- There is a sudden mortality, varying with species.
- The surviving number of cells decreases continuously during frozen strorage.

Christophersen (1968) added that a characteristic number of cells persists continuously during frozen storage, essentially describing a “tailing” effect.

Bacteria differ in their resistance to freezing; usually survival of gram-positive cocci (e.g. *Staphylococcus*) is higher than of gram-negative rods (e.g. *Salmonella*). Stationary phase cells are more resistant than log-phase cells. The survival is also varying considerably among different strains of one species. Many kinds of food constituents like protein and carbohydrates increase freezing viability, whereas low pH decreases survival (Georgala & Hurst 1963).

During freezing the same mechanism of ice formation is working as in cellular food, even though bacteria are smaller by several orders of magnitude. Most water freezes outside the cells, causing dehydration of the intracellular space. Intracellular freezing is occurring at higher freezing rates. Mazur (1966a) summarized that the effect of freezing on microorganisms is largely determined by solute concentration and intracellular freezing, which is deadly (Mazur 1961; Muldrew, Acker, Elliott & McGann 2004). During slow freezing, most events occurring during freezing are consequences of dehydration (Gounot 1991; Jay 1996):

- The intracellular viscosity increases.
- Freezing results in a loss of cytoplasmic gases. Aerobic organisms lack O_2. Diffusive O_2 causes oxidation.
- pH changes occur in a magnitude of 0.3 to 2 pH units. Increase or decrease of pH is possible.
- Cellular electrolytes are concentrated.
- Protoplasmic proteins in colloidal solution are affected and in the end denatured. (See denaturation of flesh proteins above in chapter 2.1.4.)
- Temperature shock in microorganism is induced, especially in mesophilic and thermophilic species. Adaptation to cold temperatures, for example by slow cooling before freezing, increases survival due to the effect of a complete stress response.
- After freezing, cells are metabolic injured as detected by increased nutritional requirements.

Jay (1996) and Gounot (1991) also summarized the main effects of microorganisms adaptation to the cold. One major effect is the adjustment of the fatty acid composition of the lipid bilayer membranes, making them shorter and incorporating more unsaturated chains. In this

way they prevent lipid solidification and membrane breakage. Some psychrotrophs synthesize polysaccharides as their own cryoprotectant, pigments and proteins as well, particularly chaperones are produced. Bacteria can adapt to lower metabolic rates, some psychrotrophs adapt their complete metabolic pathway. Other psychrotrophs produce larger cells (e.g. *Candida utilis*) and it is known that more flagella are produced at low temperatures.

Listeria monocytogenes as a major psychrotolerant food borne pathogen was investigated in a number of studies and shall be taken as an example. It was for example shown that 98 % of the cells after freezing and storing at -18 °C for 6 months were dead, but at -198 °C cells were not even injured (El-Kest & Marth 1992). However, like in all microorganisms, cellular injury is a frequent phenomenon in *Listeria* recovering from freeze stress. Hence the survival determined in optimum recovering conditions is a lot higher than after incubation in selective medium (Flanders & Donnelly 1994). During storage special cryoprotectants, but also normal food constituents, prevent cell death and damage (El-Kest & Marth 1992).

Although intracellular freezing is not the sole cause of freezing injury, intracellular freezing leads to immediate cell inactivation due to massive ice crystal damage (Mazur 1961; Mazur 1966a; Muldrew et al. 2004). It shall be noted that there are contrary opinions stating that intracellular ice is protective in some cases (Acker & McGann 2003), however, this work covered very special treatment conditions of mammal cells, hence, it does not seem applicable for freezing of food bacteria.

The crucial question is the likelihood of intracellular freezing in microorganisms, especially bacteria, which is closely linked to the cooling rate. Most of the work in this field is linked to Peter Mazur and the following summary is based on a newer treatise (Mazur 2004). The main factors implied in the kinetics of water loss from a cell during freezing are cell size, water permeability of the cell wall, freezing rate and final freezing temperature (Mazur 1963; Mazur 1966b). At slow cooling rates the dehydration of cells progresses, making intracellular freezing unlikely over a wider range of temperatures due to high solute concentrations like it is shown in Figure 2.5.

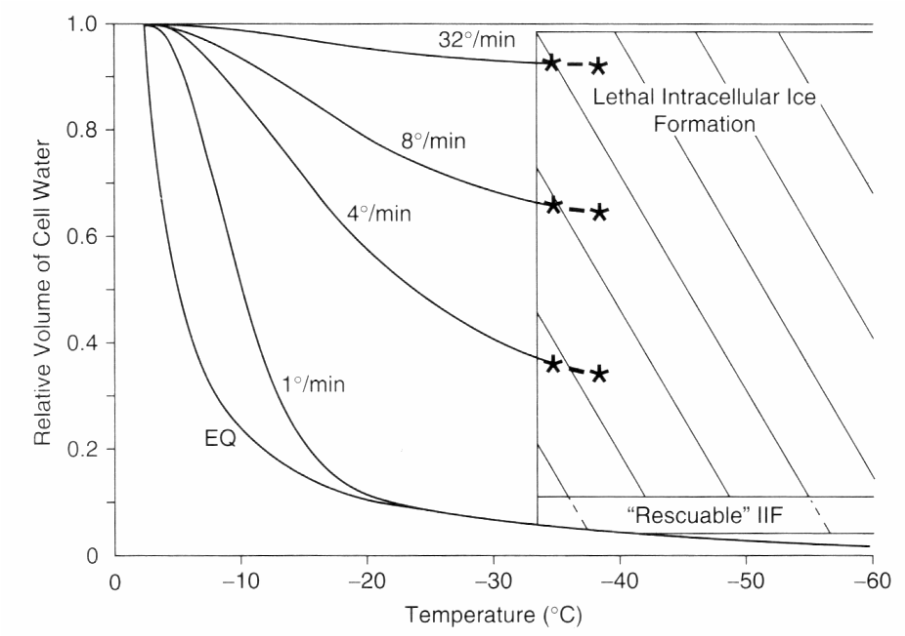

Figure 2.5 Kinetics of water loss from mouse ova as a function of the cooling rate during freezing in 1 M dimethyl sulfoxide (DMSO) or glycerol. The vertical line at -33 °C is the median ice nucleation temperature observed by Rall et al. (1983) for eight-cell mouse embryos. From Mazur (2004).

For yeast cell was reported elsewhere that at cooling rates below 10 K min^{-1} dehydration is close to equilibrium, which covers most food freezing applications, and close to its maximum at a temperature of about -12 °C (Mazur 1966b). Figure 2.5 also shows that at a certain temperature, in this case -33 °C, lethal intracellular ice formation (IIF) occurs over a wide range of cooling rates. Only very slow cooling makes it possible to prevent IIF. In mouse oocytes suspended in phosphate buffer saline (PBS), IIF was observed at about -13 °C (Mazur, Seki, Pinn, Kleinhans & Edashige 2005). Comparable data about IIF in bacteria or yeast cells are unfortunately not available. At higher cooling rates and if water efflux from the cell is limited by large cell size and low permeability, IIF is more likely to occur.

Figure 2.6 summarizes the freezing damages for a number of cells with different cooling rates. At slow cooling rates, freeze damage caused by long exposure to concentrated liquid limits the survival. At an optimum cooling rate, for yeast in a range of 1 K min^{-1} to 10 K min^{-1}, freezing survival is highest, due to dehydration during freezing, while at higher freezing rates, survival is limited by IIF. For bacteria it can be expected that the relation because of their even smaller cell size is not far from the behavior of yeast cells, so that IIF is not occurring at technical food freezing rates.

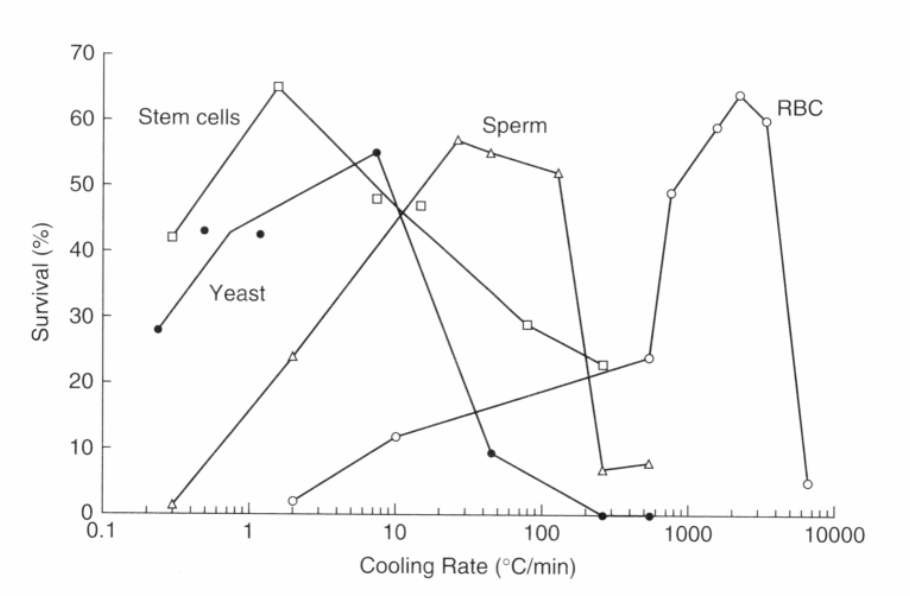

Figure 2.6 Survival of mouse marrow stem cells, yeast, mouse sperm, and human red blood cells (RBC) as function of cooling rate. From Mazur (2004).

These general relations were confirmed in other studies for *Saccharomyces cerevisiae, Candida utilis, Lactobacillus plantarum* and *Escherichia coli* (Calcott & MacLeod 1974; Dumont, Marechal & Gervais 2003; Dumont, Marechal & Gervais 2004). Furthermore both groups found increasing viability at very high cooling rates of 5000 °C min^{-1} and above as a result of vitrification.

2.2 Phase transitions under pressure

2.2.1 Phase diagram of water

According to Le Chatelier's principle water is expanding during freezing at atmospheric pressure, while the freezing point under elevated pressure is depressed to a minimum of -22 °C at 209.9 MPa. However, at higher pressure values (up from 210 MPa). Ices with a denser and more complex crystalline structure exist, leading to a continuous rise of the freezing point. First indications of ice phases distinct from the commonly known ice (ice Ih) have been detected by Tammann (1900), whereas Bridgman (1912) found several more ice phases and published an enormous amount of physical data of water and ices under pressure. Fifteen crystalline phases of ice have been described so far, which are denoted ice Ih, Ic and ice II to XIV (Salzmann, Radaelli, Hallbrucker, Mayer & Finney 2006; Chaplin 2007). Recently a model was proposed covering thermodynamic properties of liquid water and high pressure ices in the range from 0 to 2200 MPa and from –90 °C to +90 °C (Choukron & Grasset 2007). Ice Ih is commonly known hexagonal ice, whereas ice Ic has similar properties but a cubic crystal structure. It is stable at temperatures below -70 °C. Ice phases numbered II and higher are all denser than liquid water at the respective conditions.

The stability domains of the ice phases and the liquid phase in the pressure range up to 600 MPa are presented in Figure 2.7. Additionally extended phase transition lines are denoted, which indicate phase transitions of metastable phases (Bridgman 1912; Urrutia Benet, Schlüter & Knorr 2004). In the given pressure range ice I(h), III and V are the ice phases that may coexist with the liquid phase, which means, that only these ices freeze and melt. Ice IV is metastable within the domain of ice III and V and is of little practical relevance, as it is formed by heating of high-density amorphous ice (Salzmann, Kohl, Loerting, Mayer & Hallbrucker 2003). Ice II usually forms only at temperatures below the typical range of this study of -45 °C (Bridgman 1912). An interesting feature of the phase behavior of water is the possibility of phase transitions between solid phases, for example when ice I transforms to ice III upon pressurization.

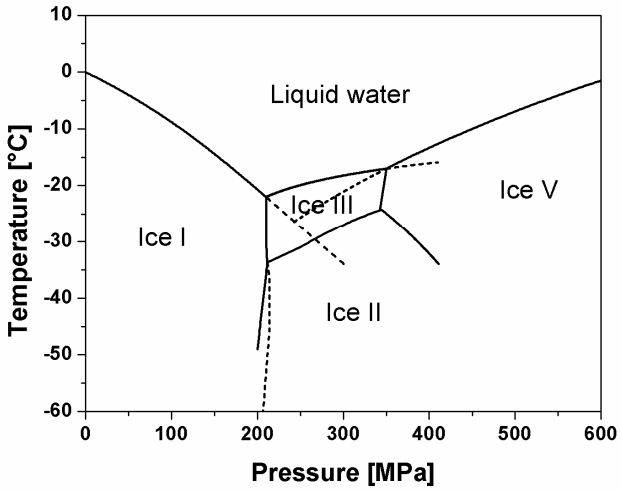

Figure 2.7 Phase diagram of pure water under pressure (Bridgman 1912). ━ boundaries of stable phases; ╍ extended phase boundaries of major phase transitions (ice I-liquid, ice III-liquid, ice V-liquid, ice I-ice III).

Table 2.2 Physical data of water phase transitions

Phase transition	**Temperature [°C]**	**Pressure [MPa]**	**Volume change Δv [cm³ kg^{-1}]**	**Enthalpy change Δh [kJ kg^{-1}]**
Liquid – ice I	0	0.1	+0.1313	-334
	-20	195.6	+0.0900	-241
Liquid – ice III	-22	209.9	-0.0466	-213
	-17	350.3	-0.0241	-257
Liquid – ice V	-20	311.6	-0.0828	-253
	0	631.2	-0.0527	-293
Ice I – ice III	-20	208.7	-0.1773	+23.4
	-30	214.0	-0.1919	+14.6
	-40	216.1	-0.1992	+2.9
	-50	214.3	-0.2023	-8.8
Ice I – ice II	-35	214.8	-0.2177	-42.5
Ice II – ice III	-25	334.5	+0.0148	+68.2
Ice III – ice V	-25	341.1	+0.0546	-3.6

Data by Bridgman (1911) with own unit conversions; pressure values were corrected according to Wagner et al. (1994); see chapter 2.2.5.

In Table 2.2 phase transition data of the relevant ices among each other and with the liquid phase are listed. Phase transitions from the liquid to ices I, III and V ("freezing") is going along with a considerable release of heat. Even though the released heat is lower under pressure compared to the maximum at 0.1 MPa (Δh=-334 kJ kg^{-1}), the values remain within the same order of magnitude. Consequently, phase transitions between these solid phases go along only with enthalpy changes which amount to less then 10 % of the heat released during liquid - solid transitions. From this point of view, ice II is an exception from the other ices discussed here as ice II cannot coexist with the liquid. When heating ice II above its area of stability, it will always convert to ice III. As the reaction is also consuming energy, the transition resembles thawing (Bridgman 1912).

The volume changes are also presented in Table 2.2 and the evolution of the specific volumes is shown in Figure 2.8. It shows that freezing to ice III and V results in a negative volume change, which is according to amount even smaller than the positive volume change during freezing to ice I. As the specific volume during freezing to ice I compared to ice III develops in opposite directions, it is obvious that the phase transitions between ice I and III go along with a considerable change of volume, as it is denoted in Figure 2.8.

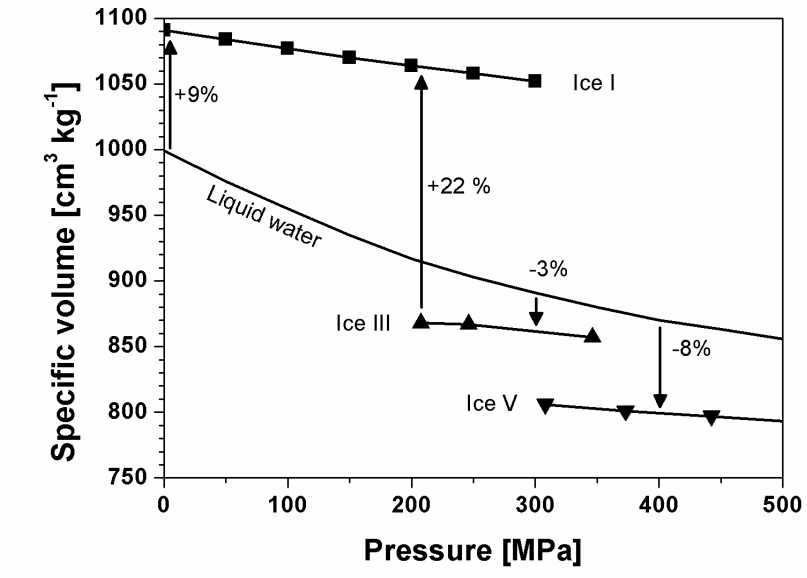

Figure 2.8 Specific volume of water and ices I, III and V along the phase transition line solid – liquid. Arrows indicate relative volume changes of the phase transitions liquid-ice I at 0.1 MPa, ice III-ice I at 210 MPa, liquid-ice III at 300 MPa, liquid-ice V at 400 MPa (from left to right, respectively).

As this change is combined with a small change in enthalpy only, the transition from ice I to III and vice versa is not limited by heat transfer. The transition can take place very fast within

parts of a second, which was validated in experiments (Luscher, Schlüter & Knorr 2005). However, Bridgman reports that in the lower temperature domain (below -50 °C) the reaction is so slow that it was not completed within several hours. It should be noted that the phase transition line from ice I to ice III is slightly concave, as it can be seen in Figure 2.7. Hence, the enthalpy change is positive above -40 °C, running through zero between -40 °C and -45 °C and negative at lower temperatures (Tammann 1900; Bridgman 1912).

2.2.2 High pressure – low temperature processes

The first developments of high pressure treatments to preserve food focused on the pure substitution of thermal pasteurization processes by so called "non-thermal" methods. Soon other processing possibilities were examined, which lead to first examinations exploring possibilities to modify the freezing food (Kanda, Aoki & Kosugi 1992). Knorr, Heinz & Schlüter (Knorr, Schlüter & Heinz 1998) published a systematic definition and nomenclature of high pressure – low temperature processes postulating the specific advantages.

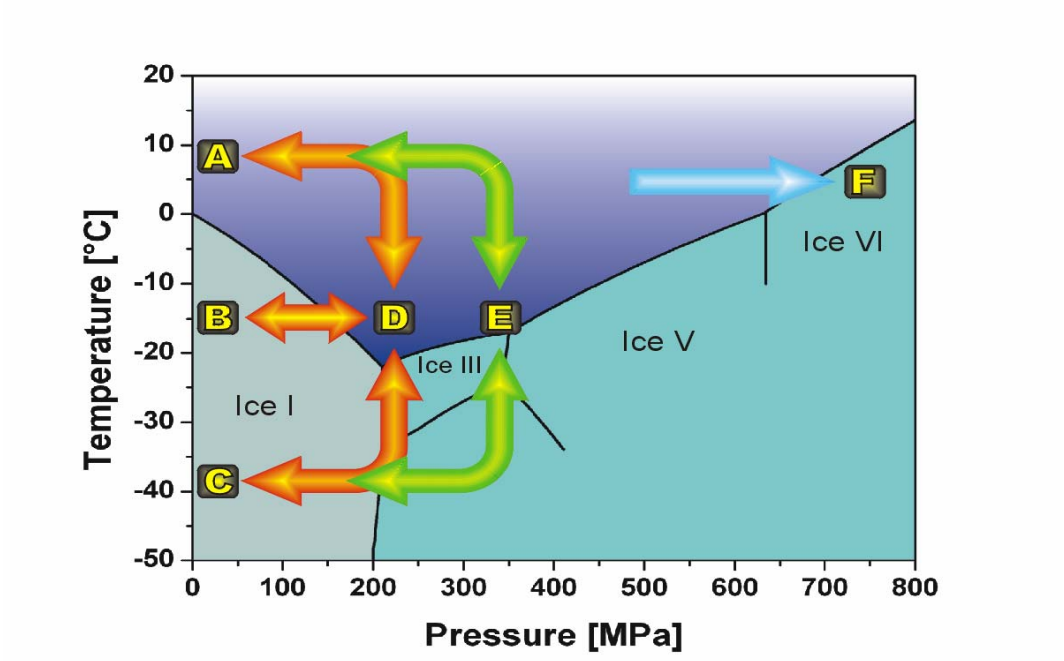

Figure 2.9 Scheme of high pressure – low temperature processes. Orange arrows: pressure-shift freezing with pressure release at point A, pressure assisted freezing and thawing through point A; green arrows: pressure assisted freezing and thawing of ice III (also possible with ice III, V); blue arrow: pressure induced freezing.

Other definitions are in use in literature (Cheftel, Levy & Dumay 2000), but within this work the nomenclature of Knorr et al. (1998) is used. A modified version of their processing scheme is given in Figure 2.9.

- By definition **"pressure assisted"** refers to freezing and thawing processes which are carried out at elevated pressure, however, the driving force is a temperature gradient, like at atmospheric pressure. Freezing (path A-D-C in Figure 2.9) and thawing of ice I (C-D-A) is possibility, but also freezing and thawing of ices III, V or VI (A-E-C and C-E-A) are possible in the pressure domain technically feasible for food processing. Benefits from these processes can be derived from the modified thermophysical properties of freezing (enthalpy, volume change) under pressure. However, time consuming heat transfer in pressure vessels is necessary to carry out these processes.
- **"Pressure induced"** is used for phase transitions in which the driving force is rising pressure. This term includes pressure induced thawing of ice I (B-D-A) or pressure induced freezing of ices III, V or VI (A-F), however pressure induced freezing was not examined so far. **"Pressure shift"** is used for pressure shift freezing of ice I (A-D-B) to indicate the sudden release of pressure during the process, which can be considerable faster than technical pressure built-up. It is expected that all pressure driven processes can be conducted faster than temperature driven processes.
- **"Pressure supported"** is used as a generic term comprising pressure induced, pressure assisted and pressure shift processes.
- Another possibility would be **storage under pressure without freezing** at subzero temperature (A-D-A). Due to the low temperature, good preservation without ice crystal formation can be achieved.

During the last 15 years high pressure – low temperature processes, especially possibilities to optimize freezing, attracted considerable interest. Due to the wealth of publication it is not possible to give a complete review of the examinations that have been carried out in this field and it is not necessary for the examinations of this study. A number of excellent reviews have been published (Cheftel et al. 2000; Cheftel, Thiebaud & Dumay 2002; Denys, Schlüter, Hendrickx & Knorr 2002; Le Bail, Chevalier, Mussa & Ghoul 2002), also the dissertations of Schlüter and Urrutia contain excellent recapitulations of the field (Schlüter 2003; Urrutia Benet 2006). Anyway, a number of papers with focus on recent years are reviewed.

Pressure shift freezing

The most intriguing high pressure – low temperature process is probably pressure – shift freezing, which is defined as the process in which food is first pressurized and cooled under pressure to a subzero temperature without freezing. Most experiments were carried out from around point A, which is roughly at 210 MPa and -20 °C. From there, instant freezing initia-

tion is possible by sudden pressure release resulting in small and uniform ice crystals. A number of papers focus on the prediction of heat transfer modeling and on the ice ratio formed during pressure shift freezing with experimental and predictive approaches (Chevalier, LeBail & Ghoul 2000; Otero & Sanz 2000; Sanz & Otero 2000; Chevalier, Le Bail & Ghoul 2001; Denys et al. 2002; Picart, Dumay, Guiraud & Cheftel 2005; Zhu, Ramaswamy & Le Bail 2005; Otero & Sanz 2006; Zhu, Ramaswamy & Le Bail 2006; Otero, Ousegui et al. 2007). It can be roughly summarized that 35 % to 40 % of the water freeze during pressure release which leads to shorter overall freezing time and a beneficial ice crystal distribution as a lot of ice nuclei are present throughout the whole sample. A positive effect on the structure and texture was frequently shown in the case of cellular plant, fish or meat tissue (Fernandez-Martin, Otero, Solas & Sanz 2000; Zhu, Le Bail, Ramaswamy & Chapleau 2004; Luscher et al. 2005; Van Buggenhout, Messagie, Van Loey & Hendrickx 2005; Fernandez, Prestamo, Otero & Sanz 2006; Urrutia Benet, Chapleau et al. 2006; Van Buggenhout et al. 2006a; Van Buggenhout, Messagie et al. 2006b; Alizadeh, Chapleau, De Lamballerie & Le Bail 2007; Tironi, Le Bail & De Lamballerie 2007; Urrutia Benet, Balogh, Schneider & Knorr 2007), but also in gels (Fuchigami, Ogawa & Teramoto 2002; Fuchigami & Teramoto 2003a; Fuchigami & Teramoto 2003b; Fuchigami, Teramoto & Jibu 2006; Lille & Autio 2007) or ice cream models (Levy, Dumay, Kolodziejczyk & Cheftel 1999; Thiebaud, Dumay & Cheftel 2002; Fernandez, Martino, Zaritzky, Guignon & Sanz 2007a). From a processing point of view it must be argued however, that the feasibility of the process is somewhat difficult, while it requires heat transfer (cooling) during pressure treatment, making extended and costly pressure holding time necessary. It can be facilitated, if the vessel is kept at a constant low temperature, and if the freezing process at ambient temperature is completed outside the pressure vessel, but still unfrozen, packaged product has to be cooled about 20 K under pressure making short time treatments impossible.

One major problem arises throughout treatment of protein rich samples like meat or fish during at all high pressure – low temperature combinations: the (cold) denaturation of protein, which causes loss of color (whitening) and other protein denaturation effects (hardening, loss of structure, gaping in fish). These reactions were found in all experiments and are discussed later in depth (chapter 2.3.3)

Pressure assisted freezing

In contrast to pressure shift freezing, pressure assisted freezing is not drawing considerable interest anymore. It was thought to be a beneficial process, because the heat of fusion of ice I

under pressure is reduced. Due to the lower freezing point, it reduces the cooling temperature gradient during phase change at a fixed cooling temperature. In contrast to pressure shift freezing, it would not only be necessary to cool under pressure before freezing, also the whole latent heat of freezing must be removed under pressure additionally making very long treatments necessary. The process however, is of academic importance as it is possible to derive insights from it, like thermophysical properties under pressure (Chevalier-Lucia, Le Bail, Ghoul & Chourot 2003; Kowalczyk, Hartmann et al. 2005). It is also noteworthy that during freezing under pressure the whole convection characteristics of the freezing process in a liquid change (Kowalczyk, Hartmann & Delgado 2004; Özmutlu, Hartmann & Delgado 2006). In comparative studies, superior quality of pressure shift frozen samples compared to pressure assisted freezing was found (Levy et al. 1999; Fuchigami et al. 2002; Fuchigami & Teramoto 2003a; Fuchigami & Teramoto 2003b; Fernandez, Otero, Guignon & Sanz 2006; Fuchigami et al. 2006).

Pressure supported thawing

According to the same argumentation made with regard to pressure assisted freezing, pressure assisted thawing at a constant pressure is interesting from a processing point of view. Without raising the thawing temperature, which is limited due to spoilage reactions, an increase of thawing temperature gradient is possible, while the freezing point of water under pressure is lower. Nevertheless the complete heat of fusion hast to be transferred, even though it is reduced under pressure. Due to the shorter thawing time, better structure and faster processing can be achieved (Chevalier, Le Bail, Chourot & Chantreau 1999; Schubring et al. 2003; Kowalczyk et al. 2004; Dumay, Picart, Regnault & Thiebaud 2006; Alizadeh et al. 2007; Tironi et al. 2007). The process has attracted some interest, however, industrial thawing is not of the same interest for food industries as freezing.

Only in a schematic way pressure induced thawing can be differentiated from pressure assisted thawing. If a frozen food sample is pressurized, it cannot be forced to thaw instantly by pressure alone due to a considerable amount of heat, the heat of fusion, which has to be transferred to the sample. So if a further pressure increase of the system is forced externally, the temperature shifts downwards along the phase transition line liquid – ice I and approaches it slowly. In this way however the temperature gradient to the thawing temperature is continuously rising, so pressure assisted thawing takes place at the same time making pure pressure induced thawing impossible. A lot of papers were published showing temperature curves during thawing under pressure supporting this relation (Rouillé, Le Bail, Ramaswamy & Leclerc

2002; Zhu et al. 2004; Picart et al. 2005; Urrutia Benet et al. 2006; Van Buggenhout et al. 2006b; Van Buggenhout, Messagie, Van der Plancken & Hendrickx 2006c). These effects were systematized by Urrutia Benet et al. (2004; 2007). A pure pressure assisted thawing process remains possible, but not a pressure induced one (Otero & Sanz 2003).

Pressure supported freezing and thawing of ices III, V and VI

Besides the freezing and thawing processes of ice I there is also the possibility to use phase transitions of ices III, V and VI for food or other biomaterial. One possibility is freezing and thawing at constant pressure to one of the high pressure ices taking advantage of the fact, that these ices shrink during freezing so that reduced ice crystal damage is presumable. Unfortunately, after freezing in the technically feasible temperature domains (warmer than -50 °C) these ices are not stable during decompression resulting in a fast phase transition to ice I with destructive effects that are shown later. This conversion would not take place at a lot lower temperatures of about -200 °C (Bridgman 1912), however, this was not even demonstrated so far for food samples as the pressure units in food science labs are all not approved for use below -50 °C by the manufacturers. There is a large number of publications (Fuchigami et al. 2002; Fuchigami & Teramoto 2003a; Fuchigami & Teramoto 2003b; Fuchigami et al. 2006) which examined freezing to the high pressure ices followed by decompression. However, some experiments with pressure assisted freezing and thawing of ice III, V and VI, that were also published, showed the expected reduction of ice crystal damage. The results of these experiments are summarized in Table 2.3. Some older publications of Fuchigami et al. are not included, as the phase transition behavior during freezing and thawing was probably not as assumed by the authors at that time.

Solid – solid phase transitions

The destructive nature of the phase transition from a high pressure ice to ice I was shown first by Edebo & Heden (1960). In recent years a number of other papers were published covering the treatment of frozen samples by high pressure (results in this thesis and Shen, Urrutia Benet, Brul & Knorr 2005; Van Buggenhout et al. 2006c; Fernandez, Sanz et al. 2007b; Serra, Grebol et al. 2007a; Serra, Sarraga et al. 2007b), which are discussed in chapter 2.3.4.

Table 2.3 Publications of pressure assisted freezing and thawing of high pressure ices III, V and VI.

Publication	Pressure and ice form	Thawing at HP or at 0.1 MPa [1)]	Object of investigation	Results
Molina-Garcia, et al. (2004)	700 MPa, ice VI	HP	Pork meat	Tissue preservation (microscopy)
Luscher et al. (2005)	320, 400 MPa, ice III, V	HP	Potato	Tissue preservation (impedance[2]), less browning, improved texture
Fuchigami et al. (2003a)	500, 600, 690 MPa, ice V, VI	HP	Agar gel with 0 to 20% sucrose	Microstructure close to control sample (electron microscopy)
Luscher et al. (2005)	320 MPa, ice III	0.1 MPa	Potato	Macroscopic destruction, more browning
Fuchigami et al. (2002)	690 MPa, ice VI	0.1 MPa	Tofu with 0 to 5% trehalose	Impaired texture, destroyed microstructure (electron microscopy)
Fuchigami et al. (2003b)	600, 690 MPa, ice V, VI	0.1 MPa	Gellan gum gel with 0 to 20% sucrose	Impaired texture, destroyed microstructure (electron microscopy)
Fuchigami et al. (2006)	600, 690 MPa, ice V, VI	0.1 MPa	Agar gel with 0 to 20% sucrose	Impaired texture, destroyed microstructure (electron microscopy)
Fuchigami et al. (2003a)	500, 600, 690MPa, ice V, VI	0.1 MPa	Agar gel with 0 to 20% sucrose	Destroyed microstructure (electron microscopy)
Özmutlu et al. (2006)	260 MPa, ice III	-	Thermochromic liquid crystals	Visualization of ice III freezing

1) Samples frozen under high pressure (HP) and thawed at 0.1 MPa were converting to ice I during decompression.
2) Impedance measurement at various alternate current frequencies allows conclusions regarding the permeabilization of the cellular membranes (Angersbach, Heinz & Knorr 2002).

Storage under high pressure at subzero temperatures

The storage under pressure at temperatures below 0 °C without freezing is a fascinating approach as ice crystal damage is completely excluded, hence, it might even be interesting for preservation of biotechnological or medical precious matter like organs. However, regarding preservation it must be considered that the water activity remains unchanged if no ice is formed. The long time under pressure has likely a considerable impact on systems with active

metabolism as it affects enzymes. To date the technical demands are too high to seriously consider this process as it would require pressure vessels for the whole storage period. Food science experiments did not exceed 24 h pressure holding at these conditions in lab scale experiments (Luscher et al. 2005). Inactivation of lytic enzymes in plant cells (potato) was shown during this treatment.

2.2.3 Nucleation and metastability

When looking at the phase diagram of water under pressure, it should always be reminded, that the zones of the ices and the liquid phase represent only the areas of thermodynamic stability. This does not exclude phase transition phenomena involving metastable states which are phases that are relatively stable outside their respective zones. One well known phenomenon is the supercooling of liquid water during cooling below the freezing point. In clean water samples it is frequently observed at ambient pressure and might reach even -38 °C (Kanno, Speedy & Angell 1975; Kanno & Angel 1977). The superheating of ice was reported only for samples with a thickness of few micrometer in the picosecond's time scale (Iglev, Schmeisser, Simeonidis, Thaller & Laubereau 2006), but visible amounts of ice cannot be superheated and melt if warmed above the melting point.

In order to understand supercooling it is necessary to deal with nucleation. Nucleation has to be separated into homogenous and heterogeneous nucleation. The spontaneous formation of a nucleus from the liquid without facilitating influences is called homogenous nucleation. It is only observed in ultra pure samples of water without contact to vessel walls, e.g. in an aerosol or emulsion. In liquids, nuclei form and decay continuously, however, decisive for ice formation is the critical nuclei size, above which the nucleus is big enough to persist and grow (Sahagian & Goff 1996). This critical size is related to temperature, for example 45000 water molecules are necessary at -5 °C down to 70 water molecules at -40 °C to form a stable ice nucleus (Zachariassen & Kristiansen 2000). Hence, nucleation is therefore a stochastic event, making freezing more likely in larger volumes and at lower temperatures. It is in principle impossible to predict the beginning of freezing for an individual droplet.

The same relationships apply to heterogeneous nucleation, describing the crystal formation which is facilitated by so called nucleators. These can be vessel walls, inorganic particles, salts (silver iodide) or more complex biomolecules, for example produced by so-called ice nucleating bacteria. As one or more of these nucleation aids are present in real foods, heterogeneous nucleation is dominating when freezing biological samples. However, supercooling of a few degrees is frequently observed in food samples, depending like noted above on time

(cooling rate), temperature, volume and nucleators (Sahagian & Goff 1996). It was reported, that adding solutes to water decreases the homogenous nucleation temperature with a ratio of 2±0.5 in relation to the freezing point depression caused by the solute (Wilson, Heneghan & Haymet 2003). This relation was found for a number of solutes including glucose and sodium chloride with concentrations (weight percentage) up to 40 %. The authors also stated that the same relation should apply for heterogeneous nucleation.

Under pressure, Kanno et al. (1975) found that the homogenous nucleation temperature of water decreases from -38 °C at ambient pressure to a minimum of -92 °C at 210 MPa. Considering the minimum of the melting point, the temperature difference increases between melting point and homogeneous nucleation temperature from 38 K to 70 K. At pressures of 210 MPa to 300 MPa, the homogeneous nucleation of ice III is observed at temperatures remaining 70 K below the respective melting points of ice III.

During pressure assisted freezing of ice I, data presented by Schlüter (2004, p.98) indicate a slight increase in supercooling under rising pressure. However, the data basis is limited as no other systematic evaluation of supercooling when freezing at constant pressure is shown in literature. Nevertheless, it is clear that supercooling when freezing other ice modifications is considerable higher. Especially in the case of ice III high degrees of supercooling are necessary to start freezing, at least -15 K, but even a maximum of -21 K of supercooling was observed in potato samples (Schlüter 2003; Luscher et al. 2005). Bridgman (1912) did not even achieve direct freezing of ice III from the liquid in pure water. Nucleation points of ice V in potato were reported, ranging widely from -5 K to -15 K of supercooling which in average seems to be lower than for ice III (Luscher 2001; Urrutia Benet 2006; Otero et al. 2007). Urrutia showed pressure-temperature domains in which nucleation of ice III and V is probable in potato tissue (Urrutia Benet 2006; Urrutia Benet et al. 2007). In meat tissue, ice VI nucleated after supercooling of 10±3 K at 700 MPa (Molina-Garcia et al. 2004). It was also shown that some molecules act as selective nucleators of high pressure ices (Evans 1967), however, these compounds have little applicability for food freezing. All in all, little data is available on the nucleation of high pressure ices from the liquid and the associated degree of supercooling. A complete characterization is of course impossible, regarding the heterogeneity of systems and conditions. It may be summarized with some remaining uncertainty that ice III shows the highest degree of supercooling, while ices V and VI show more supercooling than ice I, but less than ice III. A fact likely related to constrained nucleation is the rising viscosity of water (Först, Werner & Delgado 2000) at high pressure – low temperature combinations, as water diffusion is necessary for the formation of nuclei. High viscosities of food model solutions of

sodium chloride (Horne & Johnson 1967), sugar (Först, Werner & Delgado 2002) and protein (Först 2001) were also reported.

Ices can exist and they can even crystallize at pressure – temperature combinations outside their respective areas of stability. Due to the large supercooling of ice III, it happens frequently that other ice forms freeze in this pressure domain. For example at 230 MPa it is more likely that a nucleus for ice I forms before a nucleus of ice III during isobaric cooling. In the ice III domain this leads to the behavior that ice I usually freezes during isobaric cooling at 210 MPa to about 270 MPa. At about 320 MPa to 400 MPa, due to the similar freezing and nucleation points, it is possible that either ice III or V form, while it is more likely that ice V forms at higher pressures (Schlüter 2003; Luscher et al. 2005). The existence of ice III or V in the domain of ice I was never reported, except for parts of a second during pressure release. As the phase change of ice I to ice III upon compression is explosive, it is also likely, that ice III nuclei transform ice I to ice III rapidly (Schlüter 2003).

Another consequence of the large supercooling of ice III is the long term stability of liquid water in the zone of ice III. At pressure – temperature combinations above the freezing lines of ice I and V it is highly improbable that ice III nucleates. It was shown that liquid water is stable in milliliter volumes down to -28 °C at 240 MPa for 24 hours (Luscher et al. 2005). This point might be valuable as an optimized starting point for pressure shift freezing.

During solid-solid transformations little is known about questions of nucleation and how it forms as no water diffusion is possible. In the range above 210 MPa metastability is a common phenomenon, as ice I and V are stable in the ice III domain, but during decompression ices III and V convert to ice I quickly. A soon as they are triggered, all phase transitions of ice I, III and V in the pressure range to 500 MPa above -50 °C are running fast or even explosively. Therefore it seems reasonable to assume that as soon as a seed of the respectively stable form is present all ice transforms to the stable ice type. At lower temperatures the phase transitions are running considerably slower making metastability of high pressure ices even at ambient pressure possible (Bridgman 1912).

Another problem when treating ices or frozen systems under pressure is the question if the pressure is transmitted uniformly throughout the sample, if a sample is frozen completely in metal cylinder with contact to the pressure transmitting fluid only on one side. Bridgman (1912) compared such experiments to experiments where the ice sample was immersed on all sides in fluid and found no discrepancies.

From the insights gained about nucleation and metastability over the years of high-pressure low-temperature research the following modified processing diagram in Figure 2.10 was derived (Schlüter, Urrutia Benet, Heinz & Knorr 2004; Urrutia Benet et al. 2004; Urrutia Benet et al. 2007). It is essentially a modification and enhancement of the processing scheme of Knorr et al. (1998) and reflects the metastability of the liquid phase and other ice phases in the ice III region and the relationship of pressure assisted and pressure induced thawing.

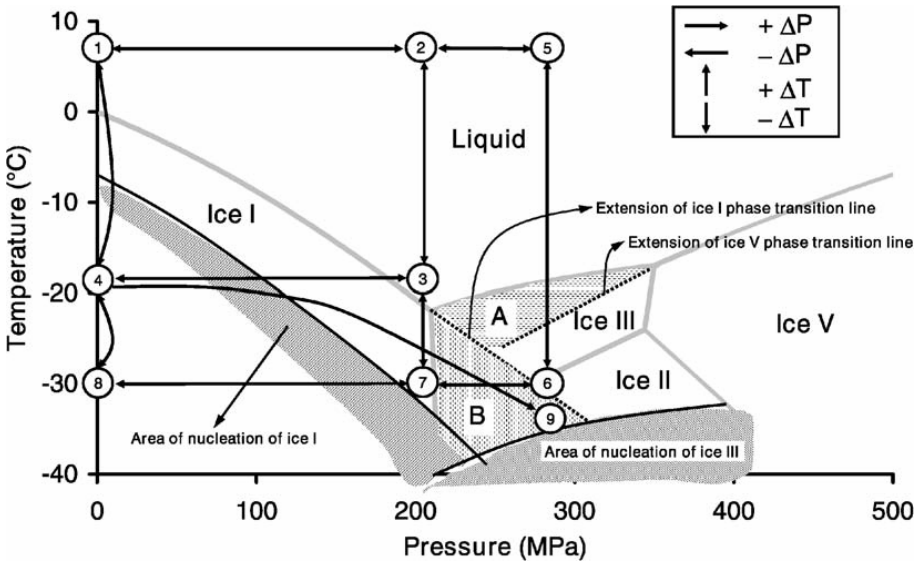

Figure 2.10 Concepts of area of nucleation, phase transition line extensions and metastable phases on the phase diagram of water. Schematic processes: 1–4–8: Freezing at atmospheric pressure; 1–2–3–7–8: Pressure-assisted freezing; 1–2–5–6–7–8: Pressure-assisted freezing to ice III, 1–2–3–4–8: Pressure-shift freezing; 8–4–1: Thawing at atmospheric pressure; 8–7–3–2–1: Pressure-assisted thawing; 8–7–6–5–2–1: Pressure-assisted thawing from ice III; 8–4–3–2–1: Ideal pressure-induced thawing and 8–4–9: Real pressure-induced thawing. Area A: metastable liquid water in the ice III region; area B: metastable ice I in the ice III region. From Urrutia Benet et al. (2007).

2.2.4 Influence of solutes on phase transitions

To get indices of the phase transitions of multi-component aqueous food systems, it is appropriate to examine the melting lines of aqueous solutions, e.g. of sodium chloride or sucrose under pressure as model systems. At ambient pressure, it is well known that solvates depress the freezing point depending on the molality of the solvate (Debye & Hückel 1923). During freezing of pure water the solutions are freeze concentrated in equilibrium until they reach the eutectic point. The eutectic of the sodium chloride – water system forms at -21.2 °C and a sodium chloride mole fraction of X_{NaCl}=0.0857 (Gribaudo & Rubiolo 1992). The eutectic of the sucrose – water system was found at -14.0 °C and $X_{Sucrose}$=0.084 (Young & Jones 1949).

Data of the pure water ice I – melting curve are among others given by Bridgman (1912) and Nordell (1990). In the ice I area the works on phase transition behavior of binary systems include examinations of aqueous solutions of 9.7 % (w/w) MgSO4 and the detection of the eutectic by differential scanning calorimetry (DSC) for this system (Chourot, Le Bail & Chevalier 2000). In another study, phase transitions of sodium chloride and sucrose solutions in a concentration range of 1.63 % (w/w) to 16.09 % and 16 % to 36 % respectively were measured (Guignon, Otero, Molina-Garcia & Sanz 2005). The water – ammonia phase diagram was reported for pressures up to 300 MPa for a number of concentrations, partly covering the ice III – phase boundary (Hogenboom, Kargel et al. 1997; Leliwa-Kopystynski, Maruyama & Nakajima 2002). The phase transitions of a number of emulsified 1 M – alkali halide solutions were examined in the pressure range up to 290 MPa including ice III; interestingly the authors also reported eutectic solidification of some of the systems (Kanno & Angel 1977).

High pressure phase transitions of more complex systems were reported in the ice I – pressure range for complex brine (Marion, Kargel, Catling & Jakubowski 2005), tuna meat (Takai, Kozhima & Suzuki 1991) and yeast suspensions (Magnusson 1977a), but not for the ice III – pressure range. Additionally, phase transition data, especially for the ice I liquid boundary can be derived from a lot of examinations, especially from pressure shift freezing experiments, if the pressure – temperature recordings are measured and presented in an appropriate way. During pressure shifts the temperature moves along the phase transition line, because the system is freezing and the pressure is continuously changing (Schlüter 2003; Schlüter et al. 2004). When freezing to other ice modifications is examined, single phase transition points can be derived, e.g. freezing points of agar gel with sucrose concentrations of 0 to 20 % were reported at 500 to 686 MPa (Fuchigami & Teramoto 2003a).

The conclusion to all these reports is that aqueous solutions and more complex aqueous biological samples show a parallel shift of the ice I - phase boundary according to the melting point depression at ambient pressure. However, little is known about the other phase transitions and complex phase transition phenomena like the eutectic state.

2.2.5 Equations describing phase boundaries

Before considering the definition of equations that describe the phase transition boundaries of water, a remark has to be made to the experimental data and numerical values that are circulating. The data published by Bridgman (1912) are still the main basis of most phase transition lines. He presented the pressure values given in the unit kg/cm³ and not in Pascal (Pa),

which can be easily converted using earth's gravity g_N. However, the pressure value of the triple point liquid/ice I/ice III is then converted from p=2115 kg/cm² to 207.4 MPa, a value which can be frequently found in literature. According to the definition of phase transition lines of water (Wagner, Saul & Pruß 1994), which are accepted by the International Association for the Properties of Water and Steam (IAPWS), the values of Bridgman have to be corrected (Babb 1963b), as the reference points of the pressure measurements shifted. Care should be taken when directly converting Bridgman's values; however, it should be easier to take the values from Wagner et al. (1994), for example the correct value of the triple point at 209.9 MPa.

The Simon equation is the standard method to describe phase boundaries not only of water, but of all kinds of substances (Simon & Glatzel 1929; Babb 1963a). It fits the curvature of typical melting curves well over a wide range of pressure, regardless of matter; however, it is empirical. Wagner et al. (1994) used them to describe the melting curves of pure water on behalf of the IAPWS. They fitted the parameters of Simon equations to the available experimental data of the ice phases I, III, V, VI and VII up to 20 GPa. It must be noted that the experimental basis of the ice III – equation is not as strong as in the case of the other ices, as the equation is only based on four data points given by Bridgman (1912).

The melting pressure of ice I (p_{mI}), ice III (p_{mIII}) and ice V (p_{mV}) can be calculated using the following internationally adopted equations. With modified parameters, the equations can be used to describe the melting curves of plant tissue material and solutions, like potato tissue (Schlüter 2003) or solutions of sodium chloride or sucrose (Guignon et al. 2005).

Ice I

$$\pi = 1 - \alpha \cdot 10^6 (1 - \theta^\beta) + \chi \cdot 10^6 (1 - \theta^\delta)$$

Equation 6

Ice III and Ice V

$$\pi = 1 - \alpha \cdot (1 - \theta^\beta)$$

Equation 7

α, β, χ, δ are fitting constants. The normalized temperature and pressure are defined as follows:

$$\theta = \frac{T}{T_n}$$

Equation 8

$$\pi = \frac{p}{p_n}$$

Equation 9

T and p are the variables, T_n and p_n are temperature and pressure value of the reference point.

Wagner et al. (1994) provided values of α, β, χ and δ for pure water. They fitted the equations to the pressure range between the respective triple points of the melting curves, so the range of validity is fixed and the equations may not be extrapolated to values beyond the triple points.

A simpler way to fit the equations to data of aqueous systems would be to shift the curves to lower temperatures according to the freezing point depression found at atmospheric pressure by modifying p_n and T_n and using the parameters of Wagner et al. (1994). However, it was shown that during high pressure – low temperature processing of these substances the existence and formation of high pressure ices in domains outside their regions of stability is quite common (Evans 1967; Luscher et al. 2005; Urrutia Benet 2006). This is especially true for the existence of ice I and ice V in the range of stability of ice III. Hence, it is necessary to adjust the equations to new ranges of validity by adjusting the fitting constants when making adjustments to other systems.

Schlüter (2004) used the Simon equation to fit experimental data of phase transition points of potato of ices I, III and V in the pressure range to 400 MPa. He suggested two different methodologies; fitting Simon equation to experimental data by calculating completely new parameters or shifting Simon equation with parameters of pure water to lower temperatures by just using a modified normalizing temperature, subtracting the freezing point depression obtained at ambient pressure from T_n. This second method is easy to use if it is assumed that the curvature of the melting line itself does not change, but is just lowered entirely. However, modifying T_n has also effect on the curvature. If the normalizing temperature is lowered by 10 K for example, the difference between the water curve and the shifted curve at 200 MPa is lowered by only 9.2 K. It should be mentioned that parameters derived for a specific temperature and pressure range cannot be shifted to other temperature ranges with the same results. Consequently, Schlüter (2004) obtained considerable better values for a completely new fit of parameters in the case of all three ices. As an estimation method, shifting the curves could be accomplished in a modified way by subtracting the freezing point depression from the final temperature values.

Guignon et al. (2005) provided plenty of data for the melting lines of ice I of sucrose and sodium chloride in a considerable concentration range. It should be noted that the experimental findings at temperatures under -20 °C are somewhat deviant from the expected values. They fitted Simon equations to their data and obtained good fits. However, it has to be stated critically that they used T_n and p_n as parameters to be fitted, whilst they are introduced in the equation as fixed reference points. Their purpose is to normalize temperature and pressure values to transfer them to a dimensionless value. Wagner et al (1994) used the triple points of water as reference points, including the triple point solid-liquid-gaseous for the ice I curve. Using these reference parameters as fit parameters is problematic and methodically incorrect, as the reference point is an anchor point through which the curve is running. Even though the triple points of the aqueous solutions are unknown, appropriate reference points should be fixed before calculation.

It is of course possible to find other equations, which describe the phase transition lines. Schlüter (2004) for example provides an equation with 20 coefficients to get even better results in terms of fit standard error. Polynomial equations are probably usable to some extent as well. Simon equations, however, are proven as state of the art for fitting equations of phase boundaries and have a quite simple structure.

2.2.6 Crystallization of lipids under pressure

It is important to understand the pressure crystallization of lipids with interest to food science as they are part of complex natural foods, like chocolate, meat, avocado or dairy products. While there is little interest to preserve foods by high pressure that are predominately lipids, it is useful to know the phase behavior of lipid domains in foods during pressure treatment. Furthermore, pressure application could open new possibilities in lipid processing e.g. by making use of pressure induced crystallization of specific fat crystal structures.

Already at ambient pressure the phase behavior of typical edible oils, shortenings or especially cocoa butter is quite complex as a number of distinct crystalline phases can be differentiated at ambient pressure, The most common of these crystal modifications are named α, β and β'. α-crystals are the most unstable form which often solidifies first when cooling rapidly. These crystals are described as platelets with little ordering and accordingly relatively little heat release during crystallization. Macroscopically they are described as coarse crystals of translucent, waxy appearance. β and β' crystals are more closely packed needles of higher ordering and more notable latent heat release during crystallization, which are macroscopically harder, opaque (white) fats. β' crystals are usually desired in shortening production due

to their smaller size which is smoother from an organoleptical point of view, while β crystals are the thermodynamically stable form (Bockisch 1993). The phase behavior in cocoa butter is even more complex and studied in depth because of the commercial importance of optimum smooth microstructure in chocolate. It was shown that α, β and β' crystals can be differentiated not only by DSC or NMR measurements but also during cooling by their temperature response which indicates a short discontinuity due to α crystallization and a more pronounced crystallization peak during β and β' crystallization (Wilton & Wode 1963; Riiner 1970). It should be noted that crystallization of fats is very different from the crystallization of water as triacylglycerides with a wide fatty acid distribution of differing saturation level and chain length do not have one precise crystallization point but yield macroscopically a temperature range in which the fat crystallizes (Bockisch 1993).

A number of studies revealed that fats and oils have the expected common behavior that the melting point increases due to pressure influence. Yasuda & Mochizuki (1992) examined the phase transitions of cocoa butter by pressure. They found solidification by observation in a pressure vessel with window. They also found cooling curves under pressure which resemble cooling curves at ambient pressure for α and β/β' – crystals (Wilton & Wode 1963; Riiner 1970). In another study, cooling curves in coca mass showed a crystallization peak similar to the α – peak. The solidification of soy oil, sunflower oil, triolein and cocoa butter was investigated by measurement of refractive index and viscosity (Kapranov, Pehl, Hartmann, Baars & Delgado 2003). Experiments in a DSC under pressure were reported for cocoa butter, copra oil and palm oil (Le Bail, Hayert, Rigenbach & Gruss 2002). The influence of crystallization on emulsified milk fat was also studied (Buchheim & Abou El-Nour 1992). All authors described the phase transition line under pressure as linear. However, quite a variation in results can be found if results of the same lipid are compared, e.g. about 10 K difference in crystallization temperature of cocoa butter. This variation can be attributed to the imprecise crystallization peak, the difference between melting and solidification temperature melting and the biological variation in foodstuff, but it has to be stated as well that distinctions between different crystal structures were not made. Hence, slight deviations from linearity were not detectable with these methods. In pure tricaprin and trilaurin, which have a precise phase transition temperature due to their pureness, the phase transition lines under pressure were curved (Yokoyama, Tamura & Nishiyama 1998).

2.3 Effect of high pressure and low temperature on biological matter

2.3.1 Pressure effects on reactions, protein and protein rich food

All chemical reactions consequently also complex reaction effects like protein denaturation, microorganism inactivation or the loss of meat color are altered in their reactions rates not only by temperature but by pressure as well. According to a comprehensive derivation provided by Heremans (2002) the temperature and pressure dependence of a reaction is given by

$$\frac{d\Delta G^0}{dT} = -\Delta S^0; \frac{d\Delta G^0}{dp} = \Delta V^0$$

Equation 10

G – Gibbs free energy, S – entropy, T – temperature, p – pressure, V – volume, superscript "0" indicates reference conditions.

A similar expression to the activation energy is the activation volume V_a which describes the effect of pressure p on reaction rate k:

$$-V_a = \frac{RTd\ln k}{dp}$$

Equation 11

Negative values of V_a indicate reactions accelerated by pressure, like the oxidation of unsaturated lipids. As a contrary example, Maillard reactions are retarded, due to a positive values of V_a.

From these derivations it can be concluded that the whole reactivity and decay reactions of food constituents are changed under pressure in contrast to heat treatments. In this way, thermal decay reactions frequently observed during thermal pasteurization are suppressed, however, it should be noted that other reactions may come to the fore which are not so important for thermal treatments at ambient pressure.

It is important to note that during a pressure treatment, the influence of heat cannot be neglected. The evaluation of a complete thermal history during pressure treatments cannot be omitted as temperature is having an effect on reactions as well. During practical treatments the temperature rises inevitably due to quasi-adiabatic compression. Due to anisotropic compressibility and heating, starting temperature and heat capacity, treatments at constant tem-

perature are an illusion. Pressure, temperature and treatment time must always be evaluated simultaneously, which is unluckily still not the case in a lot of high pressure experiments.

Of specific interest is the stability of proteins under pressure, or in other words, the reaction rates of their unfolding and aggregation. The change in Gibbs free energy as a function of pressure and temperature is given by

$$d(\Delta G) = -(\Delta S)dT + (\Delta V)dp$$

Equation 12

Integration (with neglecting terms of higher order) and insertion of the physical meanings of the integration constants gives finally a quadratic equation

$$\Delta G = \Delta G^0 - \Delta S^0(T - T_0) - \frac{c_p}{2T_0}(T - T_0)^2 + \Delta V^0(p - p_0) + \frac{\Delta\beta}{2}(p - p_0)^2 + \Delta\alpha(p - p_0)(T - T_0)$$

Equation 13

ΔG^0 – change in Gibb's free energy at reference conditions, ΔS^0 - change in entropy at reference conditions, c_p – heat capacity, ΔV^0 – change in volume at reference conditions, β - compressibility factor, α – thermal expansion factor.

This equation describes in general the stability area of a molecule with a two-phase transition (e.g. native protein – denatured protein), however it should be that not all transitions can be described completely by a simplified two-phase approach. The denaturation of protein was already reported by Bridgman (1914). This behavior is illustrated in Figure 2.11. Due to the quadratic nature of the function, the shape of the area of stability of the native protein is elliptical, but it must be borne in mind, that the exact shape, size, rotation and location of the ellipse is specific for the protein. This relation is not only valid for protein, but in principle for other reactions and biomolecules as well, like for example the transition of starch granules form crystalline to gelatinized (Buckow, Heinz & Knorr 2007). Besides Also the phase behavior of protein was experimentally verified and considerably extended to intermediate transition states etc. in numerous publications. As an introduction several reviews to the field are available (e.g. Heremans 2002; Smeller 2002).

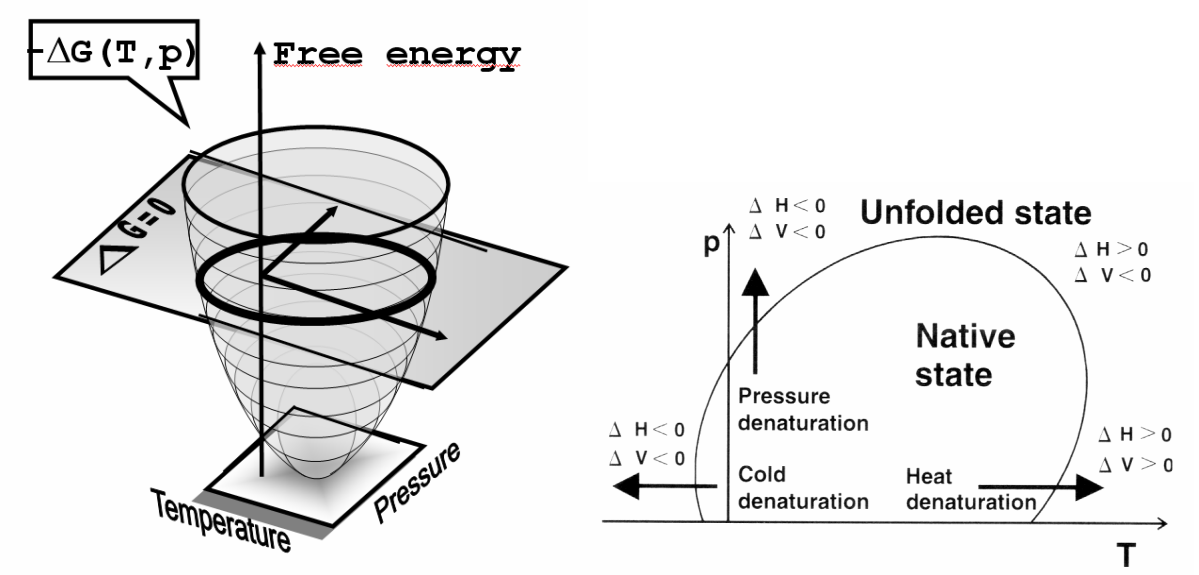

Figure 2.11 Pressure – temperature dependency of an idealized protein two-phase transition native-unfolded. Left: from Heinz (2002), right: from Heremans (2002).

Of special interest for high pressure – low temperature processes is the cold denaturation of biomolecules, especially proteins, which is facilitated under pressure due to the freezing point depression of water. For proteins the cold denaturation at high pressure was frequently confirmed by experimental results from biophysical researchers (reviewed by Kunugi & Tanaka 2002), but also for lactoglobulin aggregation (Kolakowski, Dumay & Cheftel 2001) . Pressure-induced protein gelation (Dumoulin, Ozawa & Hayashi 1998) at subzero temperatures in liquid water conditions was shown as well. The inactivation of food related enzymes, especially Lipoxygenase, was frequently reported at subzero temperatures (Indrawati, van Loey, Denys & Hendrickx 1998; Indrawati, Van Loey, Ludikhuyze & Hendrickx 2000; Indrawati, Ludikhuyze, Van Loey & Hendrickx 2000; Indrawati, Van Loey, Ludikhuyze & Hendrickx 2001), but other enzymes were examined (Kinsho, Ueno, Hayashi, Hashizume & Kimura 2002).

Typical high pressure – low temperature food processes include not only pressure treatment at subzero temperatures before freezing or after thawing, but they also include stress due to freezing, either before the pressure thawing experiment or during pressure supported freezing. Due to this double influence, it is not possible to clearly separate the effects, however typical pressure effects on meat or fish were detected especially in low temperature processes. Besides texture changes, changes in drip loss (more or less drip, depending on protein denaturation) and changes in color were frequently observed. Changes in meat color can generally be associated with changes in the myoglobin structure, which makes up most of the natural flesh

color (Mackie 1993). Myoglobin is a single-chain globular protein, containing a heme (iron-containing porphyrin) prosthetic group in the center. Its natural color depends on the charge of the iron ion. Cheftel & Culioli (1997) pointed out that during pressure treatment at temperatures above zero, two different mechanisms of color loss can be differentiated: (1) "whitening" due to the denaturation of the protein part (globin) at 200 to 350 MPa and/or release of the heme group and (2) the oxidation of ferrous myoglobin to ferric metmyoglobin, above 400 MPa, resulting in grey or brown discoloration. Due to the low pressure level with a maximum of 210 MPa in most food freezing and thawing experiments it can be assumed that the whitening effect dominates which is in agreement with color measurements made.

Chevalier et al. (1999) examined the protein changes in fish during pressure thawing and found changes in electrophoretic profiles and changes in drip, which means changed water binding capacity of proteins. Fernandez-Martin et al. (2000) found denaturation of pork and beef muscle protein during pressure shift freezing as detected by DSC, color and texture. Préstamo, Palomares & Sanz (2005) found denaturation of enzymes in potato during pressure shift freezing. Atlantic salmon (Zhu et al. 2004; Alizadeh et al. 2007) and sea bass (Tironi et al. 2007) was examined and unfavorable whitening, drip and texture changes after pressure freezing and thawing processes were found, also DSC and electrophoresis was used. Schubring et al. (2003) also examined color and texture after cooking of high pressure thawed samples of various fish species and found in most but not all species surprisingly reduced toughness after cooking of pressure thawed samples, while they were tougher before cooking. Color differential values were varying after cooking, however, cooking caused most of the color change in the majority of samples. In summary, denaturation was demonstrated in all protein rich samples. Quantitatively, often a threshold of 100 or 150 MPa was reported above which the quality changes were more detrimental. However, it is difficult to separate low temperature and pressure effect, as during high pressure – low temperature processes the temperature is decreasing with increasing treatment pressure.

2.3.2 Inactivation of microorganisms by pressure

The specific effects and damages of pressure on vegetative microorganisms are complex and cannot be evaluated detached from heat effects. Bacterial endospores are far more resistant and are usually not affected by pressure in the range to 600 MPa which is of specific interest within this study (Heinz & Knorr 2002).

High hydrostatic pressure is a physical preservation method to which a number of influencing factors that must be taken into account. These factors are pressure effects on water, adiabatic

heating and heat transfer, food composition and factors related to the microorganisms. Heat resistance of microorganisms is related to the stability of their components, which are mainly DNA, RNA, enzymes and other proteins, cellular membranes, ribosomes and the cell wall. This insight is of course not restricted to pressure, the same is true for other physical preservation methods like thermal processing. This summary follows a review by Smelt, Hellemons & Patterson (2002), which refers to vegetative microorganisms.

Pressure effects can be summarized as follows:

- *Morphological changes.* Bacteria usually remain unchanged, while changes in cell size and morphology after pressure treatment of yeast cells were observed.
- *Stress response.* Pressure is a stress event for microorganisms, to which they respond like in the case of heat or cold stress, low pH etc. However, it is not known whether they possess a specific stress response to pressure. After sublethal pressure treatments, the expression of numerous proteins which are known from other stress responses was observed. Exposure to another stress before pressure treatment or pressurization at low before influence of other stresses therefore influences the survival sometimes considerably.
- *Proteins and enzymes.* Like in the case of proteins, microorganisms often exhibit a similar oval stability diagram under pressure. The findings suggests a strong correlation of enzyme inactivation with high pressure inactivation. However, it is difficult to relate the pressure inactivation to one specific target enzyme, as isolated damaged enzymes can be repaired by the cells. Instead, it is reasonable to assume that the combined complete or partial inactivation of numerous enzymes and metabolic pathways leads in summary to cell death, which is defined as the inability to proliferate.
- *Membranes.* Membrane damage is besides enzyme inactivation usually considered as one of the main events related to cell death. Membranes undergo phase transitions and solidify under pressure, making perturbations more likely (Winter & Czelik 2000). Pressure also leads to the detachment and inactivation of membrane proteins (Ulmer, Herberhold et al. 2002).
- *pH.* The maintenance of intracellular pH is crucial for the survival of cells. Some authors related cell death predominantly to intracellular pH changes, which are however related to inactivation of enzymes controlling the acidity and membrane damages.
- *Ribosomes.* The disintegration of ribosomes in their subunits is promoted by pressure and may be related to cell death.

- *Nucleic acids.* Condensation of DNA and RNA was found by pressure, however, at higher pressures than inactivation. Pressure induced damages in combination with the inactivation of repair systems might be able to knock out the genetic multiplication process essential to proliferation.

One of the most important extrinsic factors to cell survival of pressure treatments is of course the food composition. Acidity, water activity and the presence of antimicrobial compounds are the main factors. It was also shown that the presence of antimicrobial compounds during pressure indicated transient perturbations of the membrane which vanish after the pressure treatment.

During pressure treatments microorganisms are subject to a rather smooth transition from the viable to a "death" state with many intermediate injured states which are potentially able to recover depending on the medium. On the other hand, a large fraction of cells can be excluded from growth by selective media exerting an additional stress. It was shown that flow cytometry is a potent tool to gain new insights in the states and mechanisms of cell damage of pressure treated microorganisms (Ananta, Heinz & Knorr 2004). Flow cytometry is based on the evaluation of a cells, singularized in a sheath flow. The cells scatter a laser beam, the scattered light is collected by optical sensors. It is possible to stain cells with fluorescent markers, which bind specifically to certain cell structures, and evaluate the fluorescent color of each individual cell. It is in this way possible to gain more insights with specific test which provide more insight in cell damage mechanisms than a simple live-death assay by plate count.

Listeria, as the major object of investigation in the present study, was often studied by the pathogenic species *Listeria monocytogenes*. After 15 minutes at ambient temperature, at 500 MPa 1 to 3 log cycles were inactivated, at 600 MPa already more than 6 log (Smelt et al. 2002). It was shown, that the pressure tolerance of *Listeria innocua* is within the range of variation of pressure tolerance of different *L. monocytogenes* strains (Tay, Shellhammer, Yousef & Chism 2003). Only a weak correlation of heat resistance and pressure resistance was found in 80 strains of *L. monocytogenes* (Smelt et al. 2002) making pressure resistance of a specific strain difficult to predict. The evaluation of 13 metabolic enzymes revealed that some enzymes were already inactivated at much lower pressure levels of 200 MPa, which is obviously only a repairable damage (Simpson & Gilmour 1997). It was furthermore shown, that cold shock proteins were induced in *L. monocytogenes* at low temperature as well as after low pressure treatment (100 to 200 MPa), indicating similarities in the stress response to pressure and cold (Wemekamp-Kamphuis, Karatzas, Wouters & Abee 2002).

2.3.3 High pressure – low temperature combinations

Like already mentioned, in the high pressure area at subzero temperatures without freezing, a number of studies confirmed that the elliptical shaped denaturation curves of proteins and enzymes may be extended to the inactivation of microorganisms. In an early work Takahashi (1992) compared the inactivation at -20 °C under pressure to +20 °C and found somewhat better inactivation at the low temperature, however he did not check for phase transition during treatment. Hashizume, Kimura & Hayashi (1995) showed high pressure – low temperature inactivation behavior in detail for *Saccharomyces cerevisiae* down to -20 °C, in model solutions but also in strawberry jam (Hashizume, Kimura & Hayashi 1996). Perrier-Cornet et al. (Perrier-Cornet, Tapin & Gervais 2002; Perrier-Cornet, Tapin, Gaeta & Gervais 2005) confirmed the high pressure - low temperature inactivation of *S. cerevisiae* and *Lb. plantarum*, but in their interpretation they attributed these effects mainly to differences in water structure (compressibility) and also to the cell membrane rather than to protein denaturation, which seems to be arguable. From the same group, an examination of *E. coli* showed that additives like glycerol can counteract the low temperature inactivation (Moussa, Perrier-Cornet & Gervais 2006). Some of these examinations touch the ice range during their experiments which was usually taken into account, however, there are sometimes examinations that are difficult to evaluate, due to incertain phase transitions (for example Yuste, Pla, Beltran & Mor-Mur 2002).

The state of water is different in some food science studies where the inactivation during typical pressure supported freezing or thawing experiments was studied. All found better inactivation at higher pressure and lower temperature. Picart et al. studied pressure induced thawing and pressure shift freezing of smoked salmon and found inactivation of several bacteria, including *L. innocua* (Picart, Dumay, Guiraud & Cheftel 2004; Picart et al. 2005). Le Bail et al. (2003) and Schubring et al. (2003) found inactivation during pressure induced thawing as well. All these studies show interesting results of inactivation that can be seen as a positive side effect of pressure phase transitions, even though treatment conditions were not sufficient to obtain pasteurization.

In an approach quite different from technical pressurization by a pump, it is also possible to generate pressure by the expansion of water in a closed vessel during freezing. It was shown that using this approach 140 MPa at -15 °C to -22 °C can be generated (Hayakawa, Ueno, Kawamura, Kato & Hayashi 1998). Various microorganisms were treated for 24 h and several logs of inactivation were achieved. Another group used the same approach (Malinowska-

Panczyk, Kolodziejska, Dunajski, Rompa & Cwalina 2004) and obtained even 193 MPa and showed considerable inactivation (several logs) already after 30 minutes. The simple setup of this approach is interesting and should attract more interest in the future.

In ice, however in a completely different pressure and temperature range, microbial activity was reported in ice VI at 1.7 GPa (Sharma, Scott et al. 2002), however, the results are highly questionable (Yayanos 2002).

2.3.4 Disintegration by pressure phase transitions

Edebo & Hedén (1960) showed that phase transitions between ice I and ice III can be used as a disintegration method for suspensions of cells. They disintegrated *E. coli* by passing the ice I – ice III boundary at -25 °C and were able to attribute the cell disintegration clearly to the ice phase transition. It was also shown that ice III – ice V transitions did not have a pronounced effect on the cells, due to lower volume changes.

In later works, this idea was used to design a freeze press which was called the X-press. It basically extrudes ice through a whole by applying high pressure (Edebo 1960). It is used for disintegration of cells or particles of any kind without thermal load. Also other freeze presses are described in literature (Scully 1974). The feasibility of this concept was shown for a wide range of press sizes and applications (Magnusson & Edebo 1974; 1976a; 1976c; 1976b). Concerning freeze presses, it is often argued that the ice I – ice III transition is the major cause of the disintegration. However, the thorough discussion of the authors shows that also other factors are responsible for the disintegration which are shearing between ice I crystals during extrusion and pressure gradients within the cells due to applied pressure and pressure gradient (Edebo 1960). The most interesting study showed pressure and temperature measurements which demonstrated a parallelism to curves obtained in food science studies for pressure induced thawing (Magnusson 1977a). It is likely that partial thawing of ice I facilitates the extrusion of ice with liquid water as a "lubricant". Furthermore the high concentration of cells, which is described as a paste, indicates that a high amount of water is unfrozen in this temperature range. It can generally be noted that the formation of ice III in these presses is strongly related to extrusion temperature, however, the dynamic extrusion concept makes precise measurements as well as comparisons with pressure treatments in a closed pressure vessel virtually impossible.

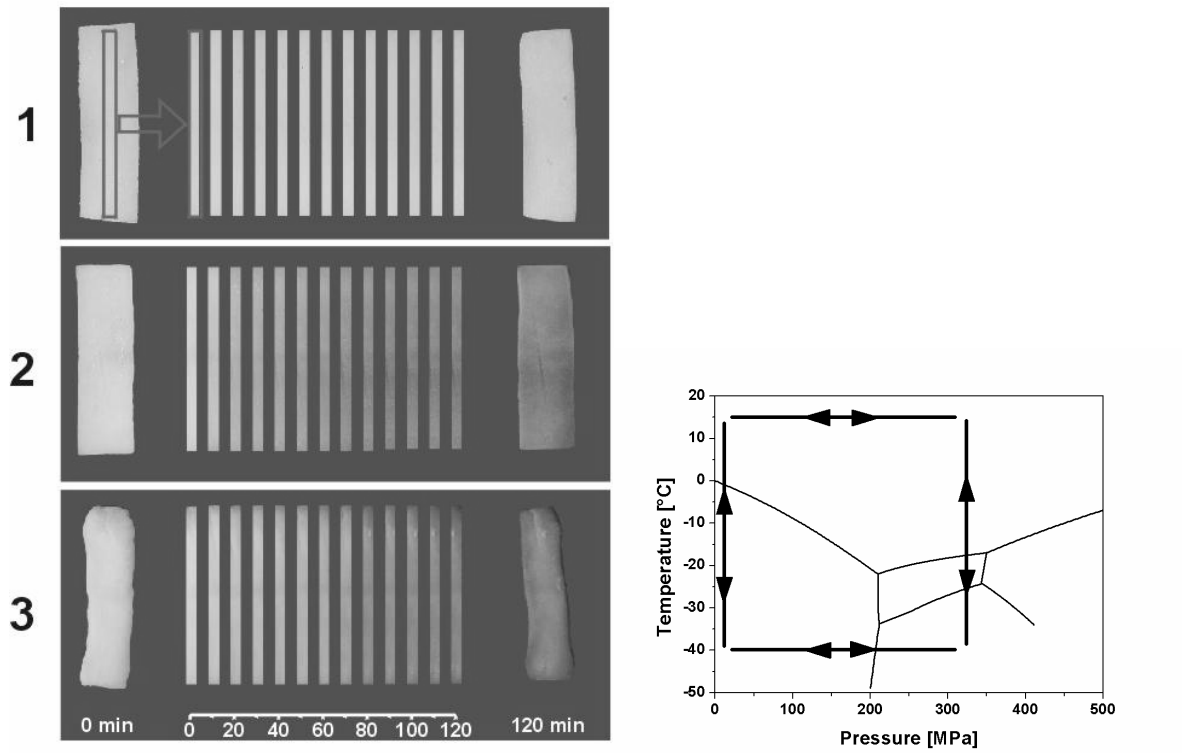

Figure 2.12 Left: Influence of ice I – ice III phase transitions on potato samples. Cylinder cut in the middle and observed for 120 minutes, as indicated by the middle stripe of the samples. Right: treatment diagram. (1) Untreated sample; (2) Sample frozen to -40 °C, pressurized to 320 MPa (ice III), thawed at that pressure and decompressed, counter clockwise cycle in treatment diagram; (3) Sample pressurized at ambient temperature, frozen at 320 MPa (ice III) to -40 °C, decompressed (ice I) and thawed at ambient pressure, clockwise cycle in treatment diagram. Modified from Luscher et al. (2005).

Like discussed earlier, the main problem if freezing food to ice modifications III, V or VI is transformation to ice I during decompression. A striking illustration of this behavior is shown in Figure 2.12. It can be concluded that the massive volume expansion in the frozen structure leads to disintegration of the tissue sample, while the shrinkage during compression to ice III causes considerably less damage. Similar derivations can be made from the experiments by Fuchigami et al. which show frequently that depressurization after freezing to ice V or VI leads to microstructure and texture damage (2002; 2003a; 2003b; 2006).

A different approach, which is summarized briefly, is the treatment of previously frozen food by pressure in order to use the effects of the phase transitions. Shen et al. (2005) found inactivation of vegetative Bacillus subtilis cells after ice I – ice III phase transitions and qualitatively confirmed the results shown in this thesis later. Fernandez (2007b) et al. examined treatments of frozen meat. They extended the pressure treatment to the ice VI pressure range at 650 MPa and found inactivation of about 2 log and no markable change of meat quality

parameters. Serra et al. (2007a; 2007b) treated frozen hams chilled in solid CO_2 in industrial pressure vessels (150 to 320 l vessel volume) without temperature control to avoid color changes during high pressure treatment. However, the temperature of the pressure medium was above 10 °C and the cycle time was 17 minutes and longer, so thawing at least of the outer zone of the ham is probably. Van Buggenhout et al. (2006c) examined the inactivation of enzymes during high pressure – low temperature treatment but found only little inactivation. Due to the measured temperature, most likely thawing of most of the sample occurred during the pressure cycle. Further results of the high pressure – low temperature treatment publications are discussed in depth in relation to the experimental findings presented later where appropriate.

3 Materials and Methods

3.1 Experimental units

3.1.1 Laboratory scale pressure vessel

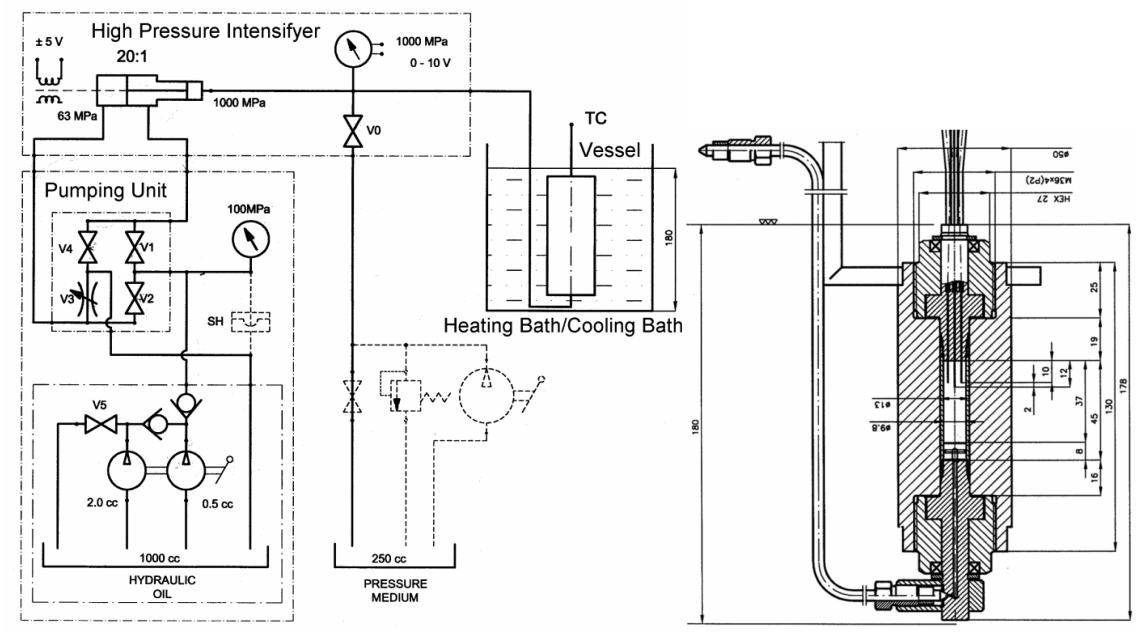

Figure 3.1 High pressure unit for laboratory scale experiments Unipress "U111 type". Left: installation scheme of the whole unit; right: cross-sectional view of the pressure vessel.

The high pressure unit used for most experiments was a special design of Unipress (Warsaw, Poland) for phase transition measurement purposes as it is shown in Figure 3.1. The dimensions of the pressure vessel are close to the dimensions of the U111 multi-vessel system, so it is named U111-type by the manufacturer. The system consisted of a manual pump connected to the pressure intensifying unit with a closed hydraulic oil circuit. The hand pump had a maximum pressure of 63 MPa with a switchable stroke of either 2.5 ml for fast pressure built-up at low pressure (to about 200 MPa in the pressure vessel) or 0.5 ml for further pressure built-up. An analog pressure indication monitored the hydraulic oil pressure during experiment. Precise pressurization as well as fine pressure release by a special release valve (V3) was possible.

The hand pump was connected to a 20:1 pressure intensifying unit, which also included the pressure gauge (EBM 6045-1000, Erich Brosa Messgeräte, Tettnang, Germany) and an inductive piston position measurement (PIZ100, Peltron, Poland). The unit was connected to the pressure vessel by a bent pressure capillary to allow complete immersion of the pressure ves-

sel in a bath. The copper-beryllium pressure vessel was connected to the pressure capillary at the lower plug, while the upper plug was opened to introduce samples and thermocouples into the internal space of the vessel. The pressure vessel was able to operate up to 1 GPa in a temperature range of -50 °C to 150 °C.

The high pressure transmitting medium was silicone oil (Huber type 6165, Offenburg, Germany) which was liquid in the desired pressure and temperature range (-50 °C, 700 MPa at ambient temperature). It was pre-pressurized before pressure built-up by an external hand pump (dashed in Figure 3.1) to allow efficient pressurization despite gas inclusions.

The vessel was operated with different set-ups of plugs which include sample holders and thermocouple apertures. The setup shown in Figure 3.1 included a sample holder with a moveable piston as a pressure transmitting plug to the bottom of the sample room. It was designed for phase transition experiments under pressure and it was used with a plug with three thermocouples type K with a diameter of 0.5 mm as shown in the figure. The two lateral thermocouples were bent to the vessel wall to record the lateral sample temperature in two places. The volume of the liquid sample was 2.79 ml (9.8 mm diameter, 37 mm length). In another setup the system was usable without the sample holder allowing an internal volume of the sample space of 5.97 ml (13 mm dia, 45 mm length). One thermocouple type K was used with this setup, protruding into the sample room with a thermocouple diameter of 0.5 mm or the same with a more robust thermocouple diameter of 1 mm. When treating samples without temperature control inside the sample, a shorter thermocouple with diameter of 1 mm was used, this measured the temperature of the silicone oil at the upper edge of the sample room.

The system was characterized by good volume ratio of sample under pressure to total volume under pressure. In this way, all changes in volume of the sample or the silicon oil directly caused changes in the system pressure. The measuring devices were able to completely monitor the experiment, especially due to the piston position measurement, which made it possible to separate internal influences to the pressure (e.g. from phase transition) from external manipulation (e.g. from pressurization or pressure release).

3.1.2 Pilot plant scale pressure vessel

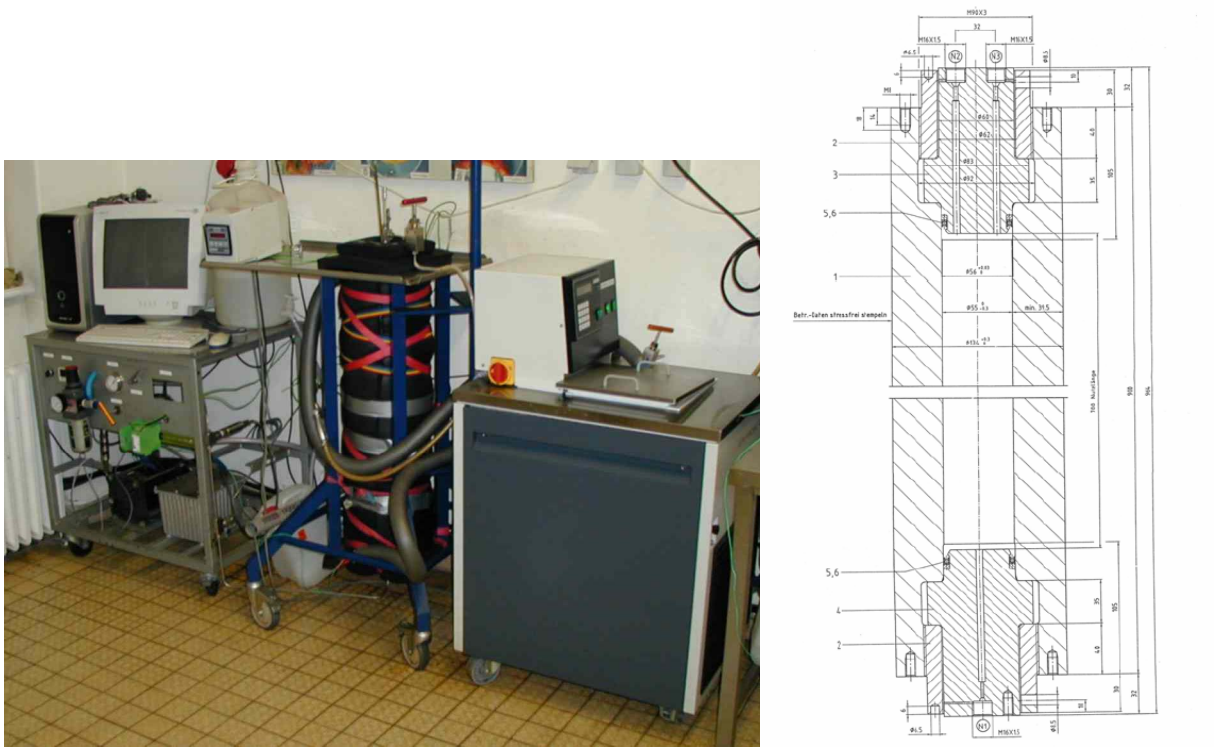

Figure 3.2 Uhde high pressure unit for pilot plant experiments, internal volume 1.66 l, with isolated heating/cooling jacket. Left: installation in the lab with cryostat Lauda RUK-50D; right: cross-sectional view.

For experiments with larger samples the Uhde high pressure vessel as shown in Figure 3.2 was available. The steel vessel had an internal diameter of 55 mm and a length of 700 mm, yielding an internal volume of 1.66 l. It was designed for use at a maximum of 360 MPa at subzero temperature to -40 °C. Silicone oil as specified above was used as the pressure transmitting fluid. A Haskel (California, USA) air driven pump DXS HF-602 was used for pressurization. For temperature control the whole pressure vessel was equipped with a heating/cooling jacket through which silicone oil (Huber, type 6163) was pumped by a cryostat Lauda RUK 50-D (Lauda, Germany). The jacket was externally isolated by a 50 mm layer of insulating foam Armaflex (Armacell, Münster, Germany). The upper plug of the vessel was opened to enter samples, two apertures for type K thermocouples (diameter 1 mm) were provided. Pressure was measured at the capillary before the pressure vessel by a pressure gauge Intersonde HP28 (Watford, UK).

3.1.3 Measurement devices

Measurement of both systems were carried out using measurement hardware STB-PC and RTI-820 for analog/digital input/output which provided an exact measurement frequency of

maximum 10 Hz to all probes. The values were all recorded in a personal computer and shown during the experiment. All thermocouples were of type K, however, different sources of thermocouples were used for the different setups as indicated. Additional thermocouples were used to measure temperatures of the cryostat or the outer vessel wall temperature. To realize precise temperature measurements appropriate grounding of all equipment was realized, however, most cables were not shielded and had connection plugs in the thermocouple wire, which is not completely ideal. Temperature calibration over the whole temperature range of the measurement was frequently carried out to check for deviations. If necessary, additional functions for correction of deviations were introduced to the software. Pressure gauges were repeatedly cross-checked with at least two other pressure gauges of EBM that were available. Pressure calibration was never necessary.

3.1.4 Freezing equipment

For most of the freezing experiments the aforementioned cryostat Lauda RUK-50 D was used. For immersion of the lab scale pressure vessel, it was deep enough and had a big enough volume to provide constant temperature down to -50 °C after immersion of the vessel. It was deep enough to completely cover the vessel. In the case of the Uhde pilot plant setup, after overnight cooling a temperature of -40 °C was realized inside the pressure vessel, however, during an experimental day the temperature was usually maintained at about -35 °C. For some additional lower temperature experiments a Haake K75-DC5 (now Thermo Scientific, Karlsruhe, Germany) cryostat was used with a minimum temperature of -60 °C. Other cryostats/thermostats were available for other tempering purposes, e.g. in thawing experiments. All cryostats and thermostats were operated with silicone oil Huber 6163.

For frozen storage experiments a walkable freezer at -20 °C (Linde, Germany) was used. For storage at -40 °C a Weiss WK1-180/40 (Reiskirchen, Germany) multipurpose storage cabinet was used. Storage at -80 °C was carried out in a frozen storage cabinet U101 for microbial cultures from New Brunswick Scientific (Hatfield, UK). All storage devices held the temperature ± 1 K.

3.2 Objects of investigation

3.2.1 Microorganisms

3.2.1.1 Relevance and characterization of the test species

Listeria innocua BGA 3532 was selected as a usually non-pathogenic representative of the *Listeria* genus, however it is pathogenic itself in rare cases (Perrin, Bemer & Delamare 2003). It was used for most of the experiments. *L. monocytogenes* is the more potent pathogenic species with a relatively low number of cases, but a high mortality. It is especially dangerous for people with immune deficiency including unborn children. In 2002 in Germany 237 cases of Listeriosis were reported with a mortality of 12 % (Robert-Koch-Institut 2003). Both species show comparable characteristics, they are Gram positive, facultative anaerobic rods. Their optimum growth temperature is 30 to 37 °C, however, they can also grow close to the freezing point. So they are psychrotolerant, which is a major characteristic of interest with regard to low temperature preservation (IIR 1998). *L. innocua* is ubiquitous, *L. monocytogenes* infections are related to meat, raw milk, raw milk products (soft cheese) and salads.

Escherichia coli K12 DH5α was selected as second major test organism. It is an ubiquitous specie commonly known as fecal indicator, some strains are known as food borne pathogens e.g. enterohemorrhagic *E. coli* O157:H7. It is a Gram negative, facultative anaerobic rod. *E. coli* is one of the most common bacteria, food borne infections can be related to all kinds of substrates, however, ground beef, raw milk and contaminated water are the main sources.

Pseudomonas fluorescens DSM 50090 was selected as a meat related spoilage organism. It is a psychrotolerant Gram negative, aerobic rod. *Saccharomyces cerevisiae* was selected to compare inactivation with eukaryotic yeast cells, which are larger than bacteria by a factor of about 10. It is a facultative anaerobic germinating organism, which is producing ascospores. Spores of *Bacillus subtilis* were used as a test organism for bacterial endospores, which were bought as a bacterial suspension. *Bacillus subtilis* is an aerobic, Gram positive rod.

Lactobacillus rhamnosus GG ATCC 53103 (LGG) represents a probiotic organism which is a gram-positive lactic acid bacterium. In freeze stress experiments it represents microorganisms susceptible to freezing, but it is also an organism which is interesting for living preservation due to its probiotic nature. All microbial data based on Schlegel (1992).

3.2.1.2 Preparation of microbial suspensions

L. innocu, P. fluorescens and *E. coli* from a storage culture were grown in 20 ml standard I broth on an incubator for 24 h at 30 °C and 120 turns per min. A dilution to 10^3 cfu/ml (10^2 cfu/ml for *E. coli*) was made in Ringer solution and 20 µl of this solution was used to inoculate another 20 ml of standard I broth which was incubated at the same condition. After that time cells were in the stationary growth phase. Growth curves of the organisms were established before (Schlüter 2003). The culture was centrifuged at 5242 g for 15 min (*E. coli*: 10 min at 2773 g). The pellet was washed twice in 0.01 M phosphate buffer saline (PBS) and resuspended in PBS buffer for standard inactivation experiments with a cell count of about $4*10^9$ cfu/ml of *L. innocua* and 10^{10} cfu/ml of *E.coli*. Further dilution steps were carried out in PBS according to the initial cell count used as noted for the experiments. For flow cytometry experiments the pellet was resuspended in 4 ml 0.05 M PBS to obtain an optical density of 10.

S. cerevisiae was grown in 20 ml wort broth for 48 h at 30 °C and 120 turns per min, diluted like the bacteria, but 40 µl were used to incubate another culture of 20 ml wort broth, incubated at the same conditions. The centrifugation was carried out at 2123 g for 10 min, to obtain a final cell count of 10^8 cfu/ml in PBS. *B. subtilis* spores were available in distilled water at a concentration of 10^{10} cfu/ml. They were diluted in PBS to obtain a culture of 10^7 cfu/ml.

LGG was grown in 5 ml MRS broth at 37 °C for 24 h without shaking. After the first incubation it was diluted by transferring 90 µl in in 9.1 ml Ringer solution. 50 µl of this dilution were taken to inoculate 50 ml MRS broth again at 37 °C for 24 h without shaking. Centrifugation was 10 min at 2773 g with double washing. All materials were obtained from Merck (Darmstadt, Germany).

3.2.2 Solutions and foodstuff

Sterile PBS with pH 7 was mixed in the laboratory from 0.01 M K_2HPO_4, 0.01 M KH_2PO_4 and 0.15 M NaCl. All chemicals were obtained from Merck.

Sucrose and NaCl in laboratory grade purification were dried overnight in a cabinet desiccator to obtain waterless substance. The solutions were prepared as weight per volume (w/v) solutions with distilled water by weighing the substance with an accuracy of 0.001 g in a flask and filling with water to 100 ml. Later the concentrations were calculated as weight per weight according to Table 4.1. The following masses were used: 5.148 g NaCl, 10.208 g NaCl,

25.130 g Sucrose, 50.108 g sucrose. Liquid dimethylsulfoxide (DMSO) containing 0.5 % water was mixed with distilled water to obtain the concentration used in the experiments.

Stearic acid and palmitic acid were obtained from Merck. Palmin (Unilever Germany, Hamburg) was used as hydrogenated copra fat and bought in a local supermarket. Partly hydrogenated rape seed fat was obtained from a fat refinery (Fettraffinerie Brake, Germany). The iodide value was 86 and the melting point according to standard procedures of the German Association of Fat Science was 24 °C.

Dilutions of baby food were made from baby food carrot puree "Früh-Karotten" (Hipp, Pfaffenhofen, Germany) which does not contain other ingredients, especially no salt. Pork *musculus longissimus dorsi* was bought as a whole piece at the experimental day in local supermarkets, which have fresh quality meat. Ground beef was bought fresh every experimental day at a local supermarket. Ice cream was "Sanobub Vanille" (Humana Milchunion, Everswinkel, Germany).

For inoculation baby food and thawed ice cream were inoculated with PBS to obtain a level of 10^7 cfu/ml and mixed. Ground beef was homogenized in a Stomacher 400 (Seward Medical, London, UK) two times for 120 seconds at the low speed setting.

3.3 Experimental procedure

3.3.1 Determination of phase transition lines

Phase boundaries of liquid model solutions were determined by using the setup of a metal sample holder with moving piston and three thermocouples as shown in Figure 3.1 and described there. The sample was filled in the sample holder and fixed to the plug. The setup was inserted in the pressure vessel at ambient conditions and closed. The sample was pressurized to the desired value and the vessel was immersed in a bath temperature that was set to a temperature about 20 K above the expected phase transition point and temperature equilibration (+- 1 K) was awaited. Then the vessel was immersed in a cold bath set 20 K below the phase transition line and the measurement was started.

During the cooling time and phase transitions, pressure was controlled by the hand pump and the special pressure valve to obtain ideally constant pressure values. After freezing the same sample was put again in the warm bath for the melting experiment in the same way.

After the experiments the phase transition point was derived like shown in Figure 3.3. Ideally freezing temperature and melting temperature should be identical, which was not always the

case like discussed with the results. The nucleation temperature was defined as the lowest temperature before rising of the temperature to the freezing temperature. Freezing temperature was defined as the highest temperature after nucleation or, if appropriate, the temperature of the plateau, if a constant plateau existed. The melting temperature was defined as the inflection point of the temperature during thawing, if a sharp inflexion point was found, alternatively the slopes of the temperature values before and after the melting point were extended, to estimate the melting point.

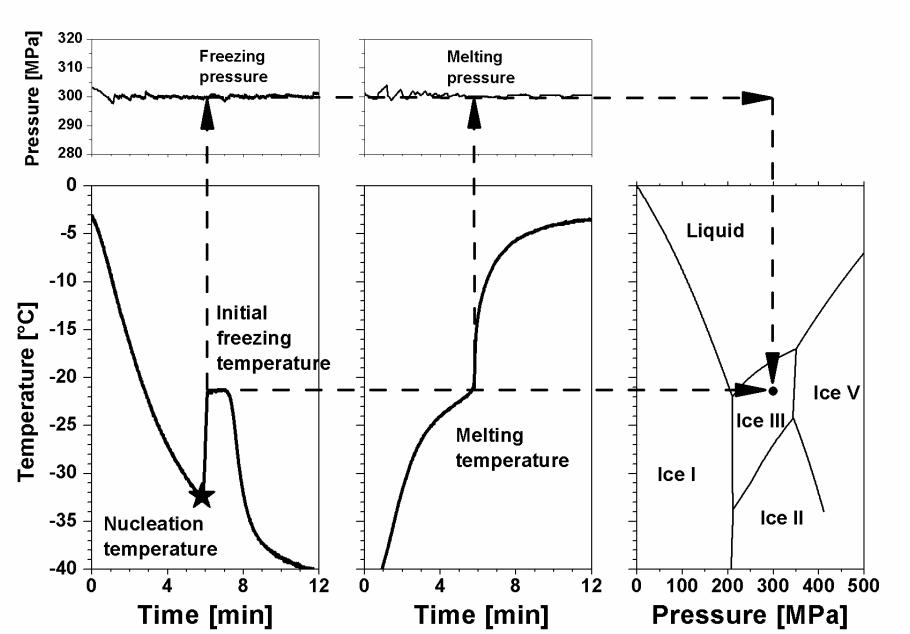

Figure 3.3 Example for the determination of phase transition points under pressure in food.

3.3.2 Phase transition lines of lipids

Complex lipids (hydrogenated rape seed fat and hydrogenated copra fat) were tempered to the desired starting point and cooled under pressure in the lab scale pressure system by programmed cooling of the cryostat. The pressure was not manipulated to follow monitor changes in system volume due to solidification. Definitions of phase transition points are found in the results section.

Pure fatty acid were investigated by pressure manipulation technique according to methods described for water freezing (Schlüter 2003; Guignon et al. 2005). This was feasible as pure fatty acids had a temperature plateau like water (see results). Samples were cooled by immersion in a cryostat that was set at a temperature close to the expected solidification point. After beginning of crystallization the sample was pressurized in steps of 10 or 20 MPa and equili-

bration for at least 10 seconds was awaited before making the next step. Towards the end of crystallization the sample temperature decreased and left the phase transition line. Special care was taken to measure reproducible temperature values by overlapping pressure manipulation cycles, so that all transition points were always determined by points at the beginning and in the middle of the experiment. Two reliable values were determined per pressure step.

3.3.3 Treatment of biological matter

For freeze stress experiments evaluated by flow cytometry, microbial suspension of *Lactobacillus rhamnosus* GG and *Listeria innocua* in PBS were prepared at an inoculum level of $5*10^7$ cfu/ml. About 30 to 40 ml of suspension were filled in Greiner centrifuge tubes (30 mm diameter, 115 mm length) with a screw plug. Samples were frozen at -20 °C in a cabinet (Weiss) with moved air or by immersion in silicone oil in a cryostat (Lauda) at -40 °C. A third group of samples was frozen by immersion in liquid nitrogen. After freezing, samples were stored for 1 to 100 days at -20 °C (walkable freezer), -40 °C (Weiss cabinet) or -80 °C cabinet (New Brunswick Scientific cabinet). Freezing equipment is defined above. Temperature fluctuations due to normal operation (opening for other samples) were possible. Duplicates of all treatment and storage conditions were processed and analyzed. After storage samples were thawed by immersion in a +20 °C thermostat (Lauda). After thawing, samples were centrifuged and the pellet of microorganisms was dissolved in less PBS 0.05 M to obtain an optical density of 10 which was necessary for flow cytometry analysis. Separate dummy samples were used to evaluate freezing profiles.

Liquid samples for high pressure – low temperature treatments were usually poured in a cryovial (Nunc CryoTube 1 ml, Wiesbaden, Germany) filled above the nominal volume almost completely with a head space estimated according to the expected treatment and phase transitions. However, during solid-solid phase transitions (ice I – ice III) this was not feasible as they were breaking. Instead a small pouch was prepared from aluminum-polyethylene composite film which was heat sealed on three edges, filled and heat sealed on the fourth side. There was no influence on bacteria due to the heat sealing, which was checked. This procedure was also carried out for food samples in the lab scale pressure system. The treatment volume obtained was about 1 ml. Samples were introduced in the cold vessel, after 15 min temperature equalization the system was pressurized and pressure was released according to the treatment time.

For pilot scale experiments bigger pouches with the same composite material were prepared. For 50 ml samples of microbial suspension an even and regular shape was desired. A tube of

steel with an internal diameter of 40 mm was cut in pieces of approximately 50 mm length. The lower end was closed with Parafilm, the cylinder filled with water, covered, and frozen in an air freezer. To retrieve the sample the cylinder was heated shortly to obtain surface thawing, the sample was than packaged in a pouch and frozen again.

For treatment appropriate temperature equalization times were used. For treatment at low temperatures the volume of the vessel was filled with precooled pressure transmitting fluid before closing the vessel to minimize the effect of adiabatic heating and warm liquid flowing in due to pressurization.

After treatment samples were sometimes stored in the frozen state before analysis, but analysis was always on the same day. Thawing of samples was carried out at room temperature in a water bath.

3.4 Analyses

3.4.1 Microbial methods

Suspensions of *L. innocua, P. fluorescens, B. subtilis* and *E. coli* were plated on nutrient agar (Oxoid, Basingstoke, UK), LGG was plated on MRS agar (Oxoid), *S. cerevisiae* was plated on wort agar (Merck). Plates were incubated at 30 °C for 48 h, *E. coli* usually only 24 h. LGG was incubated in anaerobic conditions at 37 °C for 48 h. Samples were plated in triplicate. The initial cell count was determined in triplicate each experimental day.

The dilution was usually carried out in microtiter plates (type 96 U) of 300 µl to be able to process more samples and also due to the small sample volume obtained from pouches in lab scale experiments. Food samples were first diluted and suspended in 9.1 ml Ringer solution for the first step. The feasibility was checked for a number of treatments as it is shown in Figure 3.4. The results indicate that microtiter plates are a feasible way to simplify microbial procedures. In general the same values were derived for *E. coli* (data not shown). Some deviations are possible, especially if working with food samples, however, in these cases deviations are always possible due to the heterogeneity of the samples. As an estimation method in research it is absolutely satisfying, but absolute values are subject to variation.

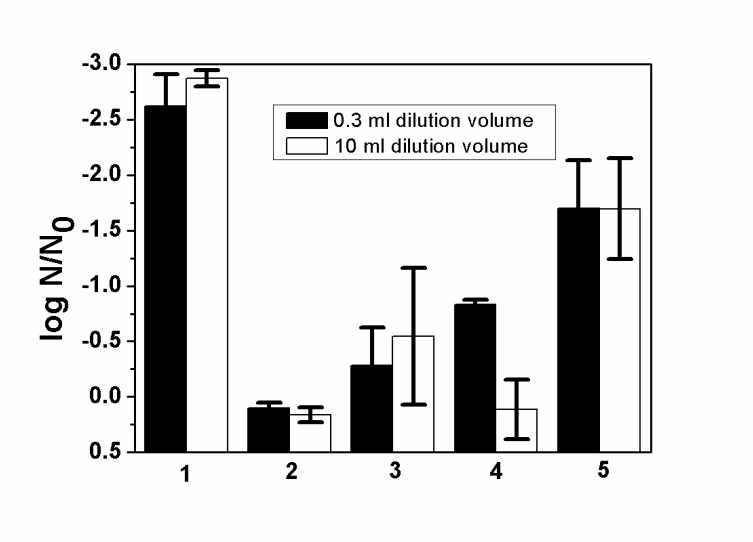

Figure 3.4 Comparison of dilution in microtiter plates (0.3 ml volume) and classical 10 ml dilution series of *Listeria innocua*. Samples 1: PBS buffer, frozen and pressure treated, 2: ice cream frozen, 3: ice cream frozen and pressure treated, 4: ground beef frozen, 5: ground beef frozen and pressure treated. All food samples were diluted in a first step in 10 ml and suspended.

3.4.2 Flow cytometry

Flow cytometry of *Lactobacillus rhamnosus* followed procedures established by Ananta (2004), *Listeria innocua* was analyzed using slightly modified protocols. Pressure treated cells with a theoretical optical density (at 600 nm) of 10 in PBS were initially incubated with 50 µM carboxyfluorescein diacetate (cFDA) (Molecular Probes, Leiden, NL) at 37 °C for 10 min to allow intracellular enzymatic conversion of cFDA into carboxyfluorescein (cF). Cells were then washed to remove excessive cFDA. This step was followed by addition of 30 µM propidium iodide (PI) (Molecular Probes) and by incubation in ice bath for 10 min to allow labeling of membrane-compromised cells To measure the performance of treated cells in extruding intracellular accumulated cF activity, cF stained cells were incubated together with glucose 20 mM for 20 min at 37 °C. To monitor the kinetics of cF-release from glucose energized cells, cF-labeled cells were incubated at 37 °C in the presence of glucose 20mM and the progress was measured every 5 min.

Analysis was performed on a Coulters EPICS XLMCL flow cytometer (BeckmanCoulter, Miami, FL, USA) equipped with a15 mW 488nm air-cooled argon laser. Cells were delivered at the low flow rate, corresponding to 400–600 events/s. Forward scatter (FS), sideward scatter (SS), green (FL1) and red fluorescence (FL3) of each single cell were measured, amplified, and converted into digital signals for further analysis. cF emits green fluorescence at 530 nm following excitation with laser light at 488 nm, whereas red fluorescence at 635 nm is

emitted by PI-stained cells. A set of band pass filters of 525 nm (505–545 nm) and 620 nm (605–635 nm) was used to collect green fluorescence (FL1) and red fluorescence (FL3), respectively. All registered signals were logarithmically amplified. A gate created in the density plot of FS vs. SS was preset to discriminate bacteria from artefacts. Data were analyzed with the software package Expo32 ADC (Beckman-Coulter). All detectors were calibrated with FlowCheck Fluorospheres (BeckmanCoulter).

Density plot analysis of FL1 (green) vs. FL3 (red) was applied to resolve the fluorescence properties of the population measured by flow cytometer. With this graph the population was able to be graphically differentiated and gated according to their fluorescence behavior. Table 3.1 describes the gate designation of stained cells.

Table 3.1 Gate designation of cells stained with cF and PI

Gate	Fluorescence properties of cells collected in each gate	Possible explanation of the status of involved cellular mechanism
#1	cF- and PI+	Esterase activity not detectable or cells not able retain cF, heavily membrane compromised
#2	cF+ and PI+	Active esterase which can still be retained, membrane minimally damaged due to PI intrusion
#3	cF- and PI-	- Esterase not active, membrane intact or - cF extruded out of the cells upon glucose addition or - empty cell cyst
#4	cF+ and PI-	Active esterase, intact membrane

Letters in gate designations like G1 or F1 have no significance.

3.4.3 Meat quality

For evaluation of the quality of meat samples, meat pieces were cut longitudinal to the fibre of pork *longissimus dorsi*, packaged in composite film pouches, frozen by immersion freezing in a cryostat at -45 °C and treated at 340 MPa, -35 °C for one minute in the pilot scale vessel to obtain a phase transition of ice I to ice III in the meat. Storage samples were stored at -18 °C in a freezer. Thawing was carried out at 20 °C in a water bath.

Color measurements were carried out with a Chromameter CR-200 (Minolta, Ahrensburg, Germany).

Roasting was carried out in a “contact grill” (Severin, Sundern, Germany) between two hot surfaces without fat addition. Samples were heated to a core temperature of 75 °C which was monitored by thermocouples. Samples were evaluated after cooling.

For texture evaluation, two methods with a texture analyzer TA.XT2 (Stable Micro Systems, Godalming, UK) were checked. A Warner-Bratzler shear blade, which is the standard method for meat texture was used at a test speed of 1 mm/s and a deformation length of 30 mm after sample contact. Sample cylinders 50 mm x 15mm were cut from the meat after roasting. However, no differences between treatment (fresh, frozen, frozen pressure treated) were found. Instead a ball probe (8 mm diameter) with a test speed of 1 mm/s and a deformation length of 5 mm after sample contact was used. Meat stripes of 10mm x 60 mm x 40 mm were used for this test.

Drip loss was evaluated by the mass loss before and after treatments. Samples were rolled on lab tissue paper in a defined way before measurement. Meat experiments were carried out 10-fold.

4 Results and Discussion

4.1 Phase transitions

4.1.1 Introduction

The knowledge of phase transition points and kinetic phenomena like nucleation or metastability is a prerequisite for the design of high pressure – low temperature processes for food or other biomaterials. Even though transition lines and phase behavior of water in foods and low concentrated model solutions in the ice I area are largely clarified, two main tasks remain on the agenda: further systematization of the complex phase transition behavior in the region of 210 to 500 MPa and the examination of high concentrated systems or model solutions in the complete pressure range to 500 MPa. The necessity to investigate high concentrated systems arises from the fact, that besides foods with low water content, the interior of plant and animal cells, as well as microorganisms, is essentially a high concentrated solution. During freezing, small cells like microorganisms are in an osmotic equilibrium with their immediate surrounding which gets freeze concentrated even in low concentrated solutions.

Sucrose solution as a solute of organic origin and sodium chloride as an inorganic ionic compound were chosen to examine phase transition lines and to propose equations to describe them (Table 4.1). Furthermore, phase transitions of various systems upon pressurization in the frozen state, i.e. pressure induced phase transitions between ice I and ice III were investigated at different temperatures to clarify the potential of these transitions for innovative food processes.

Table 4.1 Concentration of sodium chloride and sucrose solutions used in the experiments.

Solute	Mass percentage (w/w) [%]	Molality b [mol kg^{-1}]	Mole fraction of solute X_i [-]	Mole fraction of water X_w [-]	Activity [-]
NaCl	4.98	0.8967	0.0159	0.9841	2
NaCl	9.56	1.8089	0.0316	0.9684	2
Sucrose	23.37	0.8907	0.0158	0.9842	1
Sucrose	42.71	2.1775	0.0378	0.9622	1

The activity denotes the number of particles in solution per molecule or ionic compound.

4.1.2 Freezing and melting of aqueous solutions

4.1.2.1 Sucrose solution

The phase transition lines of sucrose at concentrations of 23.4 % and 42.7 % (w/w) were examined by freezing and thawing of a sample in lab scale equipment at constant pressure with three temperature probes inside the sample. Pressure was kept constant manually by either pumping or pressure release with high accuracy. The position of the pressure transducing piston was recorded, which traced whether pressure changes were caused by the sample or external influence. In this way, one nucleation, one freezing and one melting point of the solution were derived in each experimental run. It was not possible to apply techniques, which are based on pressure manipulation during freezing to move the freezing point along the transition line (Schlüter 2003; Guignon et al. 2005), due to the sometimes short and ambiguous freezing temperature plateaus. Experiments were carried out in duplicates at steps of 100 MPa. However, a lot of additional experiments were carried out, if needed to clarify the phase transitions.

Some selected freezing experiments are shown in Figure 4.1 and Figure 4.2. The reproducibility of the freezing curves was very good, as two experiments at one pressure level produced the same temperature response without significant deviations. During cooling of 23.4 % solution of sucrose, supercooling occurred and the sample temperature of the whole sample rose to the equilibrium freezing point as indicated by the long plateau of the freezing temperature. At 200 MPa, the release of heat during crystallization was developing slower, so that different temperature peaks of the three measurement points can be seen. There was no real temperature plateau any more, rather a bell-like shape of the sample center temperature. If the sample temperature was not showing a plateau phase, equilibrium freezing points cannot be derived; however the peak temperature was still denominated as freezing point. Precise equilibrium phase transition points were derived from the melting curves, which are not influenced by supercooling or slow crystallization.

In pressure domains where several ice modifications can possibly be frozen from the liquid phase, the ice phase was identified by the melting temperature of the sample. At 300 MPa the water in the solution froze to ice III with a higher supercooling than ice I, a phenomenon that was reported before in other aqueous systems. It is notable, that the crystallization is now appearing to be faster again, compared to the slow nucleation of ice I at 200 MPa. At 400 and 500 MPa ice V crystallized. At 500 MPa in both runs the temperature curves showed very unusual multiple peaks before rising to the final freezing temperature, a behavior which can-

not be explained at the time. Possible reasons are the crystallization of parts of the sample at different times, but even the occurrence of ice IV for seconds before freezing of ice V cannot be ruled out absolutely.

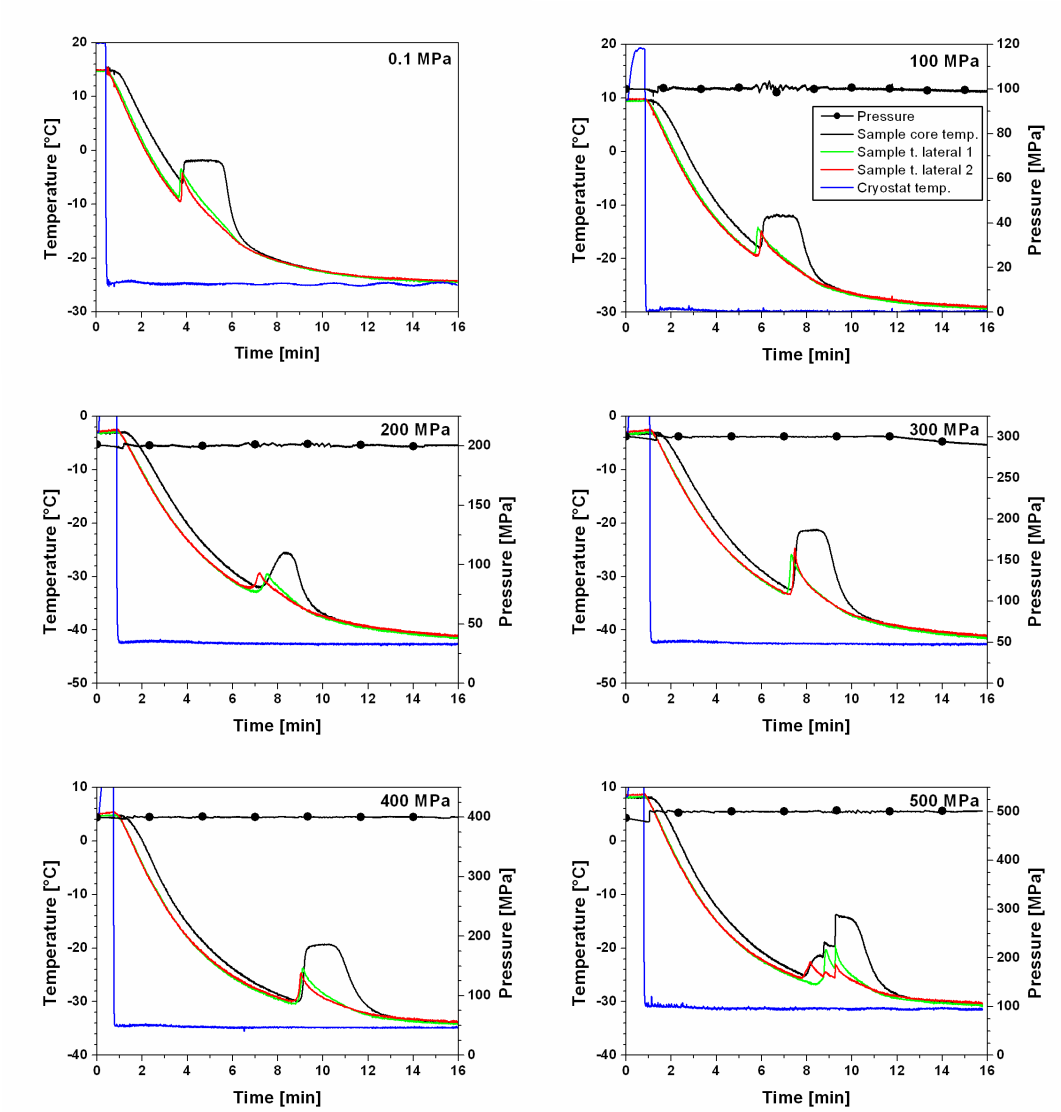

Figure 4.1 Freezing of sucrose solution 23.4 % (w/w) at constant pressure of 0.1 MPa to 500 MPa.

At the higher sucrose concentration of 42.7 % (w/w) (Figure 4.2) bell-shaped temperature peaks were observed at 0.1 and 100 MPa, indicating slower crystallization and less ice formation as more water is bound. Very slow and low temperature peaks were observed at higher pressure levels, sometimes only after a long time when the temperature was already equilibrated at the cooling temperature. Nevertheless the ice modification could be attributed to the ices I, III and V by subsequent melting of the sample. It is noteworthy, that the heat of crystallization at 400 MPa and 500 MPa (ice V) was released somewhat faster than at 210 MPa

(ice I) and at 300 MPa (ice III) leading to more pronounced temperature peaks, even though the time necessary to induce nucleation started was in some cases even longer.

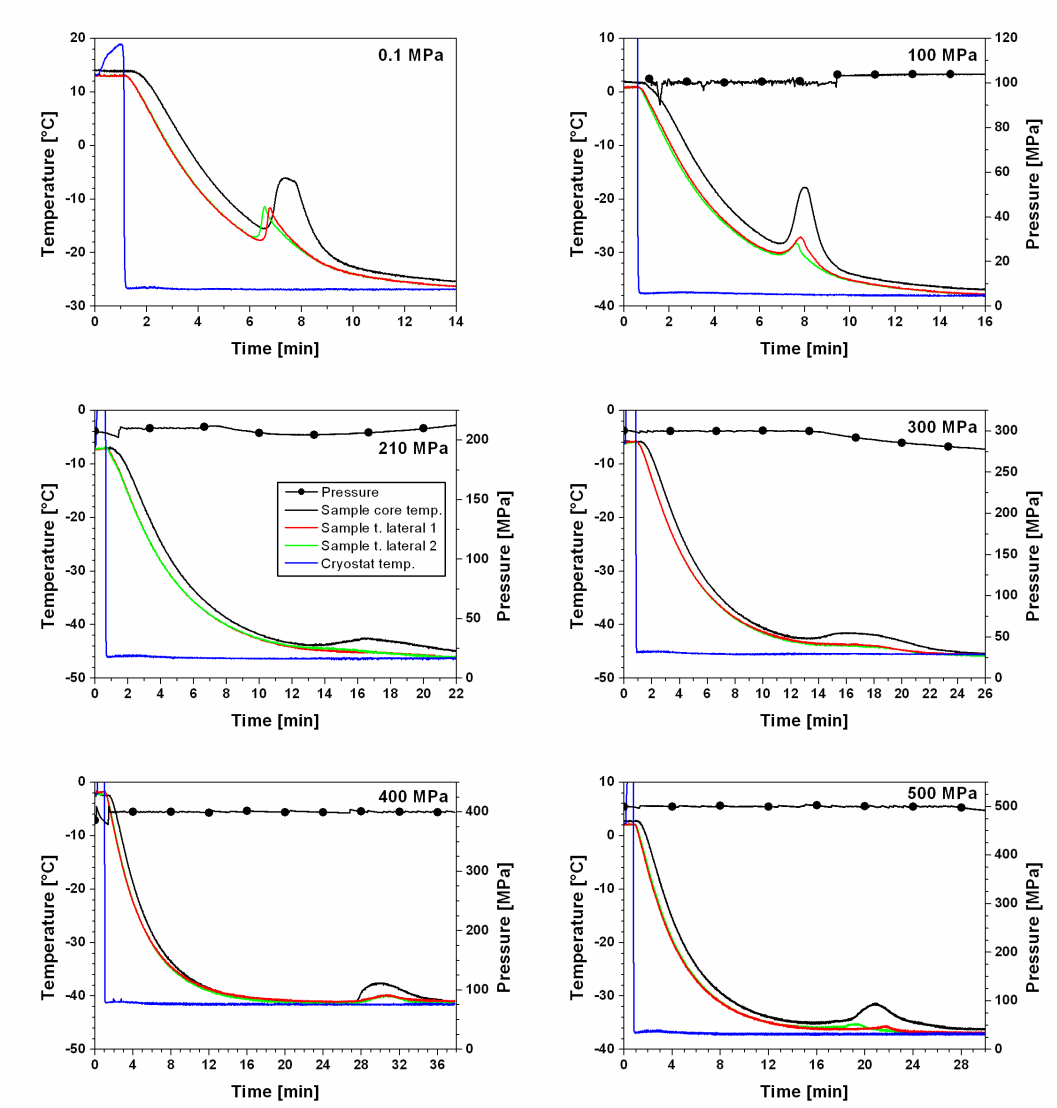

Figure 4.2 Freezing of sucrose solution 42.7 % (w/w) at constant pressure of 0.1 MPa to 500 MPa.

In summary, it can be stated that crystallization behavior of ice in high concentrated sucrose solution is decelerated under pressure. To explain the changed freezing process of ice I under pressure it should be noted that the freezing enthalpy lowers under pressure and that the viscosity is rising with lower temperature, rising pressure and increased solute concentration. Effects due to variations in cooling conditions can be excluded, as constant temperature gradients were realized by setting the temperature of the cryostat to a value 20 K below the expected phase transition point. The enthalpy change for the liquid solid transition is varying (see Table 2.2), which can explain some of the different sizes of temperature peaks. From the

supercooling behavior it can derived, that especially the nucleation of ice V at pressures of 400 MPa and above was difficult to obtain.

4.1.2.2 Sodium chloride solution

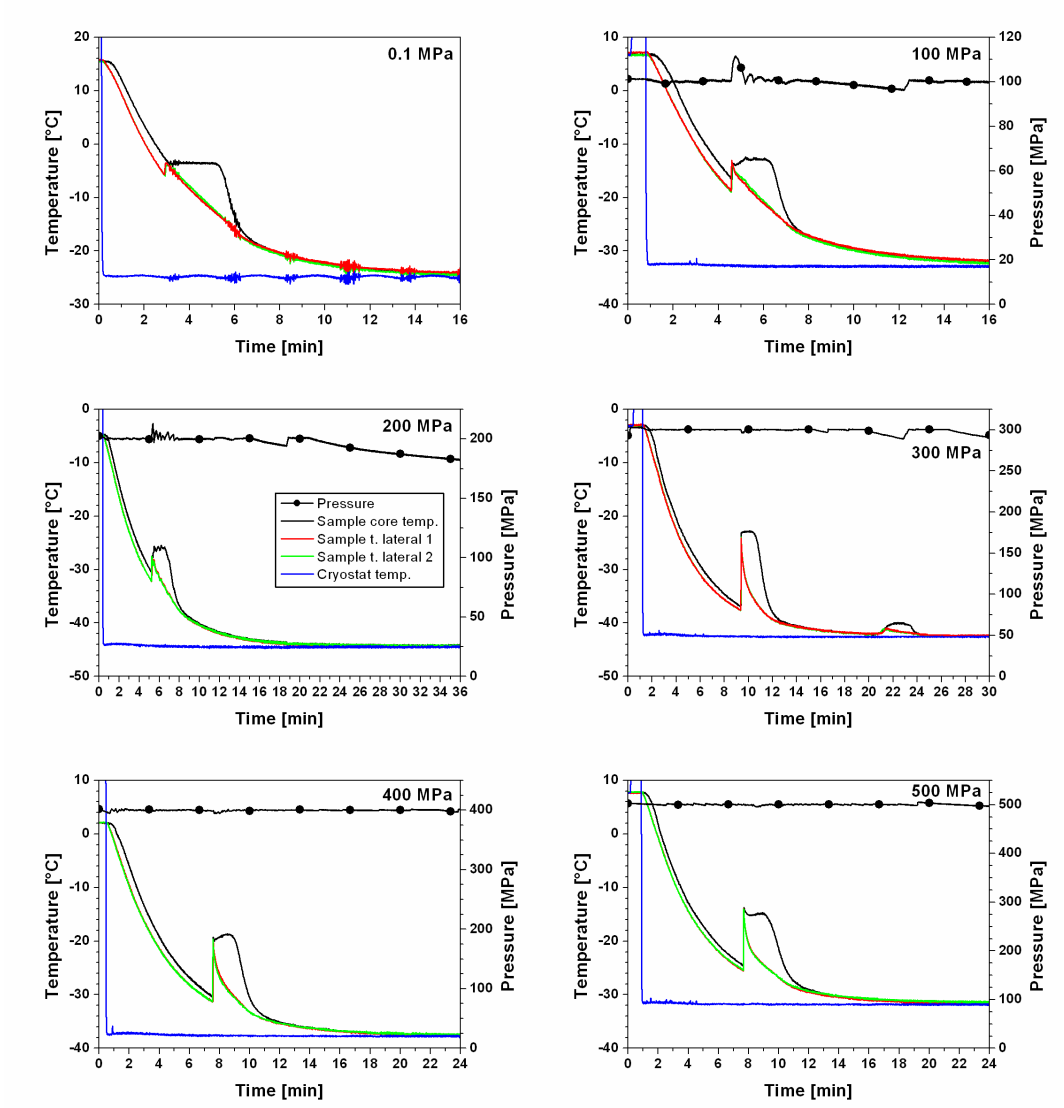

Figure 4.3 Freezing of sodium chloride solution 5.0 % (w/w) at constant pressure of 0.1 MPa to 500 MPa.

Solutions of sodium chloride of 5.0 % and 9.6 % (w/w) were used as the second model system (Figure 4.3 and Figure 4.4) with the same experimental procedure like in the case of sucrose solution. In the curves shown here, the pressure control was not always providing an absolute constant pressure (for example at 100 MPa in Figure 4.3). Supercooling behavior was about the same as in sucrose solution with a lot of supercooling of ice III and V, whereas supercooling was limited in ice I. When comparing with sucrose solution, it should be noted

that after nucleation the heat releases much faster, leading to sharper temperature peaks, which is discussed in relation to viscosity in the following section.

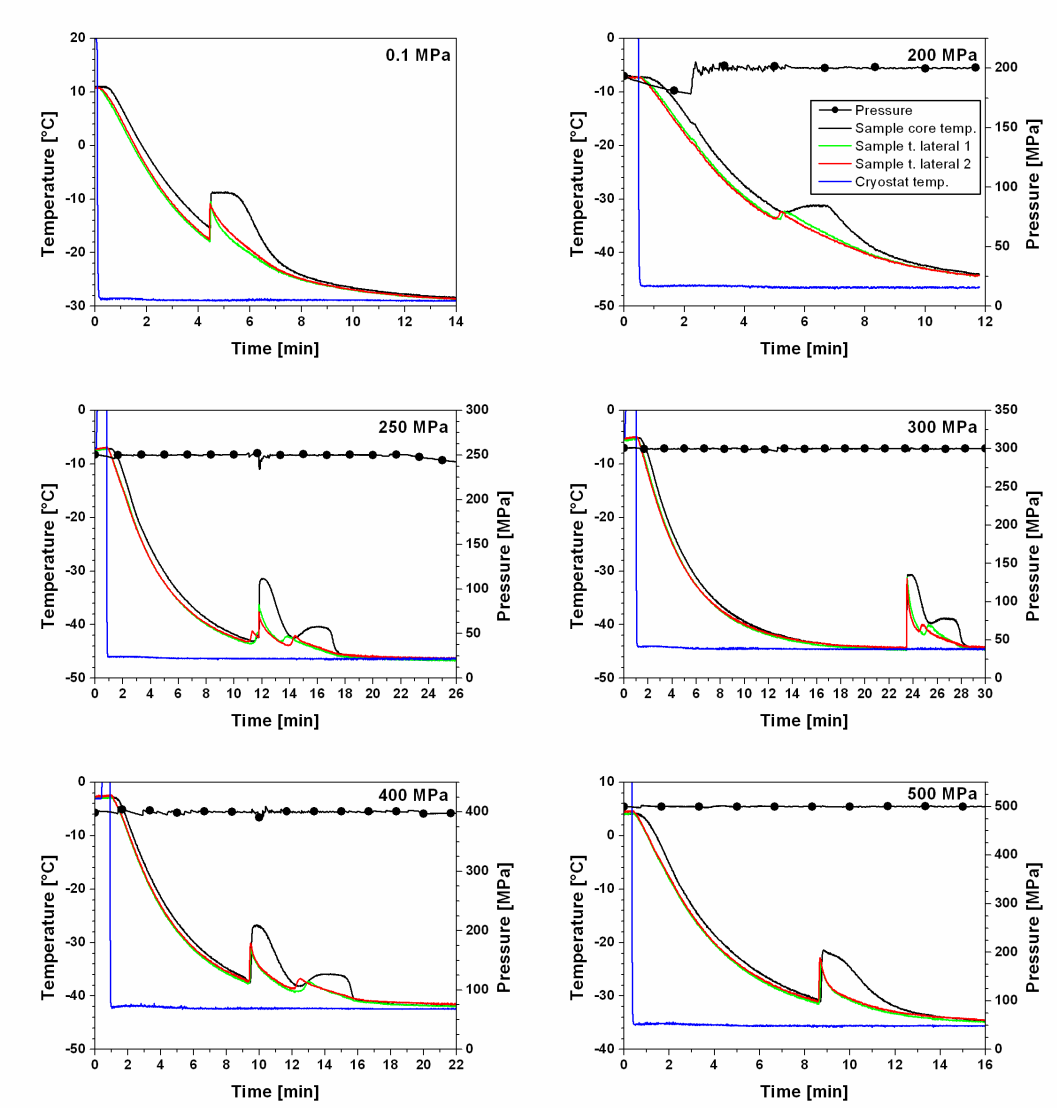

Figure 4.4 Freezing of sodium chloride solution 9.6 % (w/w) at constant pressure of 0.1 MPa to 500 MPa.

The most eye catching phenomenon in the freezing curves is the occurrence of a second temperature peak after freezing in some experiments. In the lower concentrated solution the peak occurred in both experiments at 300 MPa, in one case after 21 minutes and in the other case after 29 minutes of cooling. In the other experiments with this solution the peak was not observed, but not all freezing experiments were carried out with the same cooling times. Hence, it is possible that the second peak was missed if the cooling time was not long enough. In Figure 4.3 always the longest cooling times which were recorded before melting are selected. At the higher concentration of 9.6 % (w/w) the peak was observed more often and faster after the freezing plateau. An exact overview of all points is given in Figure 4.7. It can be stated

that with the experimental cooling conditions the second peak was observed with ices I, III and V up to 400 MPa, but never at 500 MPa. The first peak can always be attributed to freezing, as it occurred at the expected freezing temperature.

In addition to a second temperature peak during freezing, a second melting event was observed during thawing; one example is shown in Figure 4.5. It is remarkable that most of the heat is absorbed during the first melting; the second (higher) melting point corresponds to the expected melting point of the solution. The number of possible reasons for a second phase transition in a binary system is limited, thus it is the only possibility that this event is the transition to the eutectic state. A second delayed freezing event of water is not possible, as water is continuously crystallizing if its temperature is below its freezing point with ice crystals present. Glass transition can be excluded, as it would not produce an exothermic peak. Another possibility under pressure would be the occurrence of other ices, however, the second peak was also observed at ice I conditions where no other ice is stable.

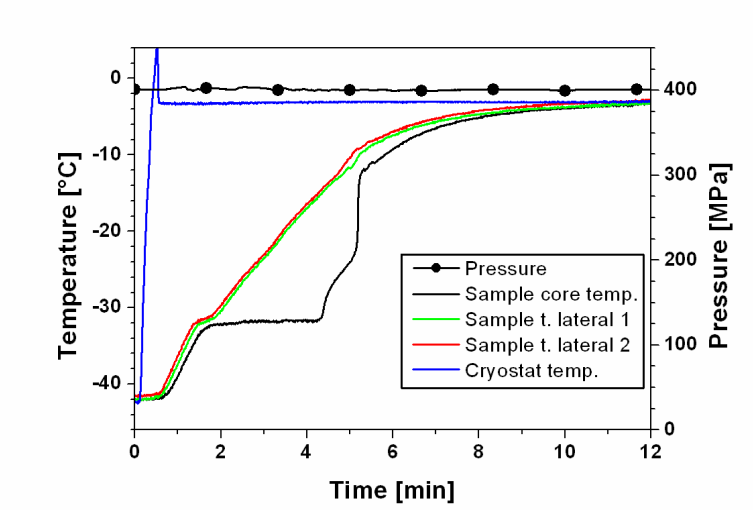

Figure 4.5 Melting of sodium chloride solution 9.6 % (w/w) at 400 MPa

The eutectic point at ambient pressure of the sodium chloride – water system is at -21.2 °C and 23.3 % NaCl (w/w). During freezing water crystallizes and leads to a freeze concentration of the remaining liquid, so that it is possible that the requirements for eutectic crystallization are fulfilled. The eutectic state of a magnesium sulfate solution (9.7 % w/w) was reported in a DSC unit under pressure in the range to 160 MPa (Chourot et al. 2000).

4.1.2.3 Relation to viscosity data

Most of the slowed freezing characteristics of the solutions under pressure can be attributed to the viscosity of the solutions under pressure. Even though there are no data for subzero tem-

peratures for the viscosity of these solutions, from the data presented in Table 4.2 the influences of pressure, temperature and solute concentration can be estimated. It can be stated, that the influence of temperature is dominating over the pressure effect in the ranges under consideration. Data on the viscosity of pure water at subzero temperatures under pressure (Först et al. 2000) tend in the same direction and allow to assume further viscosity increase of the solutions at lower temperatures. The influence of the solute and the concentration is of high importance as well. Table 4.2 shows that the viscosity of sodium chloride solution is not as high as the viscosity of sucrose solution with the same concentration, at ambient pressure as well as at elevated pressure. Accordingly, it can be derived from Figures 4.1 to 4.4 that sodium chloride is crystallizing faster than sucrose once nucleation has begun. However, considerable supercooling occurs in all solutions.

Table 4.2 Literature data of dynamic viscosity [mPa s] of aqueous solutions of sucrose and sodium chloride under pressure.

	Sucrose 20 % (w/w)				**Sucrose 40 % (w/w)**		
	5 °C	**20 °C**	**40 °C**		**5 °C**	**20 °C**	**40 °C**
0.1 MPa	3.11	1.90	1.15	**0.1 MPa**	32.95	15.54	6.97
200 MPa	3.23	2.05	1.27	**200 MPa**	42.35	21.30	9.03
400 MPa	3.77	2.37	1.45	**400 MPa**	64.80	29.77	11.93

	Sodium chloride 2.7 % (w/w)			**Sodium chloride 5.4 % (w/w)**	
	4.5 °C	**9.1 °C**		**4.5 °C**	**9.1 °C**
0.1 MPa	1.59	1.32	**0.1 MPa**	1.60	1.38
196 MPa	1.67	1.35	**196 MPa**	1.63	1.43

Data of sucrose by Först et al. (2002), data of sodium chloride extrapolated from data by Horne & Johnson (1967) and Kaufmann (1960).

Freezing is particularly difficult in sucrose solutions of 42.7 % (w/w) at pressures higher than 210 MPa. Three factors combine for a very high viscosity there: high solute concentration, very low freezing points and the effect of high pressure. In the case of sucrose solutions of 23.4 % (w/w) the temperature peaks are obviously rounded only at the pressure level of 200 MPa (ice I), but not at higher pressures. This fact cannot be explained by viscosity data, because the viscosity should be even higher at e.g. 400 MPa, where the crystallization is developing faster. It seems like ices tend to crystallize easier from solutions at higher pressure (>200 MPa) and higher viscosity than ice I around 200 MPa.

4.1.3 Phase transition points

Figure 4.6 shows all phase transition points from the experiments with sucrose solution. Each point was derived as the average of the pressure and temperature values from two experimental phase transitions points. This was feasible, because the pressure was constant and identical in both experiments with deviations below 5 MPa. The freezing point was defined as the maximum of the core temperature after nucleation, the melting point as the inflection point of the core temperature during thawing. The freezing temperature, even when a plateau is observed, might deviate from the equilibrium phase transition temperature, which should be derived from the melting points. The nucleation point was found as the lowest temperature attained before the temperature peak, taking into account the lateral sample temperatures which were usually lower in temperature. At 200 MPa the freezing and supercooling data of sucrose solution 42.7 % (w/w) was not conclusive and therefore discarded but the melting point is shown. The experiments were repeated at 210 MPa. At 350 MPa, the melting point was higher than expected for ice III, strongly suggesting that ice V was formed. The experimental error of the detected melting points of sucrose at ambient pressure in comparison to calculated values (shown in chapter 4.1.7) was -0.5 °C and -0.6 K, respectively.

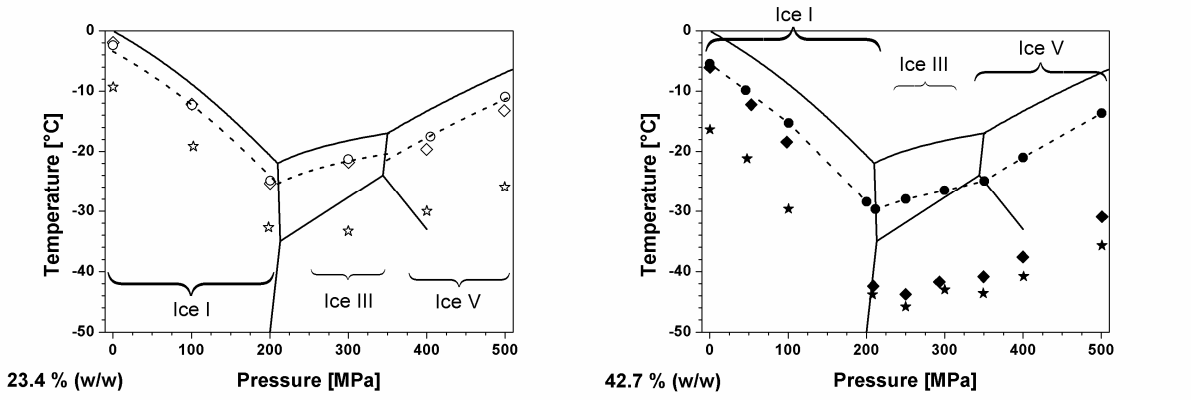

Figure 4.6 Phase transition points of sucrose solution plotted in the pT-diagram of water. ◆◇freezing points, ●○melting points, ★☆nucleation points; dotted lines are graphical estimations of melting lines.

In sucrose solution 23.4 % (w/w), the supercooling below the equilibrium phase transition point during freezing of ice I was 7 to 8 K for ice I, but 12 to 13 K for ice III and V. At 42.7 % (w/w) the supercooling was 10 to 14 K for ice I, but 16 to 22 K for ice III and V, however, the crystallization began at a point where the system temperature was already equilibrated at the cryostat temperature. Comparable supercooling values should only be derived from experiments with similar cooling conditions. Furthermore it is further notable that during freezing of

sucrose solutions the eutectic was never detected in the experiments. At ambient pressure the eutectic point of sucrose in water was not detected (-14.0 °C and $X_{Sucrose}$=0.084, (Young & Jones 1949)) even though this temperature was obtained. More than 14 K below the respective freezing point were realized under pressure, too, but no eutectic transition was found. Nevertheless, this is not surprising, since sucrose solutions are easily supersaturated.

In the case of sodium chloride, eutectic transitions during freezing were found (Figure 4.7) as described earlier. When evaluating the transition to the eutectic during freezing of sodium chloride solution, the same problem of the detection of the transition point occurred. The heat of crystallization was not sufficient to raise the sample temperature to equilibrium transition conditions. However, during melting the equilibrium temperature was detected. The location of the transition points gives further evidence that the eutectic formed as the eutectic transition occurs at ambient pressure at -21.2 °C. At 50 MPa the eutectic melted at -25.5 °C which is 21.4 K below the associated melting point of water. At the other pressure levels the temperature difference to the melting line of water was consistently about 18 K. At 300 MPa the eutectic formed at both concentration levels. As the eutectic forms after freeze concentration of the system at exactly the same concentration level, the melting points of the eutectic consequently fall on one point in both solutions, which is the case at 300 MPa in Figure 4.7. This further supports the conclusion that the eutectic was formed.

It must be stated critically, that the experimental error of the detected melting point of sodium chloride solution at ambient pressure compared to the tabulated values (Kaufmann 1960) was -2.8 K in the case of concentration 9.6 % (w/w). At 5.0 % (w/w) the deviation was -0.5 K. Nevertheless, it was decided to include the phase transition points as the general phase transition behavior is reproducible. It remains unclear why such a deviation of the expected values occurred. Systematic errors cannot be excluded, as the phase transition behavior is complex. Both experiments showed almost the same melting point (-9 °C and -9.1 °C), which excludes some random experimental errors. However, they were carried out on the same day, so errors concerning the whole experimental day might have occurred, for example the loss of electrical grounding of the equipment. To avoid arbitrary exclusion of experimental data, the data points were taken as they are.

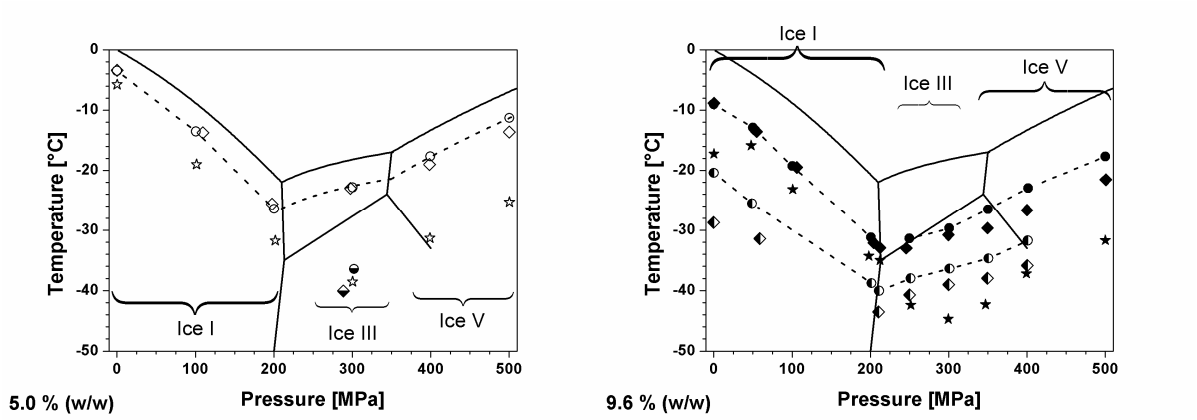

Figure 4.7 Phase transition points of sodium chloride solution plotted in the pT-diagram of water. ◆◇ freezing points, ●○ melting points, ★☆ nucleation points; ◆◆ second (eutectic) crystallization, ◒◐ melting of this (eutectic); dotted lines are graphical estimations of melting lines.

In the study covering the eutectic state under pressure of a $MgSO_4$ solution under pressure (Chourot et al. 2000) in the ice I range, it was observed, that the ice melting line in solution is running parallel to the ice I melting line of pure water. However, the temperature difference between eutectic melting and melting of ice is getting smaller under pressure, like it is the case in this study of NaCl. Absolute values of the different electrolyte solutions are not comparable but the phenomenological behavior is in remarkable accordance with the results shown here. The authors attributed this behavior to differences in solubility of the salt under pressure, which is influencing the occurrence of the eutectic.

4.1.4 Nucleation and freezing point depression under pressure

The supercooling values derived during freezing of sodium chloride solutions are shown in Figure 4.8, together with the values of sucrose solution 23.4 %. The values of sodium chloride 9.6% are not completely comparable with the values of other solutions, as nucleation occurred at end of cooling when the temperature was almost equilibrated. However, nucleation began still during cooling unlike most values of sucrose solution 42.7 %, which are consequently not evaluated in that figure. When freezing food or solutions in the milliliter range examined in this study, nucleation will always occur as heterogeneous nucleation, which means nucleus formation is facilitated by vessel walls, organic molecules, ions or simply dust. In pure water samples in micro-volumes in emulsion or aerosol nucleation occurs as homogeneous nucleation, which means by spontaneous formation of a nucleus from the liquid, however at much lower temperatures (compare chapter 2.2.3).

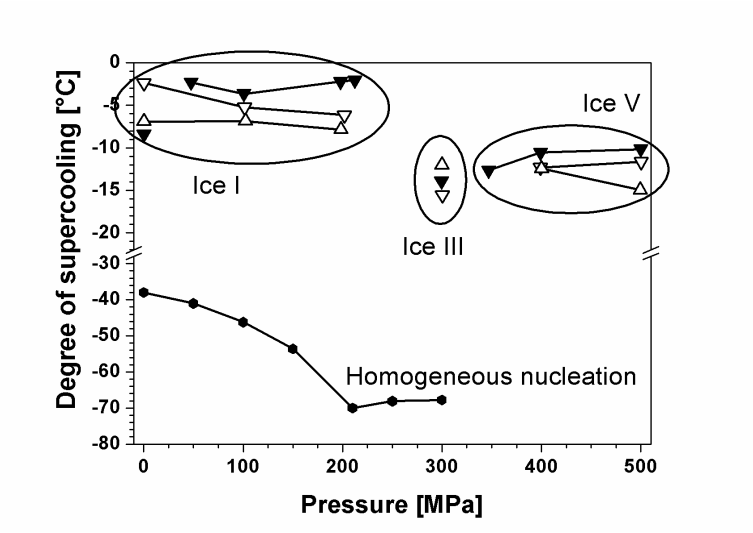

Figure 4.8 Heterogeneous nucleation in aqueous solution under pressure expressed as degree of supercooling below the respective melting point. ▽▼△supercooling during freezing of sodium chloride solution 5.0% and 9.6% and sucrose solution 23.4% (w/w), respectively, ⬢ data of Kanno et al. (1975) for homogeneous nucleation of pure water.

Figure 4.8 shows the tendency that the degree of supercooling for all freezing processes in the ice I region is almost constant with values between 2 and 8 K depending on the system. However, when freezing ice III or V at pressures up to 500 MPa, supercooling and nucleation seem to be constant between 10 and 16 K. These values of heterogeneous nucleation cannot be generalized, but they show a deviation to the homogenous nucleation behavior of water in the range to 210 MPa. In pure water the homogeneous nucleation temperature under pressure is not constant but falling to a value of 70 K of supercooling, and is more or less constant only at values of 200 to 300 MPa (Kanno et al. 1975).

The freezing point depression (FPD) as a function of pressure is shown in Figure 4.9. It was calculated from the respective phase transitions points, determined as melting temperature $\vartheta_{m,su}$, minus the phase transition temperature of water at the respective pressure $\vartheta_{m,w}$, calculated according to Wagner et al. (1994):

$$FPD = \vartheta_{m,su} - \vartheta_{m,w}$$

Equation 14

With the exception of the NaCl (9.6%) - solution whose phase transitions points are more error-prone, a clear tendency for a bigger depression of the ice I phase transition under pressure was observed. The melting temperatures at 200 MPa of these solutions were about 2 K lower than a parallel shift of the melting curve of water to lower temperatures would suggest. In the case of ice III the lower concentrated solutions of both solutes showed less FPD whereas the

more concentrated solutions showed the biggest FPD., hence a clear tendency cannot be derived. In the case of ice V it seems like FPD is getting smaller with increasing pressure.

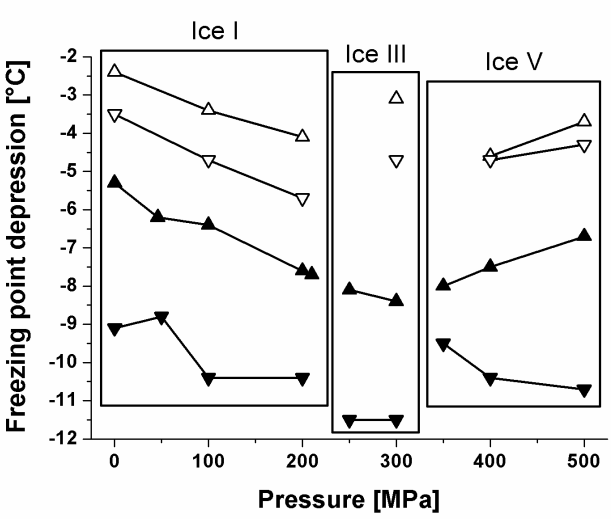

Figure 4.9 Freezing point depression of water in aqueous solutions as a function of pressure (temperature difference between melting point of the solution compared to melting point of pure water at that pressure). △▲ sucrose solution 23.4% and 42.7 %, ▽▼ sodium chloride solution 5.0% and 9.6% (w/w).

Schlüter (2004) and Guignon et al. (2005) did not find such a pressure-dependency of the FPD like it was observed here. In both studies it was concluded that melting curves of solutions or more complex systems can be derived by shifting the melting curves of water in parallel to lower temperatures. However, in both examinations most or all experimental data was based on techniques that include pressure manipulation during freezing. Especially in the case of higher concentrated solutions, freezing methods are generally less potent to derive exact phase transition points. The determinations of single melting points are obtained in independent experiments which give a more realistic insight in the phase boundary at that pressure. The data shown here indicate that pressure manipulation techniques lead to wrong conclusions regarding the slope of the transition curves. A further discussion of experimental errors in Guignon's examinations is found in the next paragraph.

4.1.5 Fit of Simon equations

As described in chapter 2.2.5, Simon equations (Equation 6, Equation 7) are the established way to describe phase boundaries by mathematical equations. Wagner et al. (1994) fitted Simon equation curve parameters to experimental data to describe the phase boundaries of pure water. They used the triple points as reference points to normalize pressure and temperature (Equation 8, Equation 9).

In this study, the same procedure was used; however, the triple points of water in aqueous solutions are so far unknown. To overcome this problem, the calculation was carried out in a two-step iteration. In a first step, the equations of the ice I phase transition were established using the experimental melting points. For this calculation the temperature of the reference point was set to the average melting point at ambient pressure. As pressure value, the pressure at the triple point liquid – ice I – vapor of pure water (0.000611657 MPa) was used according to Wagner et al. (1994), because the transition temperature difference between this triple point and 0.1 MPa is only 0.1 K for water. Preliminary equations for ice III and V were established using the experimental data with the reference conditions set at one experimental data point. In this way, triple points were determined by the intersection of these curves. In the second step, with the knowledge of these triple points, the curve fit of ice III and V was repeated to establish the equations shown in Figure 4.10 and Table 4.3 with the triple points used as reference points. This procedure was necessary, as the mathematical from of the equation requires a reference which is located on the curve without deviation.

In the case of the lower concentrated solutions only two experimental points at one pressure level (300 MPa) were available in the ice III domain, which was not enough to provide curves and triple points there. Hence, the equations of ice V are based only on experimental values as reference points.

Table 4.3 Parameters of Simon equations describing the melting lines of sucrose solution and sodium chloride solution

	Sucrose 23.4 % (w/w)	**Sucrose 42.7 % (w/w)**	**NaCl 5 % (w/w)**	**NaCl 9.6 % (w/w)**
Ice I				
T_N [K]	270.8	267.7	269.7	264.1
P_N [MPa]	0.000611657	0.000611657	0.000611657	0.000611657
α	551072	506181	545629	599225
β	-2.5715	-2.1282	-2.9902	-2.1715
χ	274730	352759	205999	372320
δ	13.6191	11.1616	17.0147	8.8946
Range T [K]	248.2 – 270.8	243.2 – 267.7	246.7 – 269.7	240.0 – 264.1
Range P [MPa]	0.000611657 – 202	0.000611657 – 213	0.000611657 – 201	0.000611657 – 215
Relative FSE $*10^{-3}$	6	12	4	20
Ice III				
T_N [K]		243.2		240.0
P_N [MPa]		213		215
α		0.3119		0.3944
β		57.5541		48.3135
Range T [K]		243.2 – 247.9		240.0 – 244.0
Range P [MPa]		213 – 346		215 – 319
Relative FSE $*10^{-3}$		22		17
Ice V				
T_N [K]	255.5	247.9	255.5	244.0
P_N [MPa]	400	346	399	319
α	0.4061	1.9808	0.9240	0.5075
β	18.0448	4.4401	9.8182	16.3219
Range T [K]	255.5 – 262.5	247.9 – 259.7	255.5 – 262.1	244.0 – 255.5
Range P [MPa]	400 – 501	346 – 503	399 – 504	319 – 500
Relative FSE $*10^{-3}$	17	8	10	11

The relative FSE (fit standard error) was derived as the fit standard error calculated during the curve fit algorithm, divided by the maximum pressure of the respective definition range. In this way, dimensionless FSE values of different equations can be compared directly.

The data shows the shift of the water transition lines if solutes are added for the example of NaCl and sucrose in considerable concentration. They show that a regular phase behavior can be expected even at high concentrations in the pressure range examined. However, each line is each only valid for one concentration level. Other melting curves can be extrapolated between the curves. Despite this regularity, it should be considered that these lines are not useful to estimate the practical beginning of freezing due to high supercooling and slow crystallization. However, ice nucleating agents, especially selective ice nucleators of specific ice types, or possibly antifreeze proteins might still change the freezing process. It can be estimated that complex biological systems based on water show comparable phase transition behavior, espe-

cially in terms of pressure induced thawing processes, e.g. concentrated foods like ice cream or the interior liquid of cells.

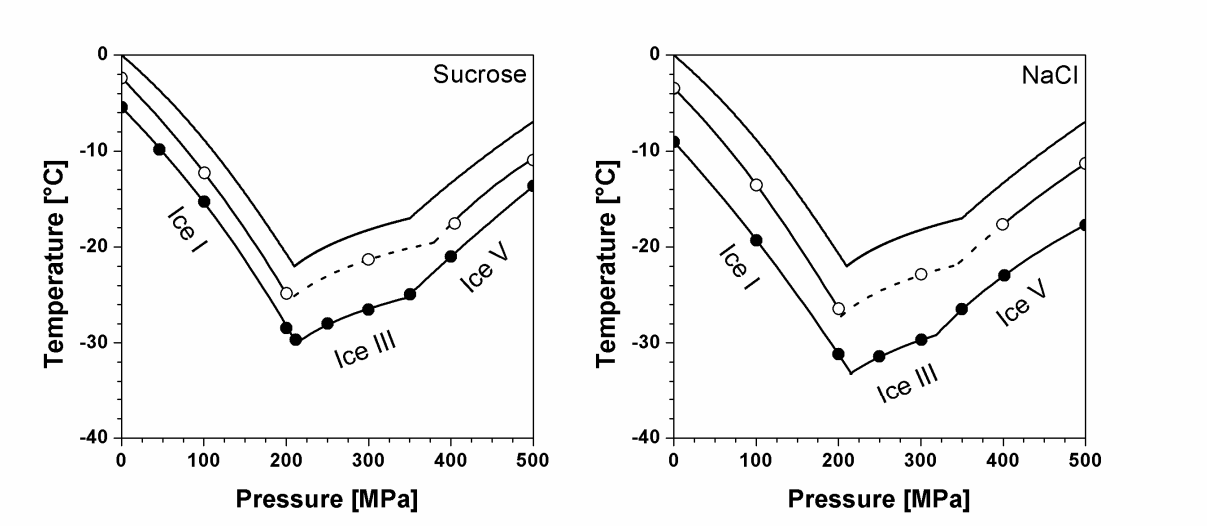

Figure 4.10 Solid – liquid phase boundaries of ice I, III and V of aqueous solutions described by Simon equations. Solid lines with symbols are phase boundaries of solutions, concentrations ○ sucrose 23.4 %, NaCl 5.0%, ● sucrose 42.7%, NaCl 9.6%; dashed lines are graphical estimations; upper line is the phase boundary of water (Wagner et al. 1994).

It is necessary to see the results presented here in relation to other examinations where Simon equations were used to describe the phase transition lines of aqueous systems (Schlüter 2003; Guignon et al. 2005). Slight but decisive differences apply, which can be summarized as:

a. Differences in mathematical approach

b. Differences in experimental approach

c. Deficiencies of the experiment (systematical errors)

a. It was already described in chapter 2.2.5, that the method used by Guignon et al. and Schlüter is questionable, as they use the reference point data as further variables to be adjusted. The method used here to overcome this deficit was described above.

b. In this study, the number of data points used to fit the curves is quite small, but each point was derived from a completely independent experimental freezing-thawing cycle, limiting the amount of melting points derived to two per day. Due to this time-consuming approach, in the other papers pressure manipulation techniques were used to find a high number of freezing points in one experimental run. From the point of view of number of experiments the data basis is not necessarily better if multiple phase transitions points are derived in one experimental run. As a result of this difference, discrepancies were found regarding the freezing

point depression. Curves presented by Guignon et al. (2005) indicate a parallel shift of the transition lines, other than the influence of pressure on the FPD. With the knowledge that thermophysical properties are pressure and temperature dependent and as the properties of electrolyte solutions are not even theoretically understood at ambient pressure (see below), there is no reason to automatically assume a parallel shift of phase transition lines under pressure. Quite likely, the behavior is a lot more complex.

c. The examinations of Guignon et al. (2005) pose two serious problems when evaluating their data. It is unclear whether sucrose / NaCl were used in a completely anhydrous state for their experiments. The mass difference between anhydrous or hydrated chemicals might add differences in concentration specifications (Kaufmann 1960; Bubnik & Kadlec 1995). A second experimental problem is analyzed in Figure 4.11. From the curvature of the melting lines found in this study, by Wagner et al. for water (1994) and by Guignon et al. (2005) it can be concluded that the data of Guignon et al. are partly deviating. It is estimated graphically as indicated by the horizontal lines in the graphs that the deviation is not connected to pressure, but to low temperatures. The deviation becomes more pronounced at lower temperatures regardless of the associated pressure level. The authors decided in their paper to exclude some points on the lowest NaCl curve, however, the slope shown here indicates that the deviation is already high at about -16 °C. The problem is difficult to analyze retrospectively, however, it is probably connected to insufficient cooling equipment or temperature calibration problems.

In Figure 4.11 the equations published by the authors were evaluated. The curves indicate that the experimental points were slightly too high, which leads to inappropriate curve fitting. As the curves are deviating to higher temperature it is possible that this experimental error overcompensates an increasing freezing point depression, which was found in the present study but not by Guignon et al. (2005). Nevertheless, within the deviations which are associated with an experimental work, the values of all curves above -16 °C are useful. In Figure 4.11 it is striking that the alignment of the concentration curves is sometimes not as expected. Experimental errors of both examinations together with the uncertainty of the real freezing point depression under pressure lead to the fact that some curves are slightly above curves with lower concentration levels (e.g. NaCl 10.9% above NaCl 9.6%). However, the mostly parallel run of the curves at least above -16 °C shows the mutual affirmation of the studies.

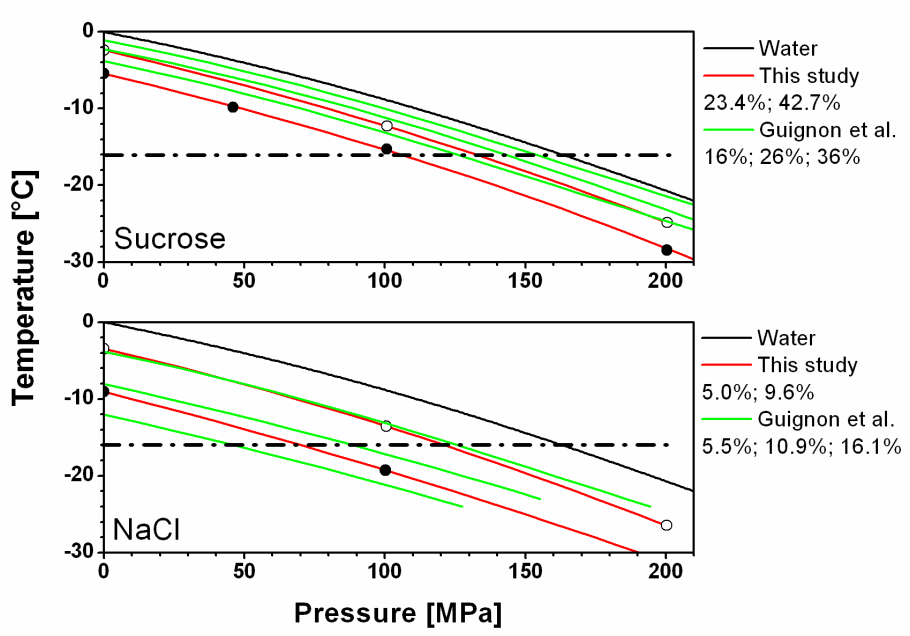

Figure 4.11 Comparison of ice I - Simon equations of sucrose and NaCl solutions. Shown are the melting curves derived in this work (red lines) and curves derived by Guignon et al. (2005) (green lines) in the given concentrations (from top to bottom respectively). Circles indicate experimental melting points from this study. The dot-dash line at -16 °C indicates the suggested limit of precision of Guignons data (see text) as estimated from the upward deviation of their data.

4.1.6 Freezing point prediction of ideal solutions under pressure

The solutions used in the experiments serve as models for food or other biomaterial. However, the equations presented are limited to their particular concentration level. A theoretical approach was made to predict the freezing point from the concentration of an aqueous solution and the Simon equations of pure water. The calculation of the freezing point in an ideal solution is rather simple, as the freezing point depression of these solutions is a colligative property. Hence, it is not dependent on the type of solute but only on its molality and on the type of solvent. However, for food studies the only relevant solvent is water. The validity of these calculations is strictly limited to the concentration range where solutions can be considered ideally. Consequently, the calculations presented here remain theoretical, i.e. without experimental verification, because the solutions in the concentration ranges examined are far from being ideal solutions. These calculations are still helpful as an intermediate step for following calculations of real solutions.

The freezing point depression in an ideal solution is calculated as follows:

$$\Delta T_f = K_f \cdot b_x \cdot i$$

Equation 15

The molality b is defined as the number of moles n of a substance x per mass of solvent m_{sv} (not per mass of solution).

$$b_x = \frac{n_x}{m_{sv}}$$

Equation 16

The van't Hoff factor i is taking into account the number of particles dissociated in solution. For sucrose is i=1, NaCl i=2, $CaCl_2$ i=3 etc. K_f is the cryoscopic constant of water, it is constant at ambient pressure, however it is worth looking at its definition.

$$K_f = \frac{R \cdot T_f^2}{\Delta h_f} = -1.86 \frac{K \cdot kg}{mol} \quad \text{at 0.1 MPa}$$

Equation 17

This means for example that every ideal one-molal solution with i=1 has a freezing point of -1.86 °C. R is the gas constant, which is independent from pressure. The freezing temperature of water T_f and the heat of fusion of water Δh_f are pressure dependent. So K_f is pressure dependent and not constant, and shall be called cryoscopic factor in the following.

$$K_f(p) = \frac{R \cdot (T_f(p))^2}{\Delta h_f(p)}$$

Equation 18

To make the calculation of pressure dependent values of K_f possible, polynomial second order equations were used to describe the pressure dependency of T_f (for the sake of simplicity) and Δh_f which are shown in Table 4.4. Equations for Δh_f were fitted to data by Bridgman (1912).

Table 4.4 Polynomial equations describing the heat of fusion and the melting temperature as a function of pressure for ices I, III and V.

y = A+Bp+Cp²		**A**	**B**	**C**	**Range**
$y = T_f$	Ice I	273,17088	-0,07321	-1,52181E-4	0.1 .. 209.9
$y = T_f$	Ice III	233,54808	0,11410	-1,41826E-4	209.9 .. 350.1
$y = T_f$	Ice V	224,36453	0,10795	-4,84477E-5	350.1 .. 632.4
$y = \Delta h_f$	Ice I	-333,80984	0,39060	4,22261E-4	0.1 .. 209.9
$y = \Delta h_f$	Ice III	-133,64409	-0,41678	1,84621E-4	209.9 .. 350.1
$y = \Delta h_f$	Ice V	-172,63224	-0,32535	2,14140E-4	350.1 .. 632.4

$[T_f]$=K; $[\Delta h_f]$=kJ/kg; [p]=MPa; all equations R^2=0.999 or better

The equations were used with Equation 18 to calculate values of K_f in the pressure range of ice I, III and V. The results are shown in Figure 4.12. Interestingly, the values of the cryoscopic factor for the ice I range are showing a similar evolution like the freezing point depression under pressure that is shown in Figure 4.9. Despite the fact that these non-ideal solutions should not be calculated by equations for ideal solutions, it is interesting to see that even for ideal solutions a parallel shift of freezing curves to lower temperatures cannot be expected, rather an increasing FPD. Unfortunately, the values of K_f for ice III and V cannot really be brought in agreement with the experimental findings for the experimental solutions. However, they indicate to some extend, that for ice III a higher FPD can be expected than for ice I and V.

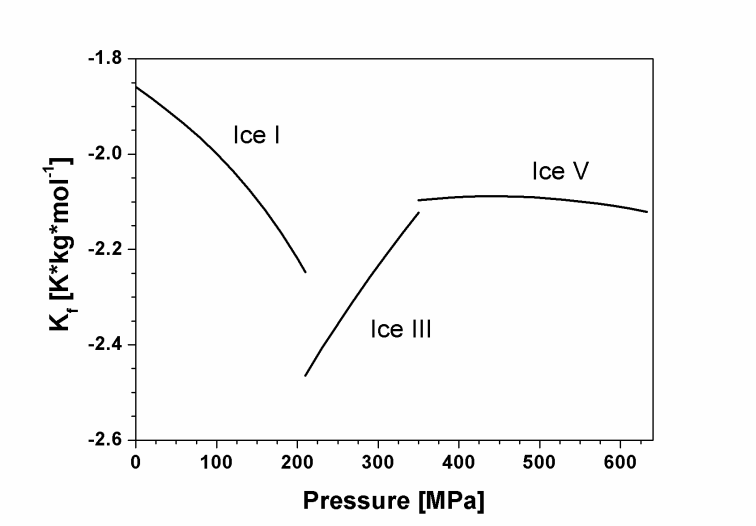

Figure 4.12 Calculated cryoscopic factor K_f of water under pressure.

The point where ideal behavior of solutions ends has to be selected according to the purpose of the examination. In terms of freezing measurements at about 17 % (w/w) sucrose, which corresponds to a molality of 0.6 mol/kg, the freezing point deviation between Equation 15 and reality is more than 0.1 K and therefore not negligible (Bubnik & Kadlec 1995). For NaCl the molal limit is even lower due to higher inter-particulate forces and the activity of two ions per molecule.

The freezing point can now be calculated by using the Simon equations for water (Wagner et al. 1994) and subtracting the calculated FPD from the temperature values afterwards. It would be very interesting to validate these deliberations with experimental data of close-to-ideal solutions, especially for ice III and V, but in this examination the real, higher concentrated solutions were emphasized. Nevertheless the ice I - freezing point depression found for high

sucrose und NaCl concentrations confirms the pressure dependent calculations of the cryoscopic factor at least qualitatively.

4.1.7 Freezing point prediction of real solutions under pressure

The next step is the freezing point calculation of real solutions under pressure. The real freezing point is deviating from the behavior of ideal solutions due to inter-particulate interaction, if the concentration is so high that the particles are close enough to interact. Consequently the ideal behavior of solutions is only a theoretical border case. The deviation from ideal behavior can be detected already at very small solute concentrations depending on the sensitivity of the measurement. In the following the behavior of sucrose solution in the ice I pressure range shall be examined. To establish a calculation approach that unifies freezing point calculation under pressure and the pressure dependence of freezing expressed by Simon equations, data on more concentration levels are necessary. Hence, equations of Guignon et al. (2005) were used in addition to the values derived in this work within the limits set in Figure 4.11.

In advance, sodium chloride is excluded from the modeling approach made here. The calculation of the freezing point of highly concentrated sodium chloride solution, as well as of other electrolyte solutions, is a very complex task already at ambient pressure. Several models based on theoretical thermodynamic approaches were published, but due to strong and complex ionic interactions the behavior is not fully understood yet (Loehe & Donohue 1997). The freezing point calculation of concentrated electrolyte solutions under pressure would exceed the dimension and goal of this work, first approaches to this topic were recently published (Choukron & Grasset 2007). In consequence, the following calculations are limited to sucrose solution, which is the more relevant model solution to food and bioscience studies.

The real freezing point of a solution at ambient pressure can be calculated according to the following set of equations (Chandrasekaran & Judson King 1971; Heldman 1974; Pongsawatmanit & Miyakawi 1993).

The Clausius-Clapeyron equation is relating the effect of pressure to the freezing temperature:

$$\frac{dT_f}{dp} = T_f \frac{\Delta v}{\Delta h_f}$$

Equation 19

T_f is the freezing temperature at pressure p, Δh_f the heat of fusion and Δv the volume change during the transition.

For ideal solutions, the freezing point is related to the concentration with the following equation based on the Clausius-Clapeyron equation (Heldman 1974).

$$\ln X_w = \frac{\Delta h_f}{R}\left(\frac{1}{T} - \frac{1}{T_f}\right)$$

Equation 20

with X_w the mole fraction of water in the solution, Δh_f the molar heat of fusion of water, R the gas constant, T_f the freezing temperature of pure water and T the freezing temperature of the solution. The mole fraction X_w is defined as the fraction of moles of water of all moles n of the system and is reciprocal to the mole fraction of the solute X_s:

$$X_w = \frac{n_w}{n} = 1 - X_s$$

Equation 21

For non-ideal solutions Equation 20 can be modified to Equation 22 (Chandrasekaran & Judson King 1971; Pongsawatmanit & Miyakawi 1993):

$$\ln a_w = \frac{\Delta h_f}{R}\left(\frac{1}{T} - \frac{1}{T_f}\right)$$

Equation 22

By definition the water activity a_w is related to the mole fraction by the activity coefficient γ_w

$$a_w = \gamma_w \cdot X_w$$

Equation 23

Combining equations Equation 22 and Equation 23 gives

$$\ln X_w + \ln \gamma_w = \frac{\Delta h_f}{R}\left(\frac{1}{T} - \frac{1}{T_f}\right)$$

Equation 24

The activity coefficient of water in a binary solution can be calculated as

$$\ln \gamma_w = -\frac{\alpha'}{T}(1 - X_w)^2$$

Equation 25

Where α' is an empirical constant characteristic for the solute (Pongsawatmanit & Miyakawi 1993) with the dimension of temperature derived from the empirical constant in Margules equation (Margules 1895). It was not possible to derive a constant value for α' in case of so-

dium chloride solution. It would probably be possible to model the freezing of NaCl solution if introducing a variable α' as a function of solute concentration, however, this would result in a completely empirical equation with little value in terms of generalization. Substituting Equation 25 in Equation 24 with using Equation 21 and rearrangement gives

$$\alpha' = \frac{T}{X_s^{\,2}}\left(\ln(1-X_s) + \frac{\Delta h_f}{R}\left(\frac{1}{T} - \frac{1}{T_f}\right)\right)$$

Equation 26

With this equation α' can be calculated from combinations of solute concentration and freezing point of its solutions. For sucrose α' was approximated with 1800 K (Pongsawatmanit & Miyakawi 1993), which fitted well to the experimental findings of freezing sucrose solutions at 0.1 MPa. Rearrangement of Equation 26 yields an equation with which the real (non-ideal) freezing temperature T of a solution as a function of the mole fraction of the solute X_s can be calculated, all other values are constants at 0.1 MPa:

$$T = \frac{\alpha' \cdot X_s^2 - \dfrac{\Delta h_f}{R}}{\ln(1-X_s) - \dfrac{\Delta h_f}{R \cdot T_f}}$$

Equation 27

Introducing the pressure dependent polynomial equations of Table 4.4 for Δh_f and T_f for water with X_s=0 for pure water in Equation 27 would give an empirical expression for the freezing point of water under pressure in the ice I range with a precision of better than 0.1 K, which is not surprising as it is essentially a modification of the Clausius-Clapeyron equation. However, introducing values for the freezing points of sucrose solutions under pressure (X_s>0) and using the polynomials for pressure dependent Δh_f and T_f in Equation 27 does not lead to satisfying results with deviations up to 1.9 K between calculated and experimental values of the solution melting temperature.

Therefore another attempt was made to relate the solute concentration, melting temperature and pressure. The empirical Simon equation for ice I relates melting temperature of pure water to pressure:

$$\pi = 1 - \alpha \cdot 10^6 (1-\theta^\beta) + \chi \cdot 10^6 (1-\theta^\delta)$$

Equation 6 (repeated)

α, β, χ, δ are fitting constants. The normalized temperature and pressure are defined as follows according to Equation 8 and Equation 9 (see page 41).

In effect, Equation 6 must be extended to a third dimension, which is the solute concentration. Equation 6 is able to reproduce the freezing point depression under pressure of different solute concentrations individually as shown previously. Now the equation is fitted to all data sets simultaneously, however, T_n and p_n are usually defining one reference point through which the curve is running in a two dimensional equation. p_n poses no difficulty and does not have to be adjusted, as all melting point curves of the varying solute concentrations of course are also valid around ambient pressure, so it is fixed to the reference pressure point of p_n=0.000611657 MPa, the pressure value of the triple point liquid-solid-vapor of pure water. T_n is now used to introduce the solute dependency to the Simon equation. It is calculated according to Equation 27 and gives the freezing temperature at ambient conditions of the respective solute concentration, as reference point specific for the solute concentration. In combination the following equation can be fitted to results for the calculation of the melting pressure of ice I of a non-ideal, regular (not ionic) solution under pressure:

$$p = p_n \cdot \left[1 - \alpha \cdot 10^6 \cdot \left\{ 1 - \left(\frac{T}{\frac{\alpha' \cdot X_s^2 - \frac{\Delta h_f}{R}}{\ln(1 - X_s) - \frac{\Delta h_f}{R \cdot T_f}}} \right)^{\beta} \right\} + \chi \cdot 10^6 \cdot \left\{ 1 - \left(\frac{T}{\frac{\alpha' \cdot X_s^2 - \frac{\Delta h_f}{R}}{\ln(1 - X_s) - \frac{\Delta h_f}{R \cdot T_f}}} \right)^{\delta} \right\} \right]$$

Equation 28

As Equation 27 is only used to calculate the reference point at ambient conditions, no pressure dependency of Δh_f and T_f has to be introduced. Introducing the values of Δh_f, T_f and R gives

$$p = p_n \cdot \left[1 - \alpha \cdot 10^6 \cdot \left\{ 1 - \left(\frac{T}{\frac{\alpha' \cdot X_s^2 - 722.78K}{\ln(1 - X_s) - 2.646}} \right)^{\beta} \right\} + \chi \cdot 10^6 \cdot \left\{ 1 - \left(\frac{T}{\frac{\alpha' \cdot X_s^2 - 722.78K}{\ln(1 - X_s) - 2.646}} \right)^{\delta} \right\} \right]$$

Equation 29

which calculates p (melting pressure) X_s (mole fraction of the solute) and T (melting temperature); α, β, χ, δ are fitting constants. Equation 29 is the equation whose coefficients should be

fitted to the available experimental data. As mentioned earlier, the data by Guignon et al. (2005) above -16 °C are valuable to be added to the data basis. The original experimental data points cannot be derived from their publication, only fits of Simon equations at the concentration levels they used. Moreover, the (few) experimental melting points derived here are not sufficient to adjust the fitting parameters in a model with three dimensions. In consequence it was decided to calculate the following data points and use them as data basis to fit the parameters in Equation 29.

- Data from the Simon equations of this work according to Table 4.3 in a step width of 0.75 K for both concentration levels of sucrose examined here, yielding 66 data points in two concentration levels of sucrose.
- Data from the Simon equations of Guignon et al. (2005) above -16 °C in a step width of 1 K, yielding 69 data points in the five concentrations levels they examined.
- Data calculated from Wagner's Simon equation of pure water for the concentration level X_s=0 in a step width of 0.35 K yielding 64 data points.
- Data calculated for the freezing point of sucrose at p=0.1 MPa in a step width of X_s=0.0006 up to X_s=0.04 according to Equation 27 yielding 67 data points.

The step width was selected in a way to establish equal weight of the four data sources by providing approximately the same number of data points. It can be argued that the result will only be a fit of other curve fits and not fitting experimental data directly, however, it is valuable as all data points are calculated with good precision from the equations used. The data basis is derived from two different experimental sources (from the data here and by Guignon et al. 2005), an international standard equation for the values of pure water (Wagner et al. 1994) and a mechanistic equation for the freezing of real high concentrated solutions, which is even valid at higher concentration levels and for other solutes (Pongsawatmanit & Miyakawi 1993). An equation which combines the different approaches with accuracy should therefore be a valid equation even though it is fitted to an indirectly derived data basis.

The curve-fit of the four fitting parameters was performed in TableCurve 3D (V. 3.12, Systat Software) by introducing Equation 29 as a user-defined function. The results are shown in Table 4.5 and Figure 4.13. Generally the function provides a good description of the data basis. The values of pure water (and probably of low concentrated solution) are somewhat deviating, especially above 100 MPa with an underestimation of the melting pressure by the equation of about 10 MPa at 210 MPa, which is the maximum error in the workspace. Nevertheless the procedure shown here is useful to demonstrate the feasibility of the calcula-

tion method for the freezing conditions of regular solutions even in non-ideal concentration ranges. It could be further extended to establish a calculation method for the freezing point of food in the ice I range, if an average molecular weight of the foodstuff for freezing point prediction (Chen 1986) can be determined.

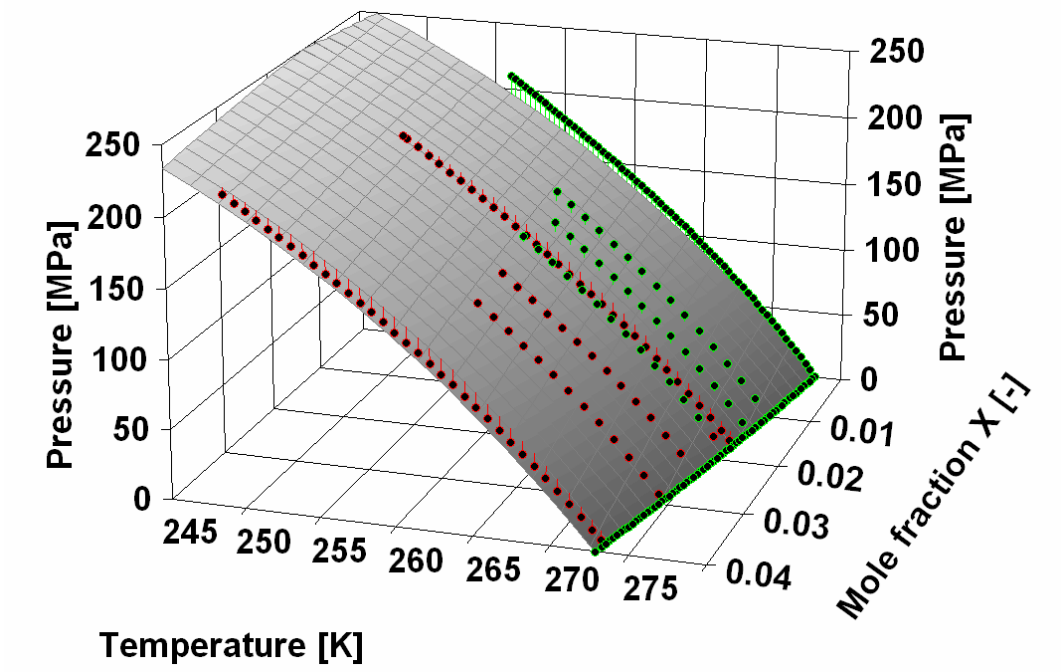

Figure 4.13 Surface graph of the melting pressure of water in sucrose solution as a function of mole fraction of sucrose and temperature according to the developed equation. Green points indicate data above the surface, red points are data sets below the function surface.

Table 4.5 Results of curve-fit of Equation 29 for sucrose solution

Parameters			
p_n	0.000611657 MPa	α'	1800 K
Fitting constants			
α	193117	β	-0.1564
χ	607983	δ	8.8379
Statistical evaluation			
FSE	6.07916	R^2	0.99177
Relative FSE*10^{-3} [1)]	28		

[1)] See Table 4.3 for definition

4.1.8 Freezing of DMSO-water mixture

To examine another solution which did not consist of solid compound dissolved in water, solutions of dimethyl sulfoxide (DMSO) in water were examined. DMSO is a liquid at ambient

conditions with a structure similar to the water molecule, though it is larger. It can be mixed with water in any quantity, so it is not influenced by solubility restrictions. It is often used as a cryoprotective agent, when freezing microorganisms or other cells. Hence it is useful to gain first insights in the phase behavior of DMSO-water mixtures to evaluate the feasibility of high pressure – low temperature processes for freezing of living biological cells.

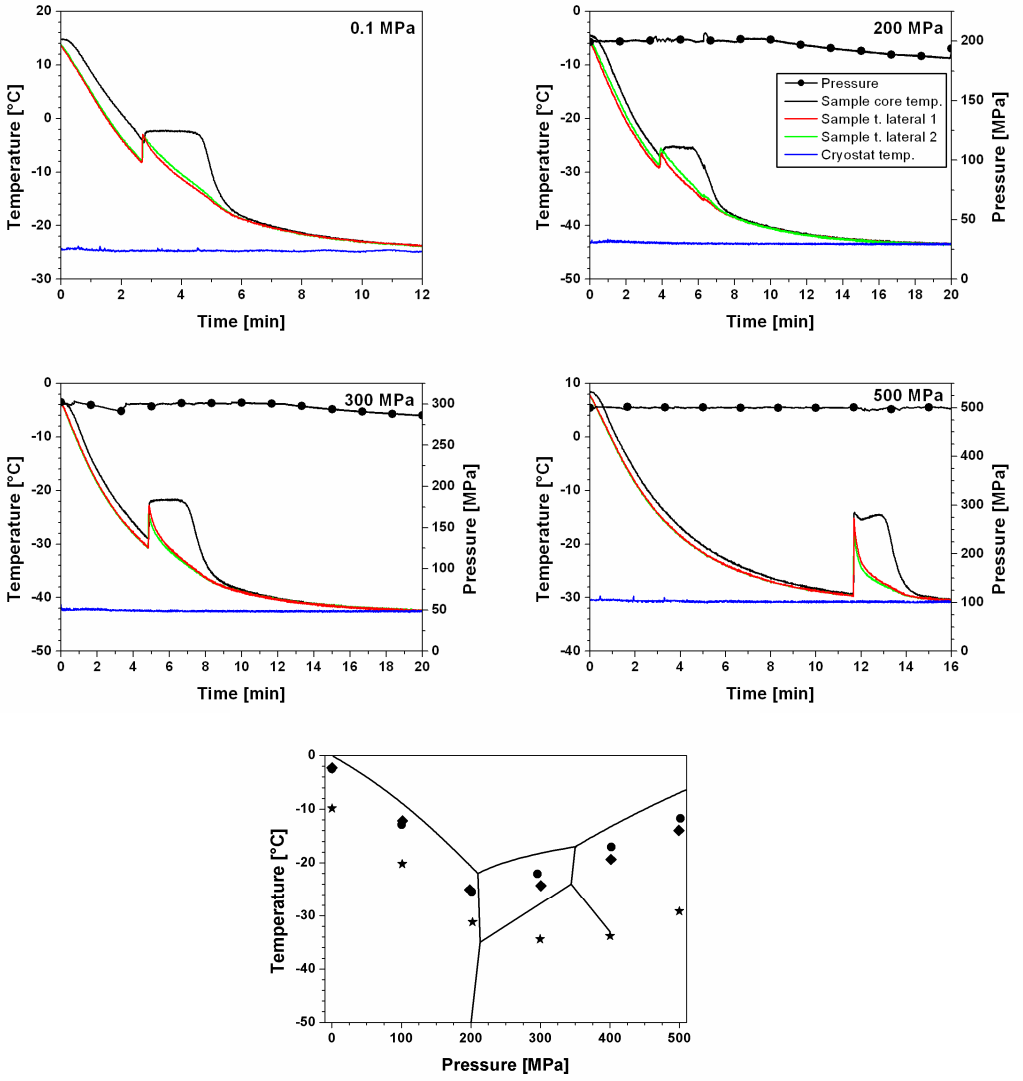

Figure 4.14 Freezing curves and phase transition points of DMSO - water mixture at constant pressure of 0.1 MPa to 500 MPa with DMSO 9.5 % (w/w). ◆ freezing points, ● melting points, ★ nucleation points.

Figure 4.14 shows exemplary freezing curves of a solution with a concentration of 9.53 % (w/w) DMSO and it shows phase transition points as an average of two experiments. Super-cooling was very high during freezing of ice V at 400 and 500 MPa and not very high for ice I. The freezing point depression at 200 MPa was 4.6 K below the freezing curve of water, however the ambient pressure freezing point was at -2.4 °C. FPD was 3.7 K at 300 MPa

(ice III) and 4.8 K at 500 MPa (ice V). The FPD for ice I supports earlier conclusions regarding the FPD and the cryoscopic constant made for solutions of sucrose and sodium chloride under pressure. In summary, no exceptional phase behavior of DMSO was found, only exceptional supercooling for ice V. Further fit of Simon equations for the solution were skipped as only one concentration level was examined as a screening.

4.1.9 Solid-Solid phase transitions of aqueous systems

It was necessary to carry out separate experiments with accurate temperature measurement inside the sample to elucidate the phase transitions occurring during pressurization of ice I above 210 MPa. The effect of the ice I – ice III phase transition on the microbial inactivation was examined, which is shown later. Figure 4.15 shows the recordings of a pressure treatment of frozen suspensions of *Listeria innocua* in phosphate buffer saline at 300 MPa for 5 minutes at -25 °C (part A) and -45 °C (part B).

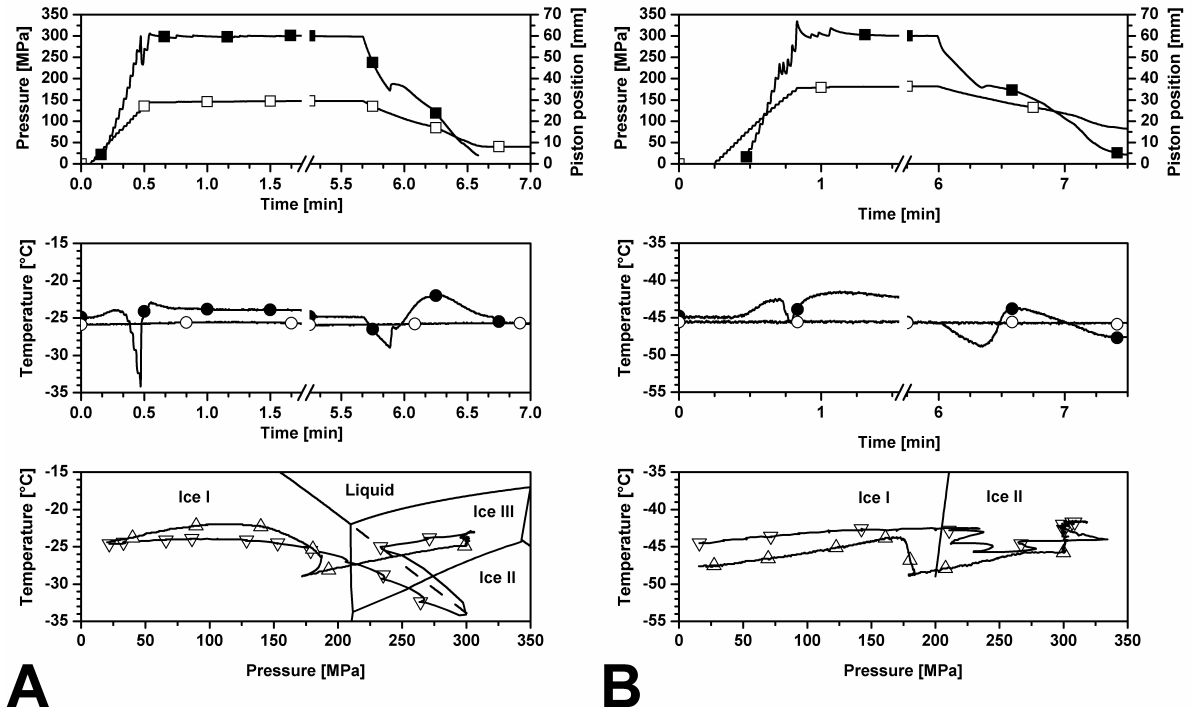

Figure 4.15 Transient solid - solid phase transition of phosphate buffer saline inoculated with *Listeria innocua* at -25 °C (A) and -45 °C (B) during pressurization to 300 MPa for 5 minutes. ■ pressure; □ piston position; ● sample core temperature; ○ cryostat temperature; ▽ sample core temperature during compression in pT - plot; △ sample core temperature during decompression in pT - plot.

During pressurization at -25 °C the sample temperature rose to -24 °C at 100 MPa due to compression heating, but during further pressure increase, the sample temperature decreased to a minimum temperature of -34 °C, which was lower than the temperature outside the vessel

(-26 °C). The temperature shifted downwards along the phase transition line ice I - liquid and approached it slowly as visualized in the plot of temperature versus pressure (pT - plot), a behavior that continued in the ice III - stability area. At about 300 MPa and -34 °C a sudden pressure drop to 230 MPa occurred in less than one second and the temperature rose from -34 °C to -25 °C. During further pressure increase, no other pressure shifts were detected and the temperature equalized within the system to -25 °C.

Decompression was going along with a decrease in temperature, but after passing the phase boundary between ice I and ice III, an increase in pressure was observed while the piston was consistently moving back. This transition was concurrent with an instant increase in temperature from -29 °C to -26 °C and up to -22 °C during further decompression.

During pressurization at -45 °C no endothermic event comparable to the experiment at -25 °C was detected. The heat of compression caused an increase in temperature to -42.6 °C. In contrast to the experiment at -25 °C a pressure decrease was already detectable at 225 MPa, soon after passing the phase boundary between ice I and ice II. A decrease in pressure was detected after each stroke of the pressurizing hand pump, accompanied by a decrease in temperature until the pressure was rising again constantly to 300 MPa. During the pressure holding phase the temperature equalized to -45.7 °C. Similarly to the previous experiment, the temperature dropped during decompression until an increase in sample volume was indicated by a period of constant pressure while the piston was moving backwards. During this time without pressure decrease the temperature rose to -44 °C .

Little is known about the kinetic behavior of water and ice phase transitions under pressure. Combined temperature - pressure recordings of these phase transition phenomena were published by Magnusson regarding the extrusion of ice through an orifice in the pressure range examined here (Magnusson 1977a). Furthermore, only the experiments of Bridgman (1912), which were carried out without temperature measurements inside the sample, were available at the time of these first experiments in 2002 to compare the data and conclusions reported here.

During the phase transition experiments different mechanisms of pressure - induced phase transitions between the solid ice polymorphs ice I and ice III at different temperature levels were observed. When pressurizing ice or frozen aqueous systems at -25 °C partial thawing occurred, which was indicated by a transient decrease in sample temperature, suggesting the energy requirement of pressure induced thawing. Due to the limitations of heat transfer this transition did not take place instantly, hence, the temperature decreased along the phase transi-

tion line and approached it slowly as thawing progressed (Schlüter et al. 2004). Ice cannot be superheated with respect to the liquid, which implies that ice I cannot exist beyond the phase transition line ice I – liquid, even though the line is extended into the area of stability of ice III.

When the pressure approached 300 MPa during thawing, ice I could no longer exist as a metastable phase in the stability range of ice II or ice III. The sudden pressure decrease indicated the conversion of ice I to ice III, which has a higher density than ice I (Schlüter et al. 2004). However, the phase transition ice I - ice III is endothermic at this temperature level, although the enthalpy change is quite small (4.5 kJ/kg for pure water, all enthalpies for water are extrapolations based on Bridgman (1912). The only possible explanation for the temperature increase was that during the ice I – ice III phase transition of the solid parts of the sample, water froze exothermically to ice III (242.5 kJ/kg at 300 MPa) in the previously thawed outer regions of the sample.

During the transition and afterwards the pressure was increased constantly to the maximum pressure and during the pressure holding time the temperature was equalizing within the system to -25 °C. It should be noted that -25 °C is only about 5 K below the melting point of aqueous biological systems, which was e.g. -19.6 °C at 300 MPa for potato tissue (Schlüter 2003). Thus it is likely, that not all water was present as solid ice III, but as liquid water, like it would be in the case of samples at -6 °C at atmospheric pressure. During decompression ice III converted back to ice I which was indicated by an increase in pressure. The exothermic nature of the transition was indicated by an instant increase in temperature to -26 °C, but the later increase to -22 °C might also be due to freezing of the mentioned liquid water.

During the experiment at -45 °C no partial thawing of the sample occurred. In contrast to the experiment at -25 °C the solid - solid phase transition to ice II or ice III began soon after passing the phase boundary ice I - ice II. An increase in sample volume indicated a transition to ice I when the sample was decompressed after the pressure holding time. The ice I to ice III transition at -49 °C is slightly exothermic (-7.7 kJ/kg), however, a rise of temperature during this period of constant pressure was detected, which is likely an effect of equalizing temperatures, as the sample was colder than the surrounding pressure vessel. As ice II and ice III have about the same density and phase transition line with ice I, it could not be concluded form the temperature and pressure measurements whether ice II or ice III was formed at about -45 °C. Despite that the ice II - stability area borders the area of stability of ice I, ice III is usually formed (Bridgman 1912) when pressurizing ice at about -45 °C above the transition pressure.

As the ice I to ice II transition is also more exothermic (see Table 2.2) than the ice I to ice III transition, a bigger rise in temperature during such a transition should be expected.

In similar experiments carried out at -35 °C, partial thawing was detected like in the case of the sample pressurized at -25 °C (data not shown), however the temperature decrease was smaller, indicating a lower extent of thawing. The complexity of the phase transitions at -25 °C and the uncertain amount of frozen water during the pressure holding time were likely to cause problems in the reproducibility and interpretation of inactivation experiments. Hence, -45 °C was chosen as the temperature level of the microbial experiments as the major focus of this work was to evaluate the effect of solid - solid phase transitions on microbial inactivation.

Magnusson reported the same phase transitions effects in frozen yeast suspensions during the development of a freeze-press (Magnusson 1977a). He also detected the melting of frozen samples upon pressurization at about -20 °C and the direct phase transition to ice III at considerably lower temperatures. Hence, these reports support the findings described here, however, it has to be stressed that the processes are difficult to compare as the dynamic extrusion of frozen material is not the same as the pressure treatment of a frozen sample in a sealed pressure vessel.

In order to examine, whether ice II or ice III was formed; a set of experiments was carried out to elucidate this phase transition behavior. Water samples were frozen to temperatures of -45 °C and -60 °C and compressed to 250 MPa, during the compression a phase transition to ice II or ice III was clearly detected. At this pressure, the sample was warmed above the transition line ice II – ice III like it is shown in Figure 4.16. During heating of the samples which were compressed at -45 °C no transition was detected, whereas samples compressed at -60 °C showed a clear endothermic phase transition along the ice II – ice III transition line that was going along with was accompanied with a slight pressure increase, like it is shown in Figure 4.16. The transition is clearly a ice II to ice III transition, which was never shown in experiments including temperature measurements before. Melting of ice I along the extended phase transition line of water might also be possible at these conditions; however, a notable pressure loss would accompany such a transition.

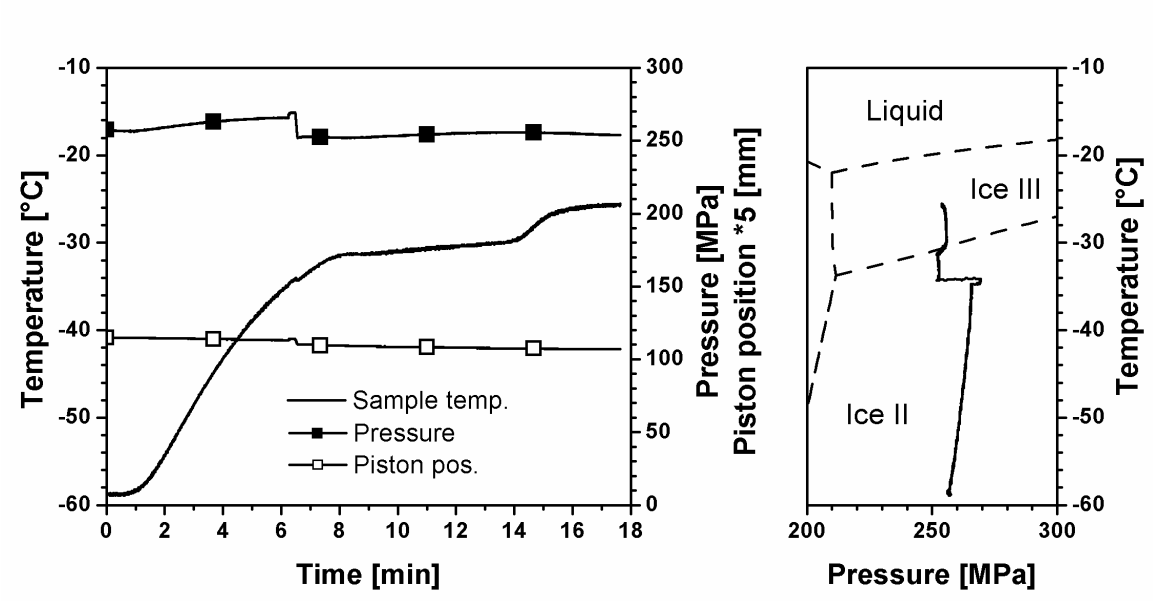

Figure 4.16 Phase transition of water from ice II to ice III. The pressure drop at 6 minutes arises from external pressure correction, as indicated by the piston position of the intensifier. Note the endothermic transition event at 14 minutes, -31 °C, 255 MPa, which is on the transition line ice II – ice III.

Bridgman (1912) noted that ice II can never be superheated above its transition line, so that a transition similar to melting occurs, due to the relatively large enthalpy difference (see Table 2.2). Later this behaviour was confirmed (McFarlan 1936). The author also stated that ice III would never transform to ice II during cooling. He explained the relationship with big differences in crystal structure between ice II and ice III. Another group reported that ice II was formed at temperatures of -73 °C, because at temperatures of -30 °C and above melting of ice I occurred (Lobban, Finney & Kuhs 2000). These reports are all in agreement with the phase transition behavior between ice I, II and III that was described here.

It was concluded, that samples compressed at -60 °C were usually converted to ice II, while samples compressed at -45 °C were usually transformed to ice III. It was not possible to check individually for each sample which ice modification was formed, however, knowing these limitations the ice formed during compression at -45 °C or higher will be referred to as ice III. As noted above, the volume changes are very similar, so the effect on a biological sample should be the same. Inactivation experiments of microorganisms treated at 300 MPa, -60 °C, compared to -45 °C are shown later.

Solid – solid phase transition experiments in the region of the highest interest at about -45 °C were also carried out with the aforementioned solutions of sucrose and sodium chloride. This was done in order to get a complete picture of phase transitions of these solutions in the pres-

sure range to 300 MPa and to get insights in the general solid-solid phase transition behavior of high concentrated solutions. Phase transition points are shown in Figure 4.17 as the onset points of the transition during compression and decompression. The onset points are by definition the first points at which notable differences from the continuous behavior are recorded. During compression this is the last pressure-temperature combination before the pressure drop of the transition and during (slow) pressure release the last point before pressure increase indicates the beginning of the ice III to ice I transition. Regarding the points in Figure 4.17 it has to be added, that during the transition of these relatively high concentrated solution partial thawing like in Figure 4.15 (part A) was detected, despite the low temperature. So no "pure" ice I – ice III transition was achieved. Nevertheless all phase transition points are in a region of about 50 MPa above the transition line (or below, respectively, during decompression). In some cases the transition in higher concentrated solution of sucrose 50% (w/w) was shifted to higher pressure (290 MPa), however in these solutions the phase transition was blurred due to lower water content. Dunand, Schuh & Goldsby (2001) showed phase transition in the same area supporting the finding in Figure 4.17. However, they attributed the transition to ice II and did not take into account that ice III can still form at these temperatures.

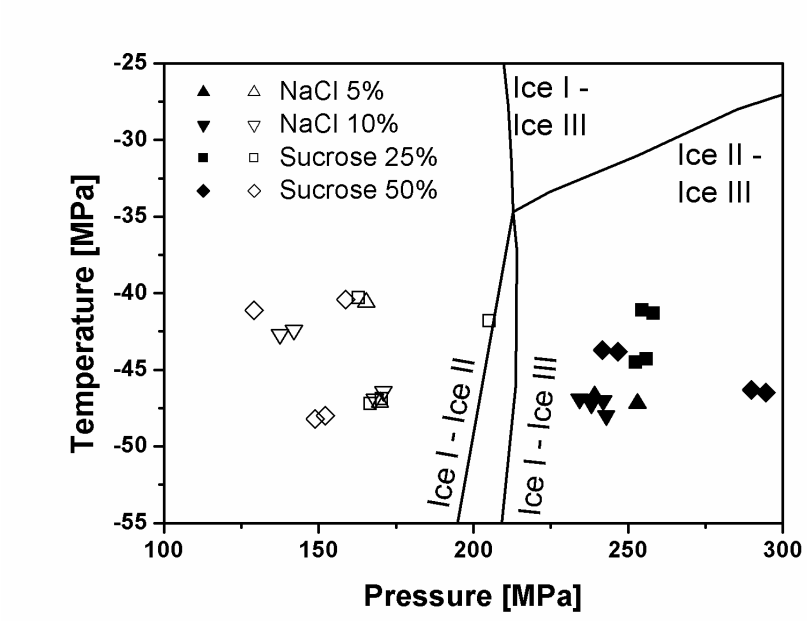

Figure 4.17 Phase transition points to ice III of frozen sucrose and sodium chloride solutions. Full symbols: onset point of transition to ice III during compression; open symbol: onset point of transition to ice I during compression; concentrations of solution (w/w); solid lines: phase transition lines of water as indicated including the extension of the iceI-iceIII line, see Figure 2.7.

4.1.10 Monitoring of high pressure treatments at subzero temperatures

During the pressure treatments of frozen biological matter for every new sample type the phase transition of the samples to ice III was first checked by treating the sample with a thermocouple at the sample center. During later experiments, especially when evaluating microbial counts after treatment, the temperature measurement inside the sample was not possible. However, the preliminary trials made it possible to identify the phase transition precisely, so that treatment of the sample with the desired phase transition was guaranteed.

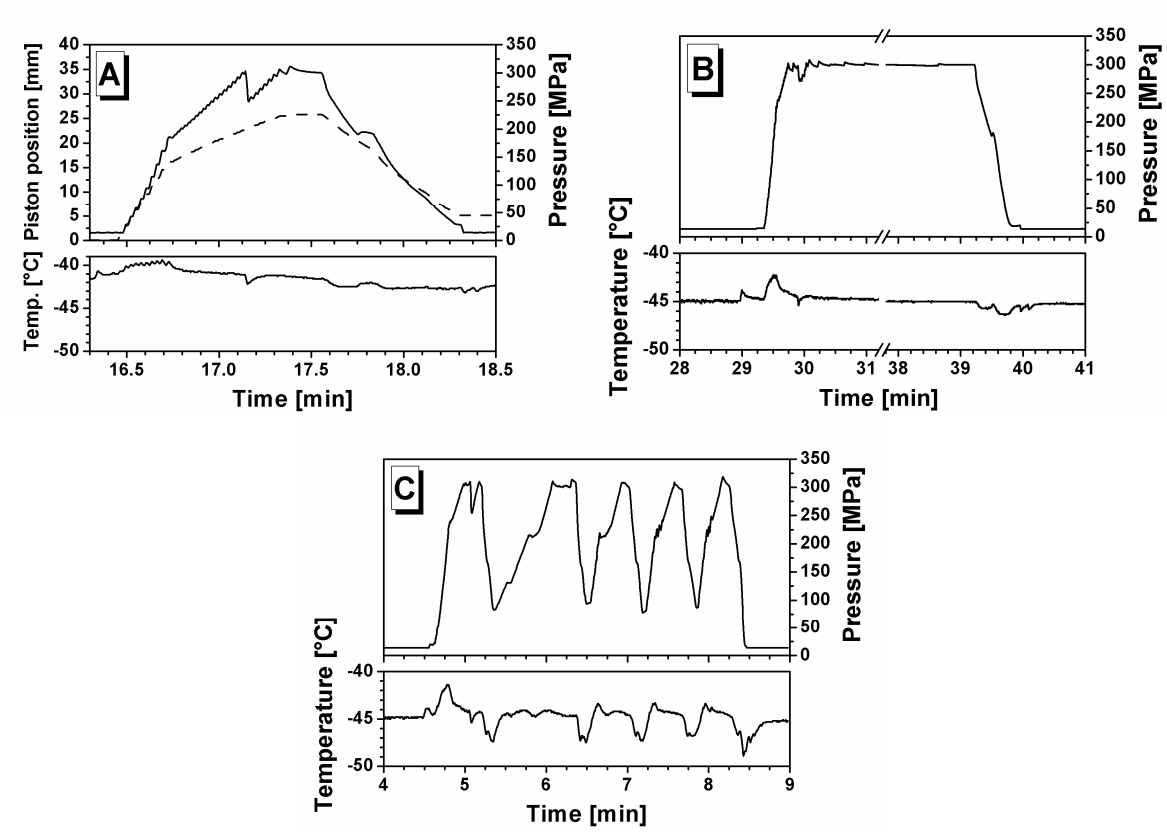

Figure 4.18 Measurement of transient ice III phase transition in buffer solution during microbial inactivation experiments with temperature probe inside the sample in the Unipress lab scale system. Sample: A,B: PBS inoculated with *L. innocua*, C: PBS inoculated with *E. coli*. Experimental conditions are denominated as follows: A: 300 MPa, -45 °C, 0 min; B: 300 MPa, -45 °C, 10 min; C: 300 MPa, -45 °C, 5 cycles. Dashed line in part A is piston position, solid line is pressure.

A lot of the experiments were carried out with microorganisms suspended in buffer solution (phosphate buffer saline) according to the results of the preliminary phase transition test shown in Figure 4.18. In part A, the phase transition occurred after 17.1 minutes, as indicated by the pressure drop, while the piston of the intensifier is not moving backwards. After some seconds at maximum pressure the pressure was released and the phase transition back to ice I

was clearly visible. Such short-time treatments are referred to as treatments with "0 minutes" pressure dwell time. The time at maximum pressure was never longer than 30 seconds, usually much shorter. The duration of a whole pressure cycle was in practice never above two minutes, as shown in Figure 4.18 A. Depending on the operator, the complete time under pressure was usually 30 to 60 seconds.

In part B of Figure 4.18 a treatment with a longer pressure holding time is shown. In this case, the phase transition occurred delayed after about 15 seconds at maximum pressure. This behavior was sometimes noted, but the transition was clearly identified by the pressure drop in each of the treatments. During holding times up to 10 minutes no other phase transition events occurred. In part C a treatment with multiple pressure cycles is shown. Here an interesting "memory effect" was visible after the first cycle. The first phase transition to ice III occurred suddenly, completely and fast during compression at about 250 MPa or above. However, during the next pressure cycles the phase transition was setting in soon after crossing the phase boundary at about 220 MPa with every stroke of the hand pump, so for a while the pressure was not rising during compression until the ice was (assumably) completely converted to ice III. Obviously, like in the case of other memory effects, some structure or remaining ice III nucleus was facilitating the next transition to ice III. During decompression no such differences were found.

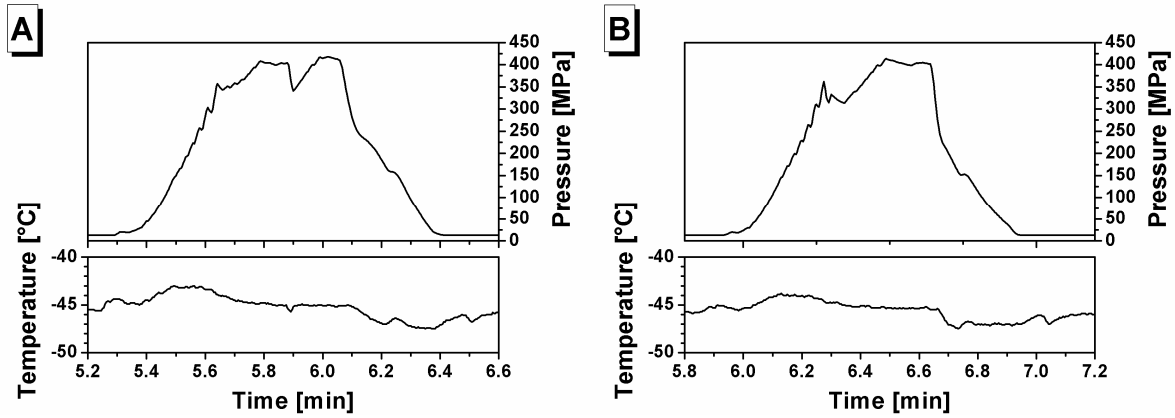

Figure 4.19 Measurement of transient ice III phase transition in food samples during microbial inactivation experiments with temperature probe inside the sample in the Unipress lab scale system. Sample: A: ground beef inoculated with *L. innocua*, B: vanilla ice cream inoculated with *L. innocua*. Experimental conditions are denominated as 300 MPa, -45 °C, 0 min.

In Figure 4.19 the phase transition is shown in two food samples (ground beef and ice cream) with a thermocouple inside the sample. The phase transition in this system sometimes occurred delayed at the maximum pressure, however, never later than 30 seconds after reaching

the maximum pressure. In ice cream samples the extent of the pressure drop during the phase transition was less pronounced due to the lower water content. Again, all phase transitions were proven by the online pressure monitoring.

The high internal volume of the pilot plant scale Uhde pressure system allowed the treatment of several samples in one experiment. Figure 4.20 shows a typical temperature and pressure measurement during a treatment of eight individually packed 50 ml samples of buffer solution that were. The temperature probe inside the vessel was located in the pressure transmitting fluid.

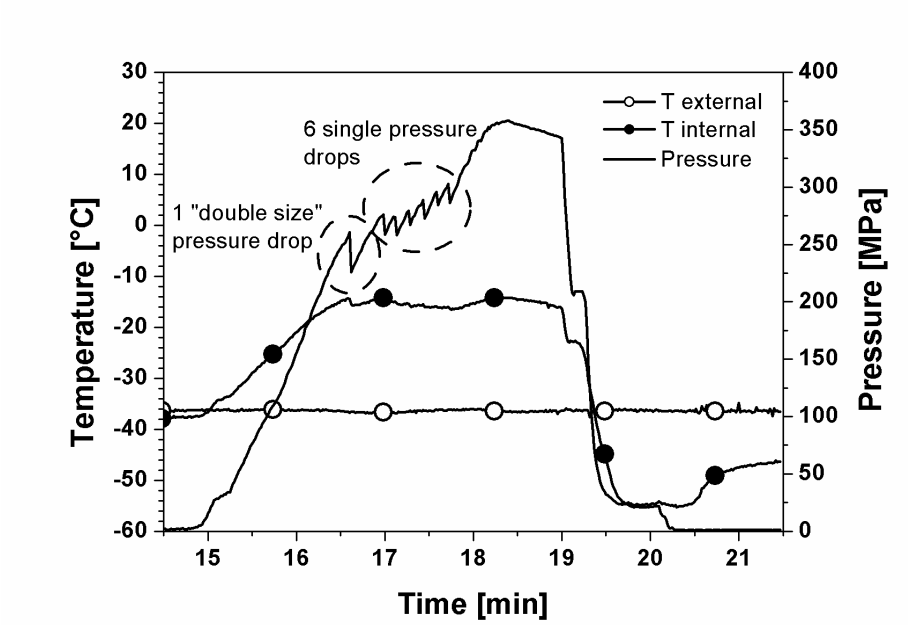

Figure 4.20 Measurement of transient ice III phase transition in the Uhde pilot plant scale system with eight 50 ml samples of buffer solution. Temperature was measured in the pressure transmitting medium (T internal) and in the cooling jacket (T external). Experiments with pressure holding times of less than one minute at maximum pressure in pilot plant experiments were denominated as “0 minutes” holding time.

During the pressure build-up small pressure drops were noted which could be counted later according to the number of samples inside the pressure rig. This shows the individual phase transition of each sample and underlines the stochastic character of nucleation even in this solid-solid transformation. In Figure 4.20 the first two samples undergo a phase transition at the same time (about a double pressure drop, while the samples were equally sized), followed by the six other samples which changed phase one by one. It was not possible to count these events during the experiment, so a pressure dwell time of one minute was realized (and defined as “0 minutes” treatment) in order to assure that the phase transition of all samples occurred. Due to the quasi adiabatic heating the temperature in the pressure medium was rising

faster than in water or the aqueous samples. These temperatures may lead to thawing of the outer edge of the bigger samples during the treatment as these temperatures are above the freezing line at that pressure. Furthermore it must be taken into account that the temperature distribution in such a pressure vessel is varying considerably, like shown in fluid dynamical modelling (Hartmann & Delgado 2003; Hartmann, Schuhholz et al. 2004), however, the thermocouple position shown here was close to the upper end of the vessel about 15 cm from the top, so that the lower parts of the vessel should be colder.

4.1.11 Phase transition lines of pure fatty acids and food fats

Figure 4.21 shows cooling curves of two of the lipids that were examined. The left diagram shows cooling of pure stearic acid (C18, saturated) with a pronounced plateau temperature which is as constant as it can be expected for a pure substance. It was concluded that phase transition points under pressure can be obtained by pressure manipulation during crystallization to obtain multiple phase transition points in one crystallization experiment. In the right part, the cooling of partly hydrogenated rape seed oil ("rapeseed 24") was examined under pressure. Two different crystallization events were obtained. The small first peak was identified as α – crystallization according to analogies in curves given in literature (Wilton & Wode 1963; Riiner 1970) and due to experiments at respective ambient pressure experiments in which the optical appearance of the fat was without doubt characterized as α, which is described as coarse waxy translucent crystals. Accordingly the same was possible with the second peak which was harder white fat, however it cannot be identified optically and by the cooling curve if it was β or β' crystals.

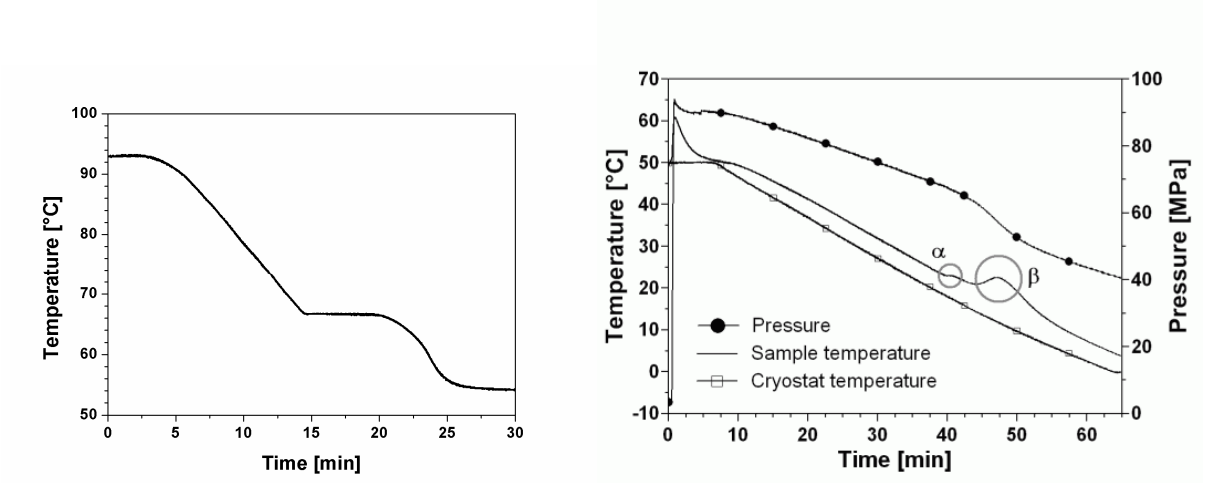

Figure 4.21 Cooling curves of lipids used in the experiments. Left: stearic acid at ambient pressure; right partly hydrogenated rape seed oil under pressure.

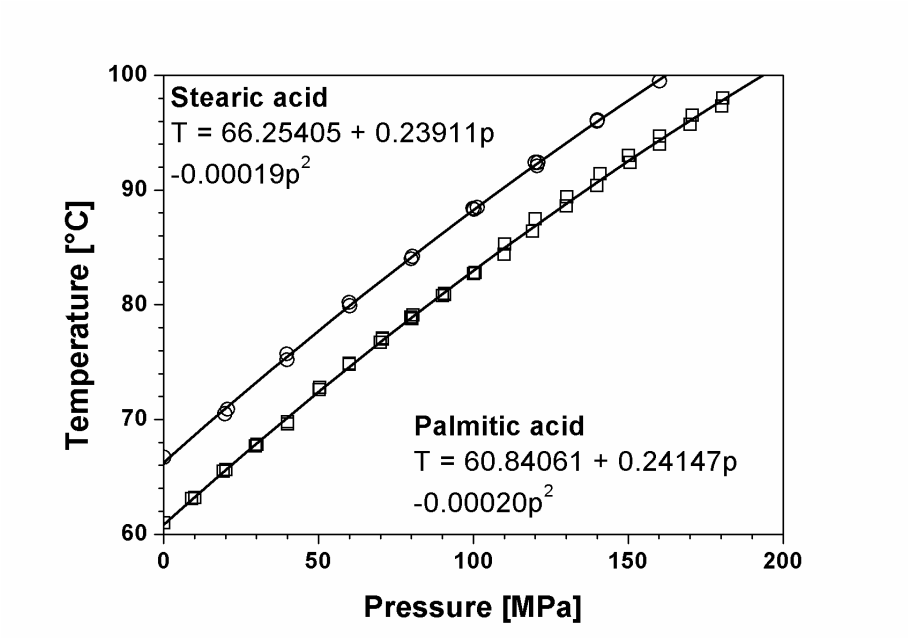

Figure 4.22 Phase transition points of pure fatty acids as obtained by pressure manipulation during crystallization.

The phase boundaries of two pure fatty acids are shown in Figure 4.22. A curve fit of a second order polynomial function revealed a slight curvature of the points; however, a linear function would give results which are only slightly less precise in terms of degree of determination. More pronounced curvature was found in other experiments with fatty acids in literature (Yokoyama et al. 1998). While in general it is assumed that fats have a linear phase boundary under pressure, it is concluded that the curved appearance of the phase transition of fatty acids should in principle exist in complex edible fats and oils as well, however, this is practically not detectable due to difficulties in fat crystallization measurement as mentioned in the literature review. Heremans (2002) stated that the elliptical phase diagram of a two state transition transforms to a linear curve if differences in compressibility, thermal expansion and heat capacity between the two phases vanish, like it is the case for most lipids. This leaves however space for curvature of lipid transition curves if slight differences still exist.

The phase behavior of rapeseed 24 is shown in Figure 4.23 by representative cooling curves, like the cooling curve from Figure 4.21, plotted in the pressure - temperature phase diagram. Phase transition points of some additional cooling curves that are not shown in detail were added. It should be noted that melting points of the fats are higher than the crystallization temperatures. α and β (which might also be β') phase transition shifted to higher temperatures under pressure. The α transition temperature peak was only very small and it was not detected above 120 MPa. β was more varying in temperature values, but was clearly detectable up to

the maximum pressure experiment at 170 MPa. The slopes of α and β phase boundaries were not the same since the Clausius-Clapeyron equation shows that the slope is governed by latent heat and volume change which is different for the two transitions.

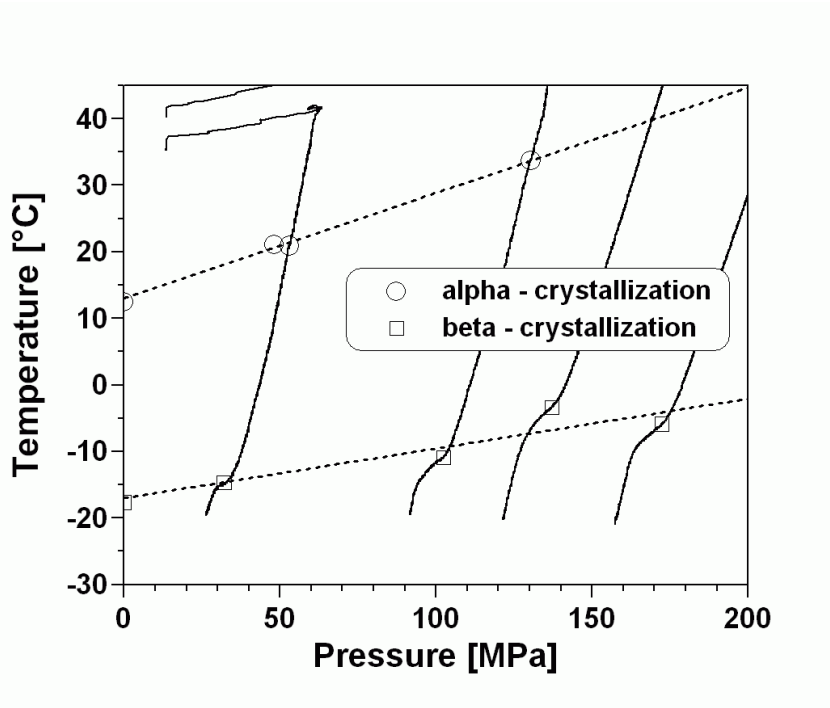

Figure 4.23 Crystallization points of partly hydrogenated rape seed oil under pressure.

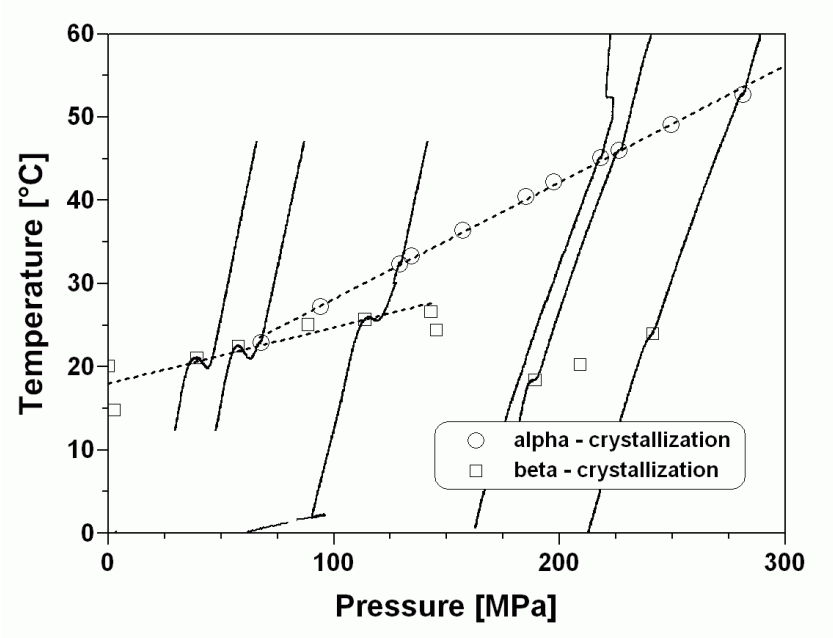

Figure 4.24 Crystallization points of hydrogenated copra oil (Palmin) under pressure.

The phase behavior of hydrogenated copra oil revealed some interesting details, though not all can be explained. At ambient pressure no α transition was found. However, under pressure of

60 MPa an α transition was noted which was very close to the β (or β') transition. Due to differences in slope of the two transitions that was also found in rapeseed 24 the phase was more clearly distinct from the β phase at higher pressure. The α phase was clearly detectable in the whole higher pressure range. The temperature peak of the β transition however was under pressure becoming less pronounced and was not detectable in the range from 160 to 190 MPa as shown by one cooling curve which showed only α transition. However, at the higher pressures of 190 MPa and above another crystallization was noted which is shown in the diagram as β even though its nature is unclear. Possibly the crystallization up to 160 MPa was β' and the transition at 190 MPa and above was β which has a lower crystallization point at ambient pressure. Other explanations are however possible as well, like a completely different only pressure stable crystal form.

It should be noted that these phase diagrams of two examples of edible fats serve only as an example to demonstrate the possibilities that pressure opens for fat crystallization. The melting point and crystallization point in food fats are not identical, which makes it possible to induce stable fat crystals by pressure. Palmin melted and tempered at 35 °C was e.g. stable crystallized after pressure treatment at 600 MPa, 30 °C, 10 min in a Unipress U 4000 pressure vessel. Potentially it might be possible to induce other crystal forms under pressure or to obtain desired fat crystals by pressure for example in complex systems with high commercial value like cocoa butter / chocolate. DSC and NMR experiments preferably under pressure are necessary to identify crystal changes directly and precisely.

4.2 Damage of microorganisms during frozen storage

4.2.1 Treatment parameters

A frozen storage experiment of microorganisms was designed to evaluate cell damage during frozen storage by flow cytometry and to get insights in the damage mechanisms and potentially in the location of ice crystals, which can be intracellular or extracellular. The location of ice is crucial to evaluate the later experiments of pressure treatments of frozen food. The object of investigation were suspensions of two microorganisms in buffer solution (PBS). *Listeria innocua* as a model for cold resistant bacteria was compared to probiotic *Lactobacillus rhamnosus* GG which is a of potential interest to survive freezing as a storage method, but still it is also more freeze-susceptible than *L. innocua*. It was not possible to carry out experiments in a real food matrix, due to flow cytometry analysis. The inoculum level was about 10^7 cfu/ml to make conditions a little more realistic, however, it could be set lower, as a considerable number of cells was necessary for flow cytometry.

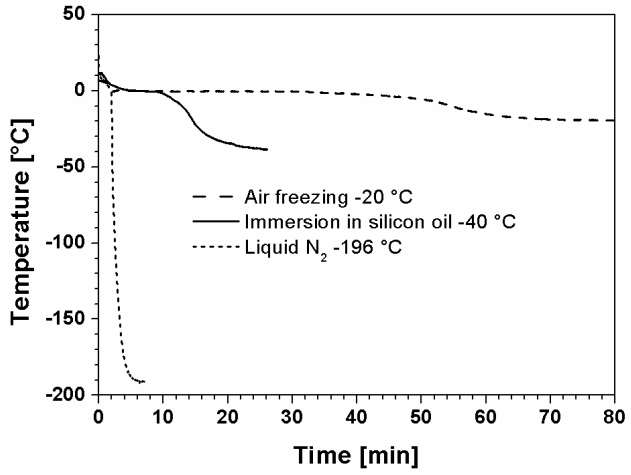

Figure 4.25 Freezing profiles of samples for storage test of bacteria frozen in buffer (PBS). Sample was a Greiner centrifuge tube (30 mm x 115 mm) filled with 35 ml of PBS inoculated with *Lactobacillus rhamnosus* GG.

As the major part of the experiment two freezing conditions, slow freezing in air and somewhat faster freezing by immersion in cold silicone oil were selected and combined with two different storage temperatures, as indicated in Table 4.6 and Figure 4.25. Freezing in liquid nitrogen with subsequent storage at -80 °C was used as a comparison which is known to obtain the viability well, as it is used to store bacterial cultures. Thawing was standardized and cautiously monitored, however not varied as an experimental parameter, as the number of

samples was limited. It should be noted that very slow thawing might lead to additional cell death, so that inappropriate non-standardized conditions may lead to experimental error.

Table 4.6 Treatment conditions of samples for evaluation of freeze damage in bacteria.

Sample reference	Freezing conditions	Cooling rate [K min^{-1}]	Freezing rate [K min^{-1}]	Storage temperature [°C]	Thawing
A -20/-20	Air blast cabinet, -20 °C	0.4	0.2	-20	Immersion in silicone oil, +20 °C
B -20/-40	Air blast cabinet, -20 °C	0.4	0.2	-40	
C -40/-20	Immersion in silicon oil, -40 °C	2.0	1.3	-20	
D -40/-40	Immersion in silicon oil, -40 °C	2.0	1.3	-40	
E -196/-80	Liquid nitrogen, -196 °C	370	140	-80	

For definition of freezing and cooling rate see chapter 2.1.2.

Flow cytometry makes the evaluation of cells on a single cell basis possible. By using different stains, conclusions regarding physiological parameters possible. In this examination two stains were used simultaneously. Propidium iodide (PI) enters cells with damaged lipid membranes, as it does not pass intact membranes, subsequently it binds to DNA giving a stable red fluorescent color. Carboxyfluorescein diacetate enters all cells as it diffuses through the membrane. It is split if active esterase is present giving green fluorescent carboxyfluorescein (CF) which cannot pass the membrane anymore, giving a stable colored green cell, indicating essentially only active esterase, however, it can be seen as an indicator of active cellular enzymes in general. Green colored cells also indicate cell integrity, as CF can only be retained if the cell membrane is not damaged. A third parameter derived can be obtained by adding glucose to CF colored cells, which are in buffer solution in a passive state due to absence of energy rich substrate. By metabolizing glucose, ATP is produced making active ATP-driven membrane transport of CF possible. Hence, viable cells lose their green color upon glucose addition. Gates were set in the PI vs. CF plot to discriminate different subpopulations (see Table 3.1). To show all treatments efficiently in diagrams, the following parameters were defined: PI colored cells are all cells in gate 1 and 2, CF colored cells are all cells in gate 2 and 4 and the CF extrusion activity is defined as the number of cells in gate 2+4 before incubation minus cells in gate 2+4 after glucose incubation.

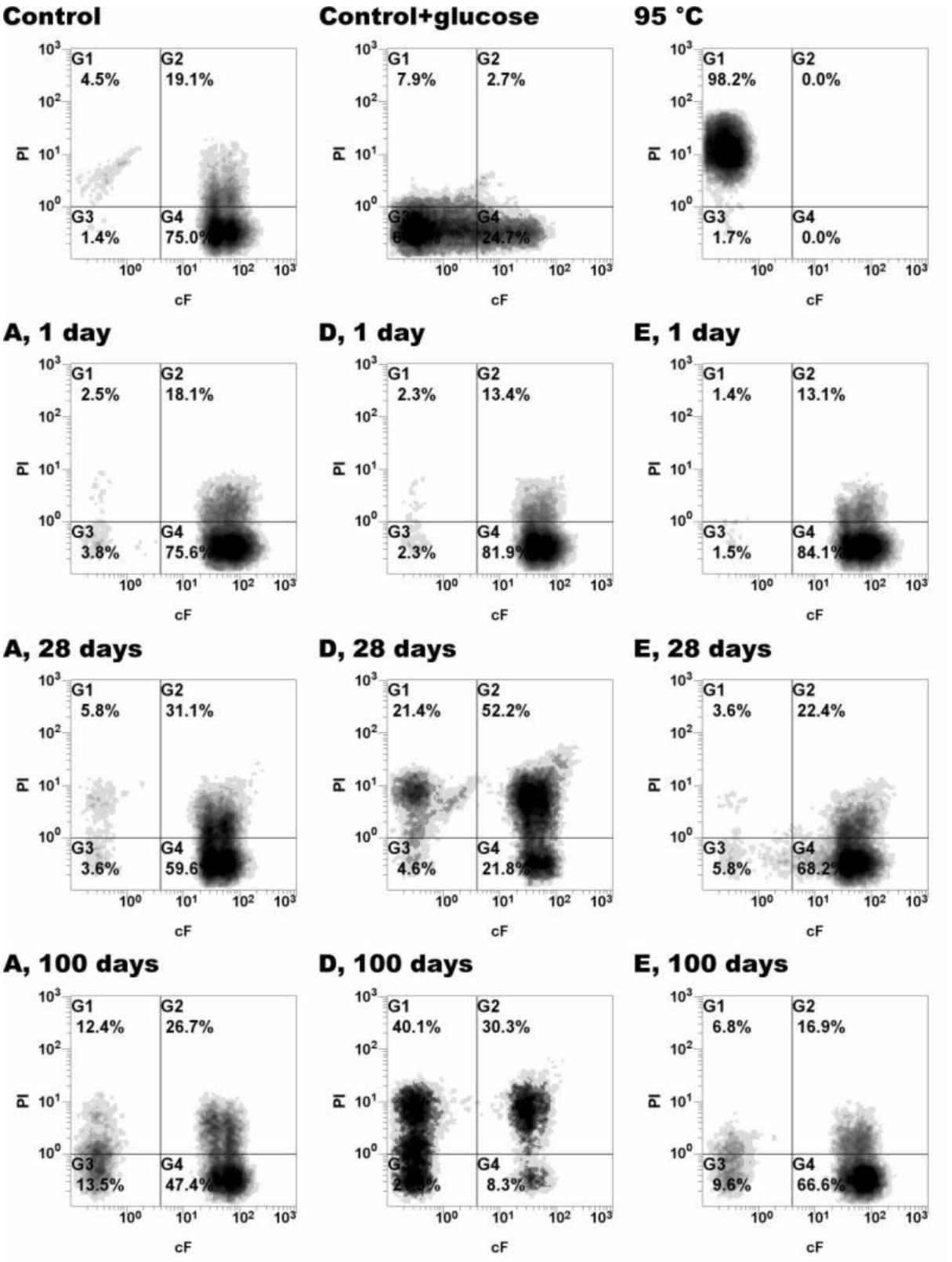

Figure 4.26 Selected flow cytometry results of *Listeria innocua* stored in frozen buffer solution (PBS): plots of PI colored cells versus CF colored cells. Treatment conditions A -18°C/-18°C, D -40°C/-40°C, E -196°C/-80°C, see also Table 4.6.

4.2.2 Freezing and frozen storage of *Listeria innocua*

Untreated control samples in Figure 4.26 are colored by CF but not by PI (gate 4), control samples activated by glucose lose also their green color (gate 3). Completely inactivated cells (heat treated at 95 °C) are PI colored, due to membrane damage, but cannot form CF anymore, due to enzyme inactivation (gate 1). A part of the population of *L. innocua* always is PI colored as indicated by the control (gate 2), which was observed also in many other studies. The glucose driven CF exclusion is always slower than in LGG, even though double incubation time was used.

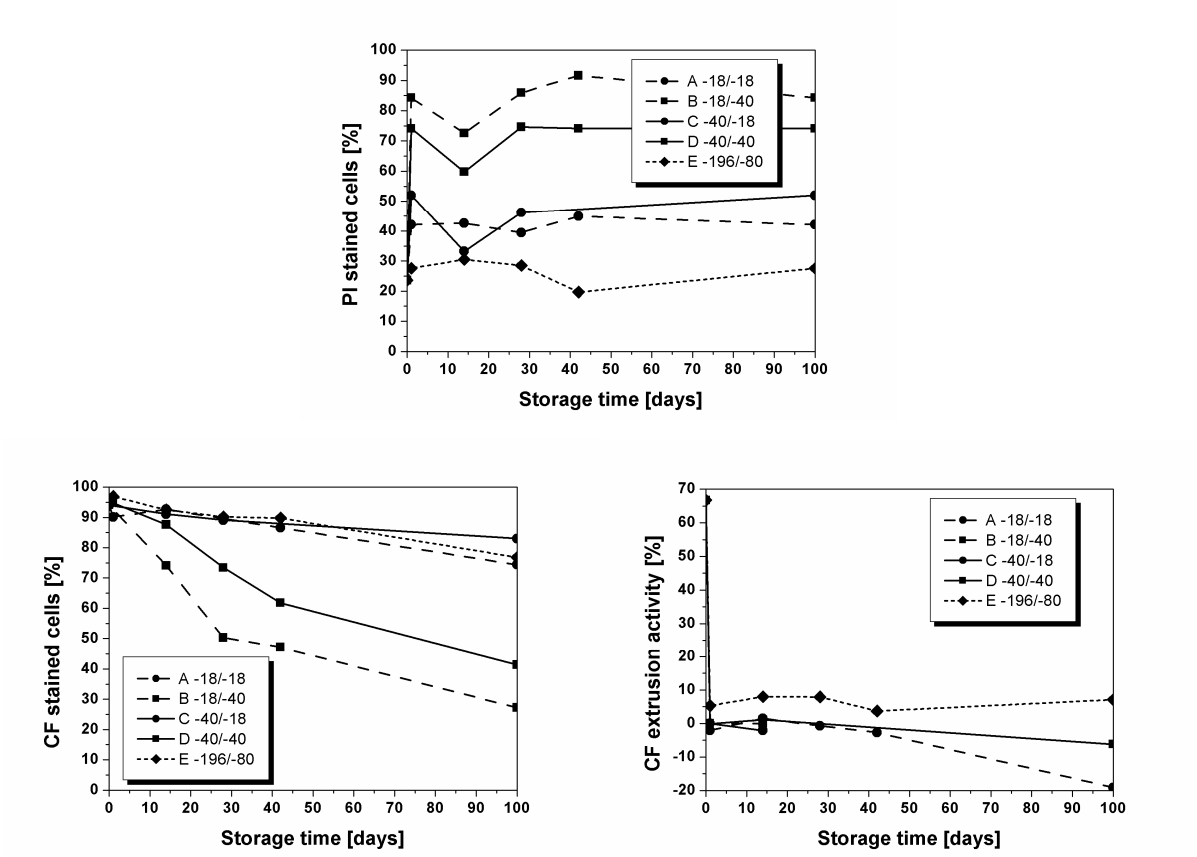

Figure 4.27 Evolution of flow cytometry parameters PI stained cells, CF stained cells and CF extrusion activity of *Listeria innocua* frozen in buffer solution during storage for 100 days. Freezing and storage parameters as indicated and in Table 4.6 (first number: freezing temperature, second number: storage temperature).

PI stain results in Figure 4.28 indicated an increase in PI stained cells already after one day of frozen storage especially for cells stored at -40 °C, whereas cells stored at -18 °C exhibited a PI colored cell fraction of 40 to 50 %. Cells frozen in liquid nitrogen and stored at -80 °C (sample E) did not show remarkable increase of PI colored cells. During storage the values for PI stain did not change markedly, the transient decrease at 14 days of storage should probably be attributed to inexplicable deviations during thawing or staining. Anyway it should be borne

in mind, that deviation of a few percent in flow cytometry are always possible. Results shown here are averages of two separate storage samples, which explains deviations in values of Figure 4.26 and Figure 4.27. CF stain results showed that both samples stored at -18 °C, as well as cells stored at -80 °C did not show changes after one day and only a slight decrease to 80 to 90 % CF stained cells after 100 days of storage. *Listeria* cells stored at -40 °C did not show changes after one day of storage, but during 100 days the CF values decreased considerably to 27 % (sample B frozen at -18 °C) and 41 % (sample D frozen at -40 °C). Sample B also showed somewhat higher PI values.

The flow cytometric profile of PI versus CF plot indicated little qualitative change for samples stored at -18 °C and -80 °C (A, C, E) while samples B and D, stored at -40 °C showed a movement from gate 4 to gate 2 and later to gate 1, indicating increasing cell damage as shown by esterase activity and cell membrane integrity. The occurrence of cells in gate 2 is somewhat contradictory, as it indicates enough membrane damage to allow passage of PI, however, CF is still retained inside the cell. In fact, it indicates cells are highly stressed and damaged, however, they show still some viability and may potentially be able to resuscitate in optimal conditions after thawing. Similar effects were shown for high pressure treated bacteria, which usually show high numbers of damaged but repairable cells (Ananta et al. 2004).

CF extrusion activity which is anyway slow in *Listeria innocua* in contrast to LGG was not detectable after freezing in all samples, except samples E, which showed some remaining activity of CF extrusion throughout storage. Negative values indicate that more cells were CF stained after glucose incubation than before, which is not difficult to explain. It might be the case that glucose enables some repair mechanism in cells making a recovery of esterase activity possible, but this assumption is quite speculative.

In summary, these results clearly indicate that storage at -40 °C is more detrimental to *L. innocua* than at -18 °C. The rate of freezing showed no considerable influence. Freezing in liquid nitrogen and storage at -80 °C was giving the best results which was expected. The viability on microbial plates, which essentially only differentiate life or dead cell, was only performed after storage of 100 days (Table 4.7). Samples A and C showed 3 to 5 % viable cells, in sample E still half of the cells were able to grow on agar. More than 99 % of samples B and D were inactivated. These results are substantial agreement with the flow cytometer findings.

4.2.3 Freezing and frozen storage of *Lactobacillus rhamnosus* GG

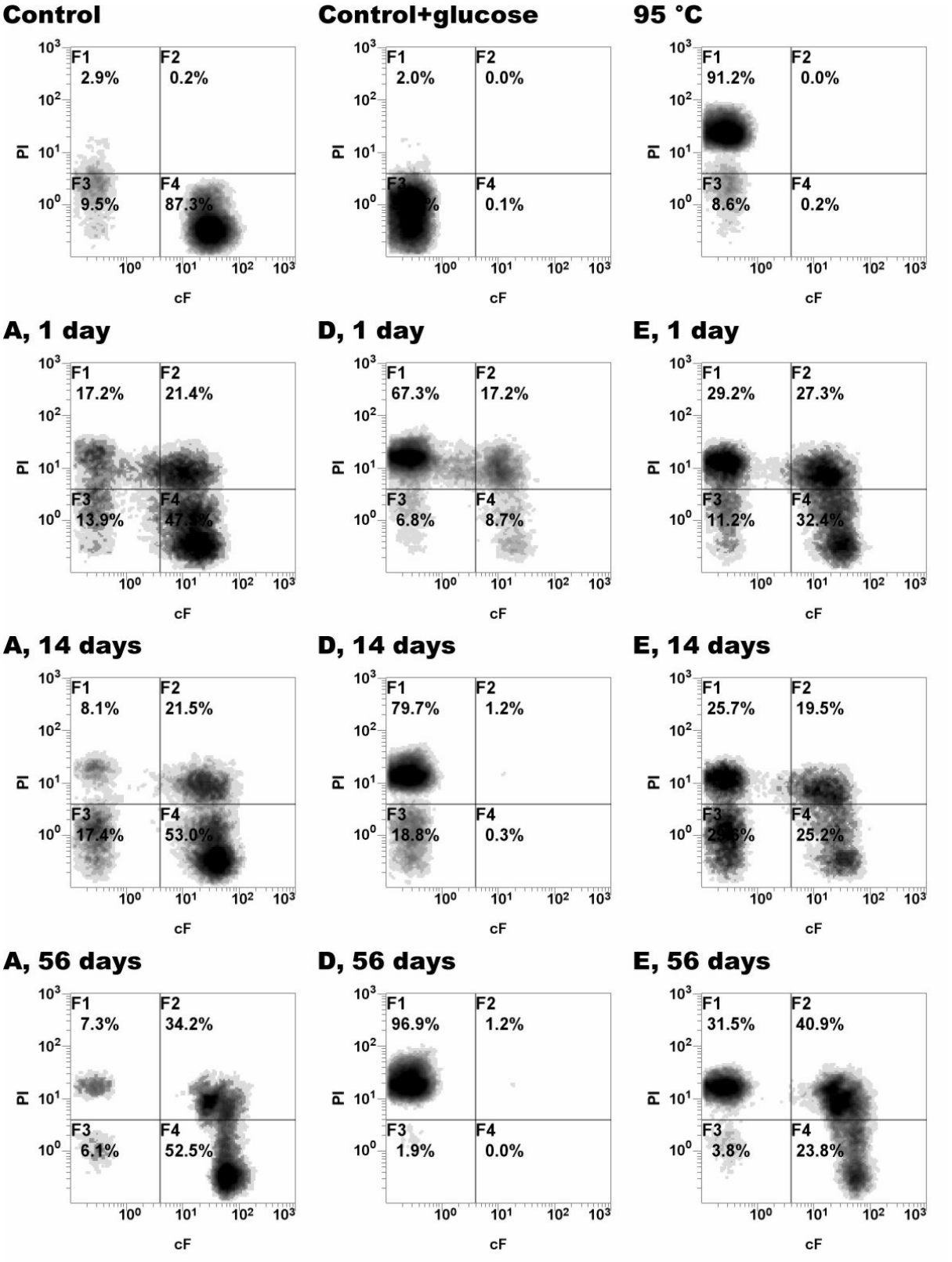

Figure 4.28 Selected flow cytometry results of *Lactobacillus rhamnosus* GG stored in frozen buffer solution (PBS): plots of PI colored cells versus CF colored cells. Treatment conditions A -18°C/-18°C, D -40°C/-40°C, E -196°C/-80°C, see also Table 4.6.

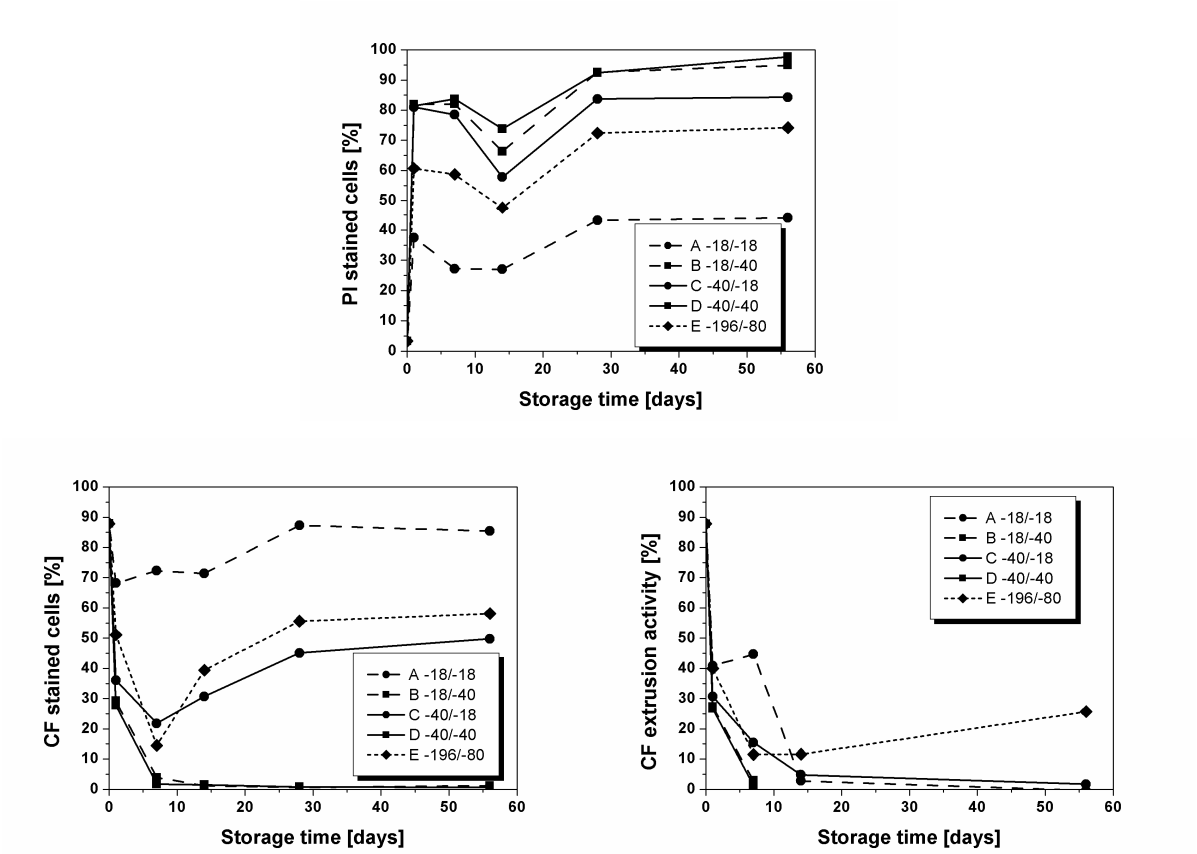

Figure 4.29 Evolution of flow cytometry parameters PI stained cells, CF stained cells and CF extrusion activity of *Lactobacillus rhamnosus* GG frozen in buffer solution during storage for 56 days. Freezing and storage parameters as indicated and in Table 4.6 (first number: freezing temperature, second number: storage temperature).

The results for *Lactobacillus rhamnosus* GG are summarized in Figure 4.28 and Figure 4.29. The overall freeze damage was higher for all treatments even after frozen storage of only one day. It should also be noted, that the total frozen storage was terminated after 56 days in contrast to100 days for *L. innocua*. However, the same trends of freezing damage in relation to storage and freezing temperature are visible. PI stain of sample A was lowest, while samples B, C and D showed detrimental membrane damage already after one day of frozen storage. Surprisingly, freezing in liquid nitrogen also induced membrane damage of 60 % after one day as detected by PI stain. Esterase activity was not present anymore in samples B and D after 1 week, sample A showed CF color in 70 to 85 % of the cells until day 56. Samples E, but also C, showed about 50 % of CF colored cells at the end of the storage period. For both parameters, CF and PI, a slight increase is notable, however, this is not explainable for CF and could caused by experimental error. Also the minima at 7days (CF) and 14 days (PI) should not be overestimated. CF extrusion was more robust in LGG and still detectable in all samples

after 7 days of storage, while it decreased afterwards, except for sample E which showed remaining extrusion activity until day 56.

The inactivation of LGG was examined throughout the storage. It can be found that sample A is less stressed than the samples B and D, showing still 17 % survival after 28 days. However, during the next 28 days this viability vanished. Sample is C is still somewhat more viable than sample B and D until that day. Even though CF and PI indicated more damage to sample E than for sample A, a lot more cells are able to resuscitate.

Table 4.7 Survival of *L. innocua* and *LGG* as detected by plate count standard methods during storage in PBS buffer.

	Listeria innocua									
	log (N/N_0)					**Percentage [%]**				
	A	**B**	**C**	**D**	**E**	**A**	**B**	**C**	**D**	**E**
100 days	-1.3	-3.0	-1.4	-2.3	-0.3	5.2	0.1	3.8	0.5	54.4

	***Lactobacillus rhamnosus* GG**									
	log (N/N_0)					**Percentage [%]**				
	A	**B**	**C**	**D**	**E**	**A**	**B**	**C**	**D**	**E**
1 day	-0.3	-0.6	-0.6	-0.5	-0.4	54.7	24.8	24.8	32.3	38.5
7 days	-0.2	-1.6	-0.9	-1.4	-0.4	62.1	2.7	11.8	3.9	41.0
14 days	-1.2	-2.2	-1.5	-2.0	-0.4	5.8	0.6	3.0	1.1	41.0
28 days	-0.8	-3.3	-1.4	-2.9	-0.4	17.4	0.04	3.6	0.1	37.3
56 days	-4.3	-3.6	-4.2	-4.1	-0.5	0.01	0.02	0.01	0.01	31.1

Treatment conditions A to E as indicated in Table 4.6. Inoculum size for *L. innocua* 1.25E8, *LGG* 8.05E8

For LGG the same relationships as for *Listeria innocua* apply. However, it seems that even short contact with -40 °C during freezing (about three hours) was quite damaging, even when the samples were stored at -18 °C (sample C). It is unlikely that cells were frozen at -18 °C and the results indicate that at this temperature level bacteria can persist a considerable time, which is however species dependent.

Storage at -40 °C induced the biggest damage. Regarding the number of PI stained cells it seems reasonable to assume that intracellular ice formed at this temperature, however this is species dependent, too. While LGG was not able to withstand -40 °C and was inactivated quickly, it seems like that in both microorganisms after one week the maximum membrane damage was already obtained as detected by PI. It was shown in literature that intracellular ice formation is like any freezing event a stochastic question of nucleus formation and is clearly taking place even after longer frozen storage (Mazur 2004; Muldrew et al. 2004). Esterase

inactivation was progressing slowly in *Listeria* showing the time dependent inactivation of the enzyme. The general behaviour is in accordance with the model of cell freezing proposed by Mazur (2004) which is summarized in Figure 2.5. Regardless of freezing rate, reaching -40 °C was detrimental instantly, especially in LGG, due to intracellular ice. However, freezing *L. innocua* frozen for only one day at -40 °C probably did result in intracellular ice yet or maybe only in a very limited way. At -18 °C cells are dehydrated and intracellular freezing can be excluded.

The mechanism of cell behavior at -196 °C in buffer solution without cryoprotectant cannot be derived clearly from literature. The formation of intracellular ice is associated with cell death and dehydration at this fast cooling rate seems unlikely. Another possibility is the vitrification of the cell interior, however literature on the vitreous state of bacteria is connected to the application of cryoprotectants, so the state of bacterial cells cooled by liquid nitrogen without additive cannot be elucidated by literature study (Mazur 2004; Muldrew et al. 2004). However, the high viability of cells frozen at -196 °C gives reason to assume that the cells were vitrified.

4.3 Inactivation of microorganisms in the frozen state under pressure

4.3.1 Approach of the studies

As a main part of this thesis, the inactivation of microorganisms in frozen food by making use of pressure induced phase transitions between ice I and ice III was studied. These studies were triggered by the drastic disintegration of plant tissue due to the ice III to ice I transition after freezing to ice III (Luscher et al. 2005, see figure 2.12). Edebo & Heden (1960) showed that disruption of frozen bacteria for biotechnical cell disintegration purposes due to ice I – ice III transitions is possible.

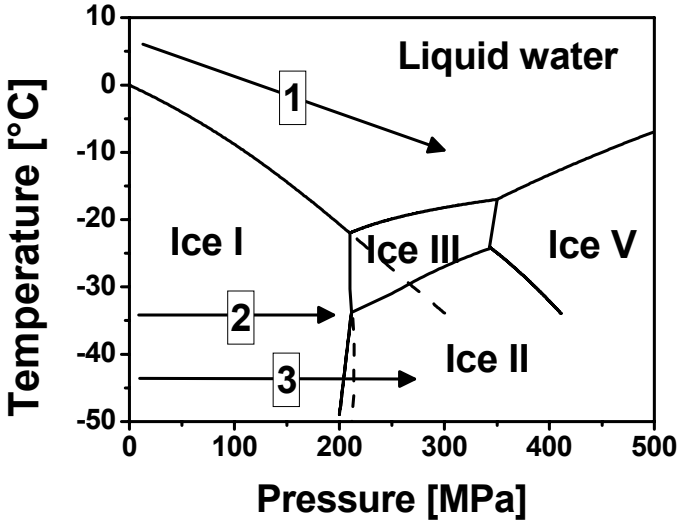

Figure 4.30 Treatment scheme of *Listeria innocua* in buffer solution to identify inactivation mechanisms. (1) pressure treatments in the subzero temperature liquid phase; (2) pressure treatments in the ice I pressure range; (3) pressure treatments in the ice III pressure range including pressure induced ice I – ice III transitions; temperature range for (2) and (3) -25 to -45 °C.

It was first tried to establish processing conditions for inactivation which lead to interpretable and reproducible results and to understand the mechanisms of inactivation at these conditions. To reduce the number of influences, *Listeria innocua* in buffer solution (PBS) was selected as a model. In a first step, the examination covered the investigation of phase transitions at high pressure – subzero temperature conditions in the liquid phase in comparison to pressure treatments of frozen material in the range of -25 to -45 °C, to examine the influence of pressure treatments in the ice phases I and III, as well as the effect of the phase transition (see Figure 4.30). The microbial experiments presented in this section are in close relation with the

developments of treatment conditions presented in chapter 4.1.9, especially Figure 4.15. The mechanism of inactivation was examined by viable cell counts and flow cytometry. Later the examinations were extended to other technical influences like freezing rate, rate of pressure release and scale-up, biological influences by examining other microbial species and effects of the food matrix by applying the findings to selected food systems.

4.3.2 Inactivation of *L. innocua* in liquid and frozen conditions

The inactivation kinetics of *L. innocua* in liquid conditions under high pressure at low temperature was linear as shown in Figure 4.31 (part A) and Table 4.8. The general expectation that the inactivation should be higher at lower temperatures was met, however it remains unclear, if the inactivation was higher due to lower temperature or due to partial freezing during pressure release. The inactivation was time-dependent, like it can be derived from the regression analysis of inactivation as a function of time in Table 4.8. Time-dependent inactivation is the usual behavior found for pressure treatments. The results are in substantial agreement with the inactivation of other microorganisms at these conditions (Hashizume et al. 1995; Perrier-Cornet et al. 2002; Perrier-Cornet et al. 2005; Moussa et al. 2006). During pressure release, freezing of the sample was detected, which was only slight in the case of experiments at 0 °C, however, freezing was more pronounced at -10 °C. This freezing event, which is comparable to pressure shift freezing, exerted additional stress on the bacteria and is presumably one cause of the higher inactivation at 300 MPa, -10 °C.

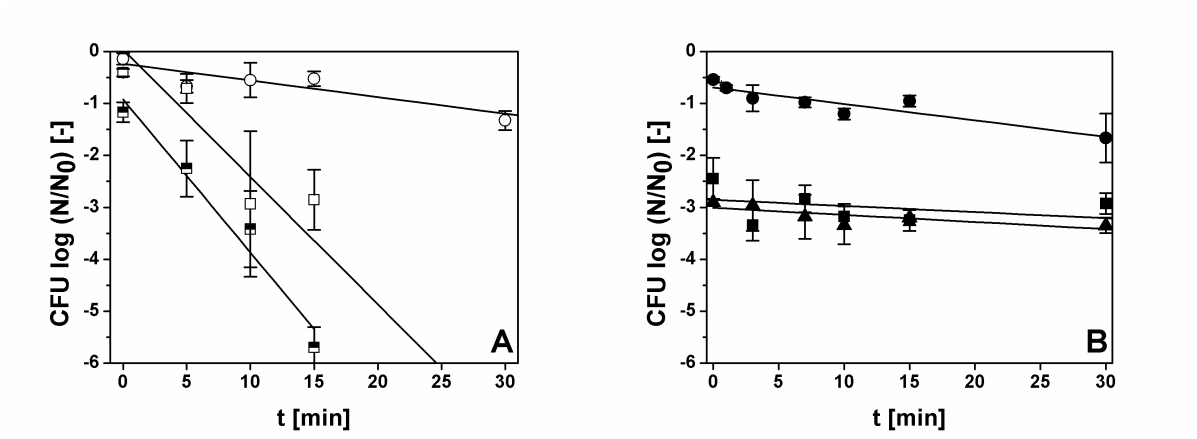

Figure 4.31 Inactivation of *Listeria innocua* in buffer solution at high pressure - low temperature conditions in the liquid phase of water (part A) and frozen at -45 °C (part B). ○ 200 MPa, 0 °C; □ 300 MPa, 0 °C; ⬒ 300 MPa, -10 °C; ● 200 MPa, -45 °C; ■ 300 MPa, -45 °C; ▲ 400 MPa, -45 °C. See Table 4.8 for remarks about regression lines and their coefficient of determination.

In comparison to the experiments in the liquid phase a substantially different behavior was detected during high pressure treatments of frozen microbial suspensions at 300 MPa and 400 MPa (Figure 4.31, part B). It is obvious that the beginning of the regression line is shifted to higher inactivation results. The shift is big enough to exclude the action of pressure during the compression and decompression time as a reason for this behavior. It is also higher than the usual standard deviation during these determinations. However, after this inactivation in the beginning the inactivation is progressing slowly. The inactivation kinetics at 200 MPa and -45 °C are in contrast only slightly different from the inactivation at the same pressure at 0 °C. The shift of the initial inactivation at 0 minutes pressure holding at pressures higher than 200 MPa without leading to time-dependent kinetics of the treatment suggests that a single event during the treatment was responsible for this exceptional behavior. However, the only event being different during these treatments at 300 MPa and 400 MPa was the phase transition from ice I to ice III and back to ice I, which was detected in every experiment at 300 MPa and 400 MPa at -45 °C by the characteristic pressure drop (treatment diagram in Figure 4.15B and Figure 4.18AB). The sudden change in the surrounding crystal structure of the bacteria was going along with a rapid decrease in sample volume (respectively increase during decompression), leading likely to mechanical stress acting on the bacteria.

Table 4.8 Parameters of the regression analysis of the experiments in Figure 4.31 for the linear equation $\log(N/N_0)=A+Bt$.

Treatment conditions	A	B	N	R	R^2	SD
200 MPa, 0 °C	-0.237	-0.032	12	-0.887	0.786	0.370
300 MPa, 0 °C	0.036	-0.245	10	-0.951	0.905	0.916
300 MPa, -10 °C	-0.922	-0.295	8	-0.951	0.904	0.621
200 MPa, -45 °C	-0.694	-0.032	13	-0.796	0.634	0.256
300 MPa, -45 °C	-2.855	-0.012	15	-0.269	0.072	0.422
400 MPa, -45 °C	-3.012	-0.014	12	-0.427	0.182	0.308

N: number of independent experiments included in regression analysis; SD: standard deviation; R: coefficient of correlation; R^2: coefficient of determination. The regression lines were fitted on the basis of results of the single experiments. Some experiments not shown in Figure 4.31 were included in the regression analysis.

Like in normal freezing preservation, it seems reasonable to assume that the low water activity due to the frozen conditions as well as the lowered reaction speed due to low temperatures reduce the impact of pressure on microorganisms, like it was frequently reported in the case of other systems under pressure with reduced availability of liquid water (Smelt et al. 2002). This reduced impact of pressure lead to much slower inactivation kinetics compared to liquid

conditions and there was also almost no difference in inactivation at 300 MPa and 400 MPa. This low impact was statistically proven by the low coefficients of correlation in Table 4.8. High pressure is transmitted uniformly through frozen samples (Bridgman 1912; Kanda, Kitagawa & Fujinuma 1993), hence, it cannot be assumed that the slow inactivation arose from the fact that pressure was not acting on bacteria suspended in the solid ice matrix.

Besides the analysis of inactivation experiments, one observation supported the assumption that cell disintegration occurred after ice I – ice III phase transitions. Cell suspensions after treatment were highly viscous with a slimy appearance. The same structure is found when homogenizing cell suspensions in a bead mill, indicating the release of DNA and protein.

Another series of experiments was carried out, examining the inactivation after repeated pressure cycles that also takes into account the treatment temperature. The pressure and temperature measurement of such treatments is shown in Figure 4.18C, however at -25 °C the repeated transition includes partial thawing like shown in Figure 4.15A. During repeated pressure cycles, which means also that the solid - solid phase transition of ice was acting on the sample repeatedly, the inactivation at -45 °C was enhanced by one log cycle (Figure 4.32). After treatments at -25 °C and at -35 °C that included partial thawing, the difference in the results was not very big. It can be assumed that the combined application of high pressure at low temperature in liquid conditions during partial thawing might be responsible for the inactivation at the higher temperature levels, because the water activity is considerable higher than in frozen conditions. Deeper insights in the inactivation mechanism cannot be derived from these plate count experiments. All experiments show that there is a small fraction of the initial bacterial population which is not affected by repeated solid – solid phase transitions. This fraction might survive due to an inhomogeneity during the phase transition or due to higher resistance of some bacteria. Although the pressure is homogeneous throughout the vessel, it seems reasonable to assume that bacteria at the outer edge of the sample, which are not completely surrounded by ice, are not exposed to the same mechanic stress as bacteria in the middle of the sample.

Like stated earlier (chapter 4.1.9) it is not completely clear if ice II or ice III forms during pressurization of ice I at -45 °C, but there is reason to assume that it is ice III. At -60 °C, Bridgman (1912) described that ice II is usually formed, which was verified at least for one sample in own experiments (Figure 4.16). As this temperature was the lowest temperature that could be obtained in the cryostats, the influence of freezing and pressurization at -60 °C was examined. Inactivation of *L. innocua* after treatment at -60 °C, 400 MPa without pressure

holding was -2.1 log and -2.7 log after 7 minute pressure holding at these conditions. As a side note to freeze damage experiments it should be noted that at -60 °C no inactivation due to freezing for a few hours was found. The inactivation after this pressure treatments was a little lower than at -45 °C. If the assumption is true that ice II was formed at -60 °C, the inactivation due to the ice II transition can be described as slightly smaller, however this should probably be attributed to the temperature level.

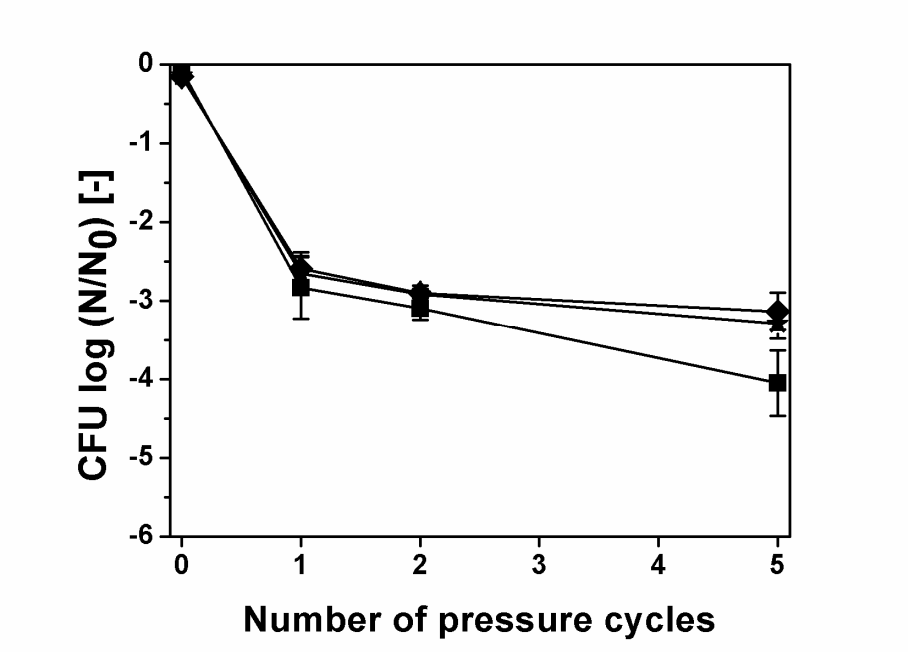

Figure 4.32 Inactivation of *Listeria innocua* in frozen PBS after multiple pressure cycles to 300 MPa without holding time at maximum pressure at various subzero temperatures. The data points for zero pressure cycles indicate the inactivation due to freezing for 2 hours at the respective temperature. ◆ -25 °C; ★ -35 °C; ■ -45 °C.

These inactivation results are in excellent agreement with the experiments reported by Edebo & Hedén (1960). They used a pressure cycling method to disrupt *E. coli* in frozen conditions suspended in buffer solution. Repeated passing of the phase transition line ice I - ice III at -25 °C produced mechanic stress and yielded the best cell disintegration compared to pressure cycling at other pressures including other phase transitions of water. However, there was also no temperature measurement inside the sample, hence, it is doubtful that a direct solid - solid phase transition of ice I to ice III took place at this temperature level, due to the close phase boundary ice I - liquid. Nevertheless, the results give no reason to cast doubt on them, but as the method was developed to disintegrate cells, the disruption was not detected by cell counts but by measuring the release of intracellular components via extinction and by analysis of the

released protein. The experiments reported by Magnusson et al. (1974; 1976b) during the development of a freeze press are difficult to compare with the results shown here due to a number of reasons. Magnusson (1977a; 1977b) himself stated the cell disintegration effect he found was probably the consequence of extrusion effects (shear, internal friction) and only partly of the ice I - III phase transition. The results he obtained were always given as a percentage of disintegrated cells detected in a microscope, which may not be equated with the inactivation results provided here. Furthermore, the sample composition is quite different as he treated yeast cell pastes that had a dry mass content up to 27 %, which is a dimensional difference compared to the aqueous suspensions examined here.

4.3.3 Flow cytometry of HPLT treated *L. innocua*

As shown in the previous part, flow cytometry can be useful to detect mechanism of damage due to physical treatments in bacteria. It was also used to demonstrate the impact of the differing conditions in this part of the study, as the approach to deduce from microbial inactivation kinetics on damage mechanisms is limited.

Figure 4.33 shows the effect of the different treatments on the flow cytometric profile of *L. innocua*. Cells in plot “a” were high pressure treated in the liquid phase. Compared to untreated cells, the profile has not changed much (viable control sample see Figure 4.28). This indicates that cells are not membrane damaged and also intracellular esterase is still active. However, an inactivation of close to 3 log was obtained. This shows that the pressure causes inactivation by a mechanism, that is not evaluable by this assay. Flow cytometry of *Lb. rhamnosus* treated by high pressure essentially showed similar results (Ananta et al. 2004). It can be stated clearly, that the cells are not disintegrated. Cells in plot “c” that were treated in frozen conditions including a phase transition to ice III and back to ice I showed in contrast severe cell damage, as most of the cells were found in gate #1. This means that they were colored by PI and CF was not detectable, likely due to membrane damage that prevented CF accumulation. A statement regarding esterase activity cannot be made if cells are disintegrated to such an extent. Even though, the inactivation was almost the same as in treatment “a”, flow cytometry shows clearly the difference in inactivation mechanisms. Cell disintegration was clearly achieved in sample “c” indicating mechanical stress.

This conclusion is further supported by plot “d” showing cells subjected to five pressure cycles in frozen conditions. Even more cells were moved to gate #1, showing the effect of repeated phase transitions at -45 °C. Cells in plot “b” however were treated in frozen conditions at 200 MPa. Even though the cells are suspended in a solid ice matrix, flow cytometry indi-

cates cell damage comparable to plot “a”, but less cells were inactivated. This indicates that also at the frozen conditions pressure acts on the cells, and it probably also does it at 300 and 400 MPa, however, this is not detectable, as the inactivation due to the ice III – phase transition superimposes this behavior, so that no real time dependent pressure inactivation behavior remains.

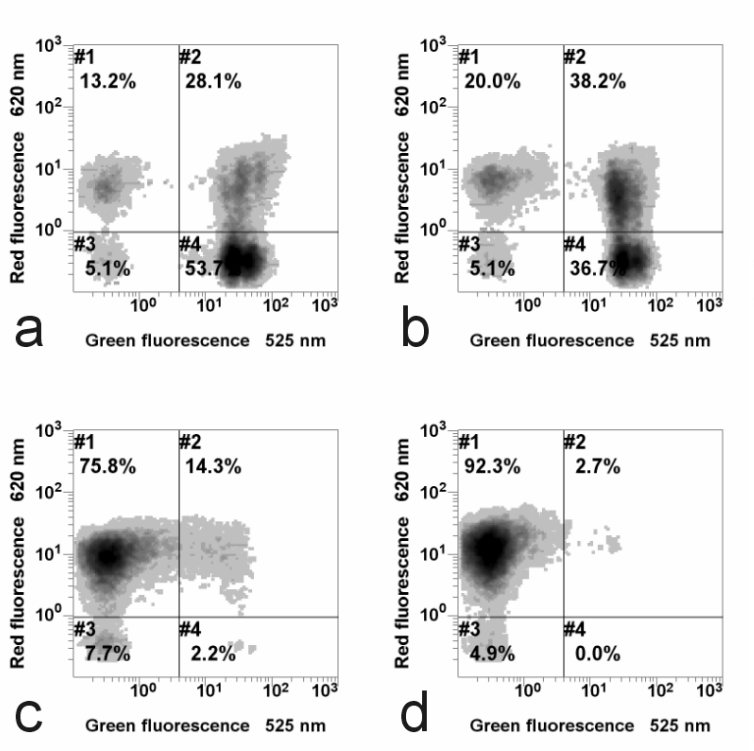

	Conditions	Log (N/N_0)
a	0 °C 300 MPa 15 min	-2.8
b	-45 °C 200 MPa 10 min	-0.6
c	-45 °C 300 MPa 0 min	-2.9
d	-45 °C 300 MPa 0 min	-4.2

Figure 4.33 Assessment of cellular damage of *L. innocua* by flow cytometry after various high pressure – low temperature treatments, as specified in the table. The inactivation results correspond to the inactivation determined for the specific sample which was used for flow cytometry.

In contrast to the disintegration shown for treatments of frozen bacterial suspension at -45 °C, the treatment at -25 °C exhibited somewhat different effects. Cells in Figure 4.34, plot “a”, were treated with a short time phase transition treatment, however, it is also reflected in the flow cytometry results that the sample is partly thawing during the treatment. A fraction of the cells is disintegrated and shifted to gate 1 and a high number of cells is found in gate 2 indicating that partial membrane damage by PI influx, while the membrane is still retaining CF inside the cell. During the treatment, a clear time dependency of the behavior was found. In plot “b” after prolonged treatment at these conditions, more cells were found in gate 1, indicating more pronounced cell disintegration. Plot “c” indicates that the same mechanism is also occurring after treatments in the ice I phase at 200 MPa and -25 °C without phase transition which are conditions close to thawing.

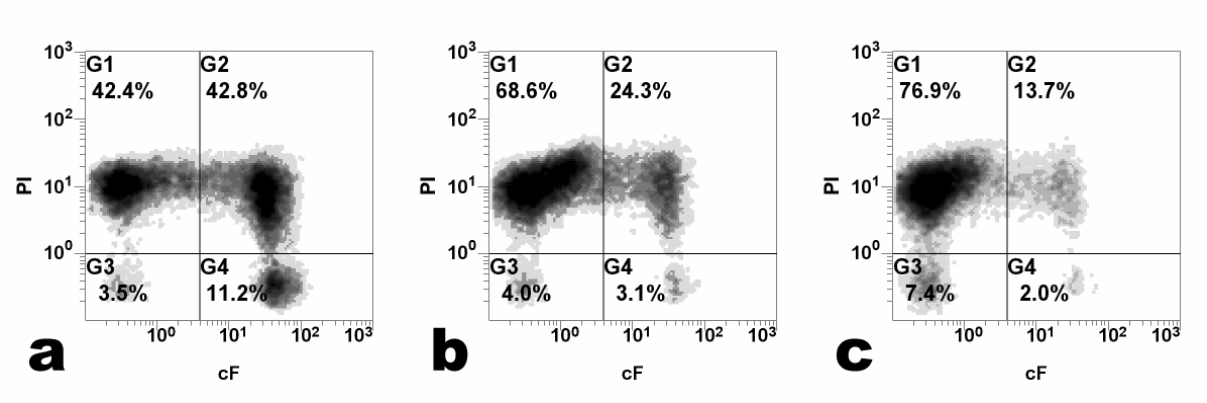

Figure 4.34 Assessment of cellular damage of *L. innocua* by flow cytometry after treatments at high pressure treatments at -25 °C. Treatment conditions: (a) -25 °C, 300 MPa, 0min; (b) -25 °C, 300 MPa, 15min; (c) -25 °C, 200 MPa, 30min.

It was concluded from the experiments, that during treatments at -25 °C "normal" high pressure action at least to considerable extent occurred, due to partial thawing in the bacterial samples. In the experiments, it was also found difficult to obtain reproducible inactivation results at that temperature level, as the phase transition to ice III after pressure induced thawing was somewhat varying due to nucleation phenomena. As the main idea was to examine ice I – ice III phase transition, the following experiments were usually carried out at -45 °C to obtain a "pure" ice I – ice III transition without thawing influence. It is not generally doubted, that interesting inactivation results can be obtained by pressure treating frozen samples at -25 °C, however, it is assumed that the mechanism is different and that the inactivation should be more dependent on treatment time. Additionally, when looking at potential food applications, it is likely that destructive pressure effects like whitening of meat and fish should occur, when samples thaw at the surface. These effects have to be considered relative to sample size as it thawing is presumably obtained to a greater extent in lab scale samples.

Shen et al. (2005) showed results comparing the pressure inactivation at -25 °C and -45 °C in the same pressure vessel like it was used in the present study. Inactivation results are somewhat ambiguous. Essentially the inactivation at -25 °C was best at 250 MPa, where the highest amount of thawing is likely, however, little time dependency of the inactivation reaction was found. The pressure – temperature curves seem to indicate differences in phase transitions at -25 °C which are difficult to interpret (Fig. 2f in their paper compared to Fig. 2g and h). The *Bacillus subtilis* culture used in this study was also quite resistant to treatments at -45 °C.

4.3.4 Inactivation of other microorganisms

The inactivation of several other microorganisms was checked as a comparison to *L. innocua*. Most the experiments where carried out simultaneously with *L. innocua* and *E. coli* in order to compare the results of gram+ and gram- bacteria. Results for the treatment of *E. coli* in buffer solution at -45 °C are shown in Figure 4.35 and basically the same results were obtained. The occurrence of the phase transition to ice III at pressures higher than 300 MPa lead to comparable inactivation kinetics with little time dependence and also to a comparable, but slightly higher extent of inactivation in the range of 3 to 4 log. One exception is only the data point at 300 MPa, 0 min which indicates only about 2 logs of inactivation. Interestingly, the extent of inactivation after repeated pressure cycles was a lot higher for *E. coli* than for *L. innocua*, reaching even 6 logs of inactivation after five treatments. A potential reason could be that gram-negative bacteria are more susceptible to this treatment due to the thinner murein cell wall.

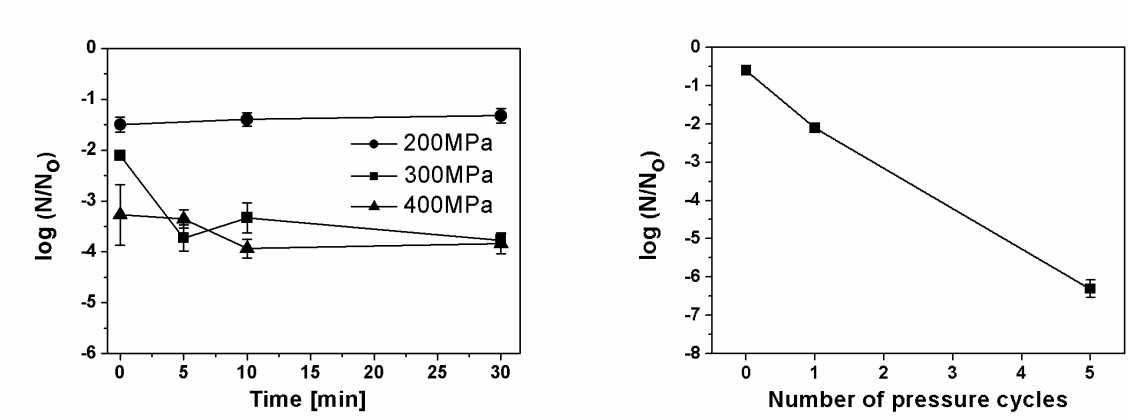

Figure 4.35 Inactivation of *E. coli* in frozen PBS after high pressure – low temperature treatments at -45 °C. Left: inactivation kinetics at three pressure levels, right: influence of repeated pressure cycles.

The inactivation of *Pseudomonas fluorescens, Saccharomyces cerevisiae* and spores of *Bacillus subtilis* were examined and also one test with *Lactobacillus rhamnosus* GG was carried out. For the first three organisms the inactivation was checked with only single experiments, however, more kinetic points were obtained. The inactivation was checked at two different temperatures. *P. fluorescens* (Figure 4.36) as a gram-negative, food related spoilage organism was inactivated 4 to 6 log cycles at -45 °C. The inactivation was even higher at -30 °C showing, that the organism is very susceptible to high pressure – low temperature conditions in general. The large variation of the results at -30 °C indicate the difficulties to obtain repeatable, stable results that were mentioned earlier.

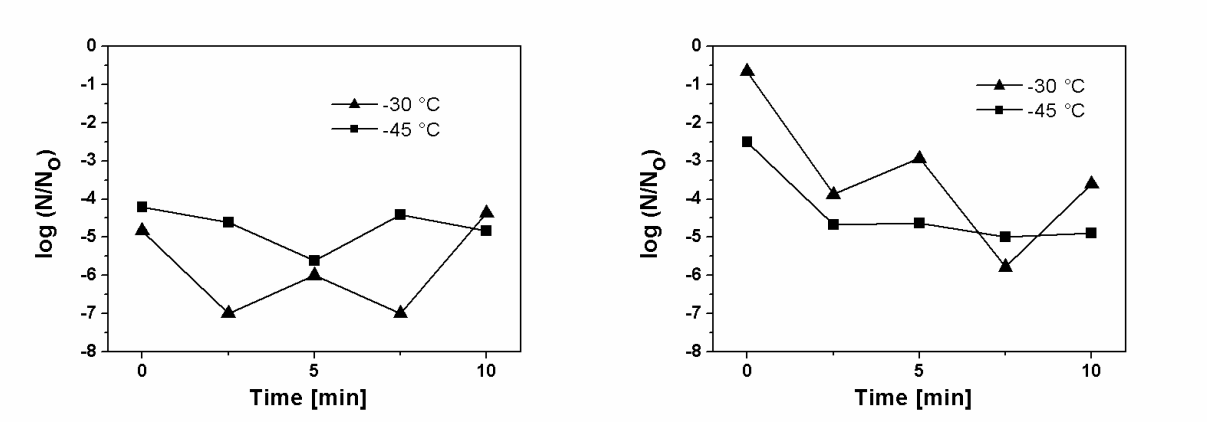

Figure 4.36 Inactivation of *Pseudomonas fluorecens* (left) and *Saccharomyces cerevisiae* (right) in frozen PBS after high pressure – low temperature treatments at 400 MPa, -30 °C and -45 °C.

Saccharomyces cerevisiae (Figure 4.36) was also considerably inactivated. It should be noted that the yeast is about one order of magnitude larger than bacteria. The inactivation was more pronounced at -45 °C as compared to -30 °C. Like *E. coli* at 300 MPa, *S. cerevisiae* showed some time dependency of inactivation at -45 °C. First the inactivation after very short treatments ("0 min") was only -2.5 log, after that the values increased to -4.7 log inactivation after 2.5 minutes. This deviation was verified in a repetition of the experiment. A clear reason for this behavior cannot be given but it might be related to different freezing or dehydration characteristics during freezing. However, together with one inactivation value of *E. coli* this was the only limitation of ice I – ice III treatments in the experiments.

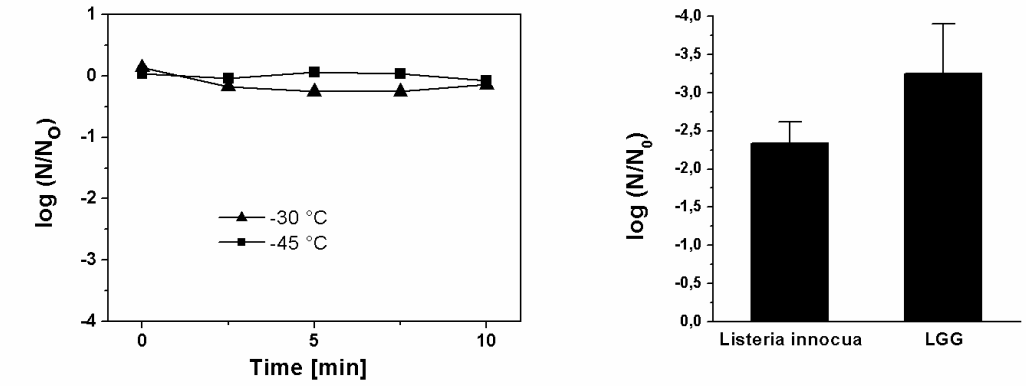

Figure 4.37 Inactivation of *Bacillus subtilis* spores (left) in frozen PBS after high pressure – low temperature treatments at -30 °C and -45 °C and *Lactobacillus rhamnosus GG* (LGG - right) after 300 MPa, -45 °C, 0 min in comparison to *L. innocua*.

B. subtilis spores (Figure 4.37) were not affected by any of the treatments which was not surprising, due to the rigid, small and resistant structure of the spore. LGG (Figure 4.37) was also

checked for inactivation after pressure phase transition of ice III, however only with one treatment parameter. The results show bigger inactivation than for *L. innocua*, however, LGG is anyway very susceptible to freeze damage, high pressure and to mechanical stress as well.

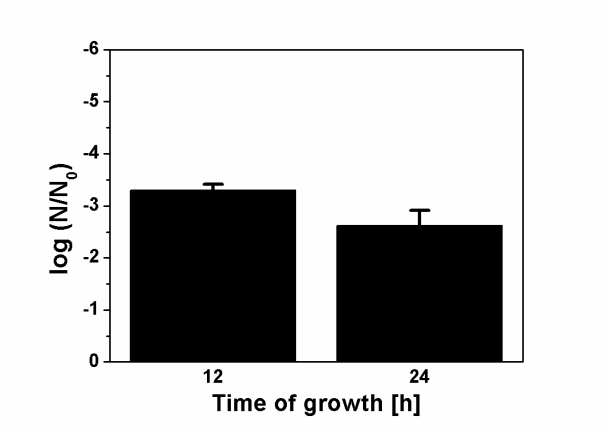

Figure 4.38 Effect of the growth phase of *L. innocua* on inactivation due to ice I – ice III phase transitions (300 MPa, -45 °C, 0 min).

The influence of different growth conditions of bacteria on the inactivation after pressure induced phase transitions is shown in Figure 4.38. After 12 h of growth, *Listeria* was in the exponential growth phase, where cells are usually less resistant to external influences, while at 24 h cell were in the stationary phase. The growth curve of this organism was shown in other examinations (Schlüter 2003). Like expected, cells were more resistant in the stationary growth phase. By this quick test it is demonstrated that the physiological state of the cells influences the inactivation results of this treatment, like in the case of other inactivation methods.

4.3.5 Effect of frozen storage after treatment

Figure 4.39 shows the evolution of inactivation if cell suspension were stored at -18 °C in a freezer with and without pressure treatment. For normal frozen storage, cells were frozen at -45 °C to obtain a similar temperature history like the treated samples. In effect, this storage can be compared to storage condition "C" in Table 4.6 of the freeze stress experiments. As *E. coli* was not examined in these frozen storage experiments, it is noteworthy that the evolution of the cell count was comparable to *L. innocua*, even though *E. coli* was slightly more inactivated if cells were not stored.

After pressure treatments with ice III transitions, *L. innocua* showed only a slight decrease during storage time. This indicates that most of the cells that were not affected by the pressure treatment initially, were not stressed or damaged enough to be reduced by frozen storage

stress during 30 days. *E. coli* however, was decreasing considerably during storage of 15 days, being reduced to more than 5 log. It can be concluded, that the combined stress of pressure treatment with phase transition and cold storage stress lead to this inactivation behavior, while the two stresses alone, did not result in more inactivation than in the case of *L. innocua*. In the period of the following 15 days, the cell count did not decrease further, indicating a very small but resistant cell fraction.

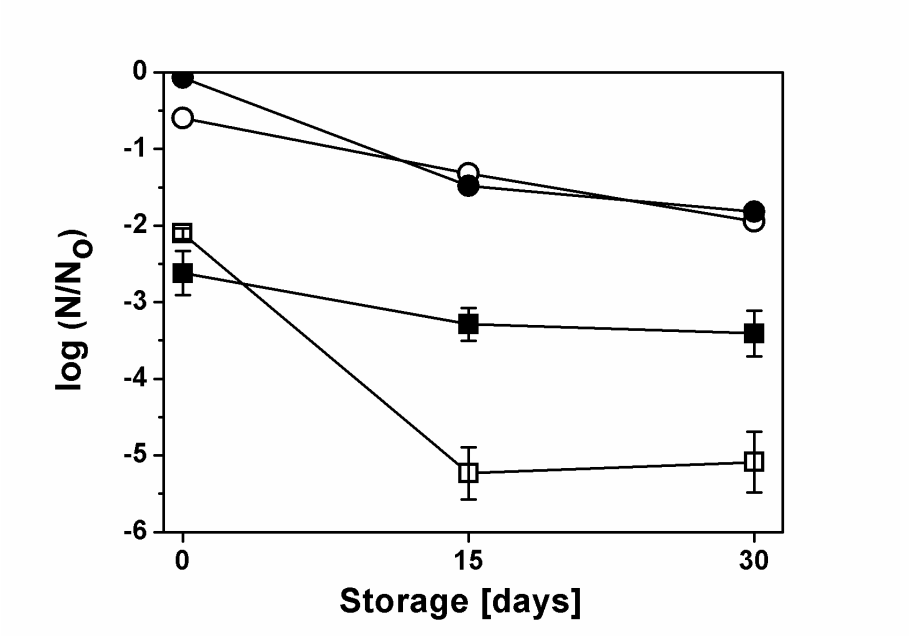

Figure 4.39 Effect of storage at -18 °C after high pressure treatment of *L. innocua* and *E. coli* in frozen PBS. ●■ *L. innocua*; ○□ *E. coli*. ○● Stored frozen without treatment; ■□ Stored frozen after treatment at 300 MPa, -45 °C, 0 min.

From a food processing point of view these results are interesting as storage of frozen food is anyway given. A combined inactivation by treatment plus storage would be easily feasible. However, the results also show that a strong species dependency has to be taken into account.

4.3.6 Influence of treatment parameters on the inactivation

4.3.6.1 Technical effects

Three technical parameters were examined that are possibly related to inactivation after high pressure – low temperature treatments with ice III transitions, which are the rate of pressure release, the application of pressure during freezing before treatment (pressure assisted freezing) and the rate of freezing before treatment.

The rate of pressure release after freezing might influence the inactivation, if shear forces between ice crystals or other processes involving ice crystal movement or expansion are a major

reason for inactivation. Experiments were carried out after two different treatments with *E. coli* and *L. innocua* with pressure release as slow as possible, intermediate speed and with pressure release as fast as possible. Due to the variation of inactivation results, definite conclusions cannot be made from the data, as all treatments resulted in approximately the same inactivation. The only slight trend that could be identified was somewhat better inactivation after very slow pressure release. During all inactivation experiments presented in other figures the rate of pressure release was close to the maximum value, as the ice phase transition was identified during pressurization and the absence of the phase transition from ice III back to ice I during decompression was not expected.

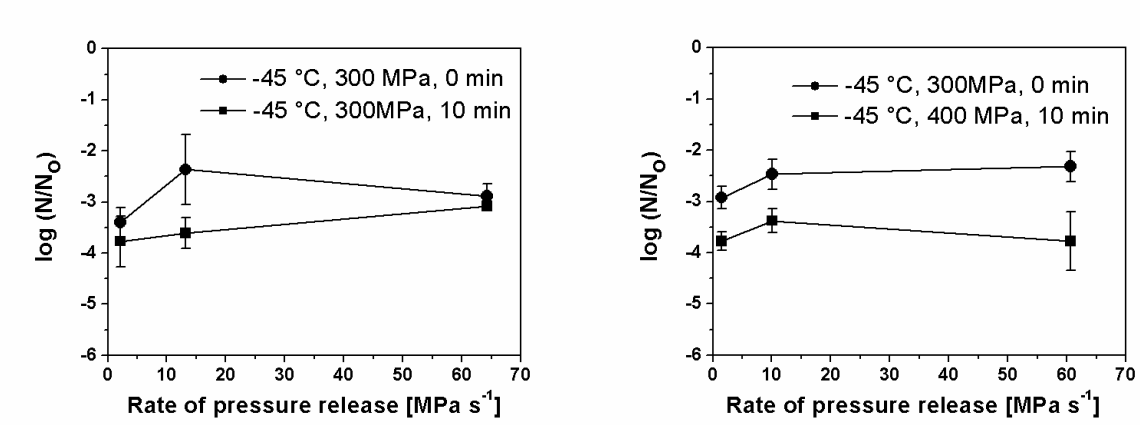

Figure 4.40 Effect of the rate of pressure release on the inactivation of *L. innocua* (left) and *E. coli* (right) after high pressure – low temperature treatments including ice III transitions.

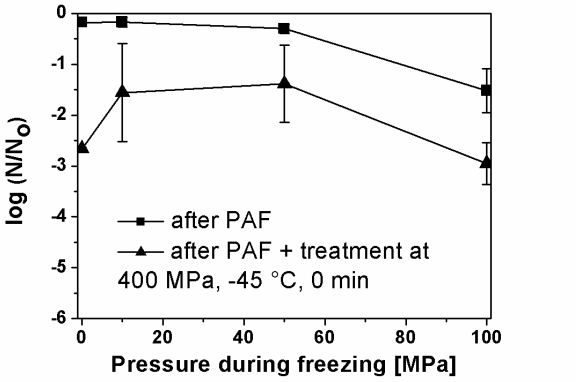

Figure 4.41 Inactivation of *L. innocua* after pressure assisted freezing (PAF) and after PAF followed by a high pressure – low temperature treatment including ice III transition.

During pressure assisted freezing (PAF) followed by thawing, notable inactivation was found only at 100 MPa. If pressure treatments in the frozen phase were carried out after PAF, the

inactivation in combination with freezing at 10 and 50 MPa was even lower compared to freezing at 0.1 MPa. However the variation in these experiments was inexplicably high. The basic idea of this set of trials was to obtain a denser ice crystal structure by PAF that prevents cavities and packs cells tighter to the ice crystals. The number of cells inactivated during ice I – ice III phase transitions should therefore be increased. Obviously this effect was not achieved.

The influence of the freezing rate was examined, as the state of the bacterial cell (intracellular ice or dehydrated) is influenced by this parameter. Three different rates were obtained by air freezing, immersion freezing and cryogenic freezing of small sample pouches, comparable to the freeze stress experiments in chapter 4.2. After freezing, samples were tempered at -45 °C and pressurized. The inactivation after these treatments in the frozen state was nevertheless not different from each other indicating that all cells frozen at 1 and 7 °C/min were in the same state, presumably in the state of dehydration. The state of bacterial cells frozen at 200 K/min is not fully understood (see chapter 4.2), and the temperature raise to -45 °C makes ice recrystallization possible. The inactivation after frozen pressure treatment is comparable to the one obtained in combination with slower freezing rates. This can be taken as an indication that the ice is distributed like in the other treatments, which could be intra- or extracellular like discussed later.

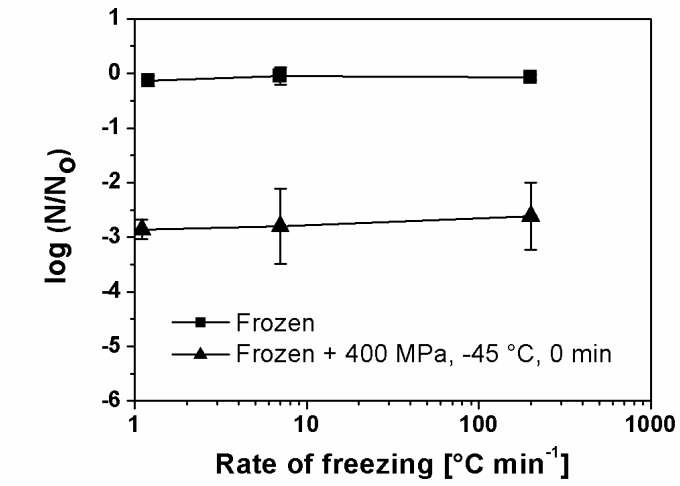

Figure 4.42 Effect of the rate of freezing on the inactivation in later pressure treatments in the frozen state.

In summary, manipulation of pressure release, pressure during freezing and freezing rate did not lead to improved inactivation results. Nevertheless the findings are useful as they give more information about the mechanisms that might be lead to cell disintegration.

4.3.6.2 Scale-up experiments

In the pilot scale experiments the vessel with an internal volume of 1.66 l was used. The samples were frozen cell suspensions in buffer solution with a volume of 50 ml in regular shaped cylinders, as opposed to 1 ml sample pouches used for inactivation experiments in the lab scale pressure equipment. Experiments were carried out at -35 °C as it was the minimum temperature in the unit. A pressure and temperature diagram of a representative experiment is shown in Figure 4.20. The inactivation results indicate the general confirmation of the studies derived in the lab scale equipment, as shown in Figure 4.43 for 0 days storage. Some deviations to the small scale experiments can be observed, like a more pronounced, yet not time-dependent *L. innocua* inactivation at 200 MPa of about 2 log. It should however be noted, that the experiments at -35 °C are likely going along with some pressure induced thawing, but it can be assumed that thawing occurred to a lesser extent due to sample size.

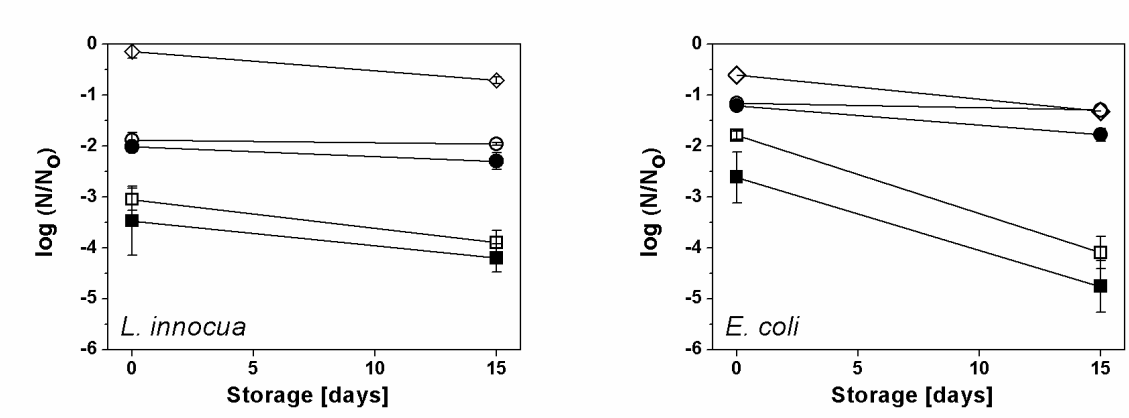

Figure 4.43 Inactivation of *L. innocua* and *E. coli* in 50 ml PBS samples after high pressure – low temperature treatment at -35 °C in pilot scale experiments, including influence of storage at -18 °C. ◇ no pressure, only frozen at -35 °C, ○ treated at -35 °C, 200 MPa, 0 min; ● treated at -35 °C, 200 MPa, 15 min; □ treated at -35 °C, 340 MPa, 0 min; ■ treated at -35 °C, 340 MPa, 10 min.

Storage experiments of samples treated at the pilot scale level show that the behavior of *E. coli* in small scale experiments during storage was confirmed. Also the slow progression of *L. innocua* inactivation was verified. This indicates that pressure treatments with ice III transitions are not influenced by the sample volume in the given range.

4.3.7 Inactivation in food systems

Ground beef and vanilla ice cream was treated in lab scale experiments with an inoculum level of about 10^7 cfu/g of *E. coli* or *L. innocua,* which were inoculated in separate samples. The inactivation results of ground beef indicate a protective effect of the food matrix on mi-

croorganims, as the reduction during pressure treatments of *L. innocua* was reduced by about one log cycle, while *E. coli* was protected even better. However, 2 log cycles of inactivation for *L. innocua*, in combination with frozen storage at -18 °C even 3 logs of inactivation were obtained, which show that the treatment is feasible for real food systems. Lower water activity is attributed to be a main effect of the food matrix. In order to interpret the results in connection to ice III transition effects, the reduced amount of freezable water in comparison to buffer solution in turn also leads to less ice crystals which would make the disintegration more difficult.

Fernandez et al. (2007b) reported about the same inactivation after frozen pressure treatments of beef in cylindrical samples of muscle flesh at -35 °C, 650 MPa and 10 minutes. They also obtained likely an ice III – ice V transition during that treatment, but did not reflect any lower pressure treatments which might be more feasible from a technical point of view. Essentially, they examined the natural flora in the samples which was about 3.5 log of total aerobic count and 2.5 log of lactic acid bacteria, which were reduced below the detection limit of 1 log.

Table 4.9 Inactivation of *L. innocua* and *E. coli* in frozen ground beef after high pressure – low temperature treatments including effect of storage

	Listeria innocua				***Escherichia coli***			
Pressure treatment at -45 °C	**200 MPa**		**400 MPa**		**200 MPa**		**400 MPa**	
Storage at -18 °C	**none**	**30 days**	**none**	**30 days**	**none**	**30 days**	**none**	**30 days**
0 min	0.1±0.3	-0.7±0.1	-1.7±0.4	-2.8±0.1	-0.5±0.5	-0.6±0.3	-1.0±0.1	-0.8±0.4
5 min	-0.1±0.2	n.d.	-1.2±0.4	n.d.	-0.3±0.5	n.d.	-1.3±0.1	n.d.
15 min	0.1±0.2	-0.8±0.2	-2.0±0.3	-2.9±0.1	-0.4±0.4	-0.6±0.2	-1.1±0.6	-1.4±0.2
5 x 0 min	n.d.	n.d.	-1.7±0.1	-3.1±0.8	n.d.	n.d.	-0.9±0.2	-1.5±0.2
Storage at -18 °C	**none**	**30 days**			**none**	**30 days**		
Frozen at -45 °C, untreated	0.0±0.1	-0.8±0.1			-0.5±0.5	-1.1±0.1		

Results are from two independent experiment with triple plate count. Water content of ground beef was 70.8 % ± 1.2 % (5-fold examination).

The inactivation results presented here for ground beef are limited with respect to the fact that the inactivation of the previously existing flora in ground beef was not evaluated separately. A study revealed about 10^5 to 10^6 cfu/g of bacteria in ground beef (Köpke 2002). Bacteria found in beef were mostly lactic acid area, *Brochothrix thermosphacta*, and *Pseudomonas* spp., but also *Enterobacteriaceae, Psychrobacter* spp., *Flavobacteriaceae* and *Acinetobacter* spp. were found. Counts and composition of the flora varied widely. Total aerobic counts of the ground beef bought for this study amounted to about 10^6 cfu/g in some representative tests before treatment and inoculation. Samples were then inoculated with *L. innocua* or *E. coli*, treated and analyzed by aerobic plate count on standard I agar. It can be estimated that some of the bacteria present in ground beef were suppressed by the high inoculum of one species added and it is also imagineable that a lot of the natural flora bacteria were not able to grow so fast on microbiological plates after treatment. Differences in colony appearance on the plates were not noted. However, a large number of these bacteria was probably counted as *L. innocua* and *E. coli*. This suggests that the true inactivation of the two bacteria in ground beef was actually higher than detected. It should also be taken into account, that the natural flora is probably better adapted to meat conditions and chilled storage. Due to the logarithmic nature of the results, the relation of microbial counts (*L. innocua* and *E. coli* 10^7 cfu/g, natural flora in total about 10^6 cfu/g) is probably explaining why it was so difficult to obtain more than 2 log cycles of inactivation. In summary, the results are quantitatively difficult to evaluate. They probably show a minimum inactivation that can be obtained in meat, but the real inactivation obtainable by pressure treatments in the frozen state is presumably higher.

In vanilla ice cream, very poor inactivation was found. Only after treatments at 400 MPa of 5 and 15 minutes pressure holding time, inactivation of 1 log *L. innouca* was retrieved, but cells were even able to recover from this treatment during storage at -18 °C. *E. coli* was not detectably affected by high pressure – low temperature treatments at all. The low inactivation can be attributed to the low water content and high amount of bound water in ice cream due to the presence of sugar. Furthermore, the fat droplets in the ice cream probably soften the effect of sudden volume change of ice during the phase transition to ice III and back. It can be concluded, that the treatment of frozen food by pressure treatments with ice III transitions is only effective in food with a high freezable water content.

In some experiments it was tried to control the water content of the sample, in order to make quantitative evaluation of water content in relation to inactivation. For sucrose solution with dry matter of 0 to 50 %, it was not possible to realize a reproducible treatment, because the phase transition at high levels of sucrose was not detected precisely. Figure 4.17 showed some

solid – solid phase transition points that were occurring at relatively high pressure, additionally the phase transition was not very pronounced. As it was not possible to detect if a phase transition occurred or to which extent, the experiments were not continued.

Table 4.10 Inactivation of *L. innocua* and *E. coli* in ice cream after high pressure – low temperature treatments including effect of storage

	Listeria innocua				***Escherichia coli***			
Pressure treatment at -45 °C	**200 MPa**		**400 MPa**		**200 MPa**		**400 MPa**	
Storage at -18 °C	**none**	**30 days**	**none**	**30 days**	**none**	**30 days**	**none**	**30 days**
0 min	0.2±0.1	0.1±0.1	-0.3±0.3	-1.0±0.5	-0.1±0.0	-0.1±0.1	0.0±0.0	-0.2±0.1
5 min	0.2±0.2	n.d.	-1.2±0.6	n.d.	-0.1±0.1	n.d.	0.0±0.1	n.d.
15 min	0.0±0.1	0.1±0.0	-1.3±0.4	-0.3±0.2	0.0±0.0	-0.1±0.1	-0.1±0.1	-0.3±0.2
5 x 0 min	n.d.	n.d.	-0.5±0.2	-0.2±0.1	n.d.	n.d.	-0.2±0.1	-0.2±0.1
Storage at -18 °C	**none**	**30 days**			**none**	**30 days**		
Frozen at -45 °C, untreated	0.2±0.1	0.1±0.1			0.1±0.1	0.3±0.2		

Results are from two independent experiment with triple plate count. Water content of ice cream was 64.0 % ± 0.2 % (5-fold examination).

Another attempt to control the water content was made with suspension of baby food (homogenized carrot) with defined addition of water. Like shown in Figure 4.44, in suspensions with 0 to 30 % of baby food the inactivation of *L. innocua* was essentially the same as in buffer solution, indicating that food with a high water content is treatable without reduced inactivation results. At 50 % or more baby food content, the phase transition to ice III was not well detectable like in the case of 50 % (w/w) sucrose solution.

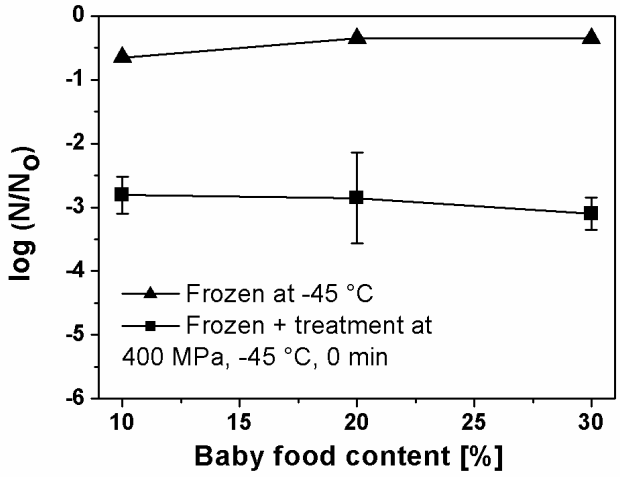

Figure 4.44 Inactivation of *L. innocua* in suspensions of baby food in PBS frozen at -45 °C with and without pressure treatment. Baby food dry matter content was 10 %.

4.3.8 Possible mechanisms of inactivation

The general result of the treatment on microorganisms in frozen environments by high pressure including ice I – ice III phase transitions is the disintegration of the cells, as it is obvious from the leakage of intracellular material, which is also shown quantitatively by flow cytometry of *L. innocua*. This behavior is different from the high pressure inactivation observed in the liquid state of water, which did not show much disintegration.

The inactivation kinetics show that a single result is responsible for cell death as all kinetic curves start with a offset already at very short treatment times. The surviving part of the bacteria is inactivated with very low time dependency likely showing a mechanism of high pressure inactivation only at a very low level, which is low due to the low water activity in the frozen environment. Only in very few inactivation curves a real time dependency during the first minute of treatment can be estimated (*E. coli* at 300 MPa, Figure 4.35, and *S. cerevisiae* Figure 4.36), but after the first minute the effect of treatment time is as low as in all other experiments.

All inactivation results are species and system dependent. It is not possible to extrapolate from one organism to the other, however, this is usually the case in every treatment. Also storage in frozen conditions acts as another stress in the case of *E. coli* for example leading to very promising inactivation results after frozen storage.

The single event thesis and the disintegration of bacteria are in agreement by concluding that the phase transition of ice I to ice III and back to ice III is involved in the mechanism of inac-

tivation. The repetition of short time pressure cycles at -45 °C further supports this assumption. It must be clearly stated that inactivation by commonly known pressure mechanisms is in this treatment almost non-existent, pressure is only used as a tool to obtain inactivation by the phase transition. It is further regarded as evidenced that the transition of ice III to ice I is the decisive step for disintegration as shown earlier with food samples (Figure 2.12).

The crucial question is however, what in detail causes the inactivation. This leads to the analysis of different temperature levels. The first proposed mechanism is quite obvious and was the working hypothesis during experiments and is shown Figure 4.45 as the hypothesis of *external disintegration*. Cells like *L. innocua* are probably still in an unfrozen state after a few hours of freezing at -45 °C like it is shown in Figure 4.26 by flow cytometry. It is assumed that they are grinded, sheared or crushed between crystals of ice III that expand during decompression.

A thorough analysis of the data, taking in to account phase transition results of frozen solutions from chapter 4.1 however gives to rise to an estimation like in Figure 4.48. It shows an estimation of the ice content of a liquid which corresponds in composition to a bacterial cell (Alberts 1995). Values were calculated according to Equation 1 to 3 taking into account the shift of freezing temperature of water under pressure. From this figure it can be estimated that every pressurization process at subzero temperatures leads to a partial melting of some of the water in biological systems. It must be clearly stated that it does not mean cells are really holding this ice content as they are responding to extracellular freezing by water loss and therefore changing their composition. However, the values show the state of water around the cells with which they are more or less in osmotic equilibrium.

Due to this analysis of water content it is clear that even at the treatment temperature of -45 °C some water is thawing around the cells. This effect is more pronounced at higher temperatures. At the time of maximum pressure, even if it is only a few seconds, cells have the chance to take up water, like it is shown in the second set of pictures in Figure 4.46. The amount of water that is effectively flowing into the cell is depending primarily on the permittivity of the cell wall for water. During pressure release, if it is fast enough, water is not able to flow out of the cell again and causes intracellular freezing which leads to disintegration. This mechanism is denoted as *internal disintegration*. Cells which are already containing intracellular ice before pressure treatment are also disintegrated by this mechanism during pressure release, however, they are already regarded inactivated due to the intracellular ice.

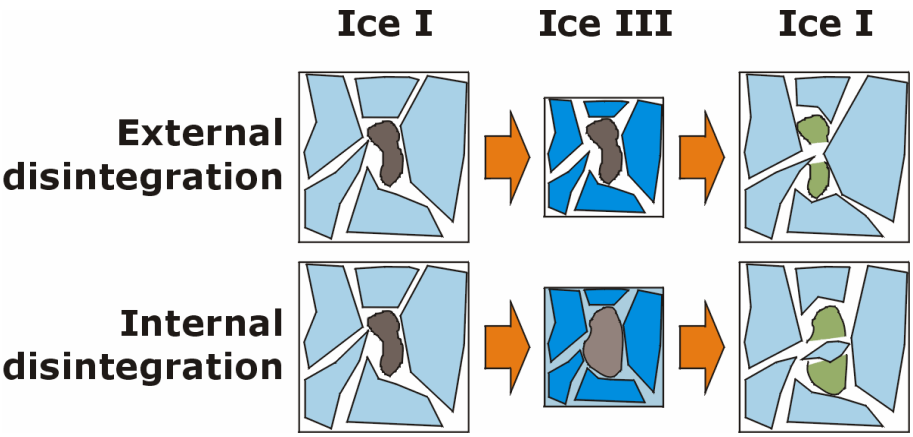

Figure 4.47 Proposed disintegration mechanisms of bacteria during pressure treatments of frozen food with ice III transition.

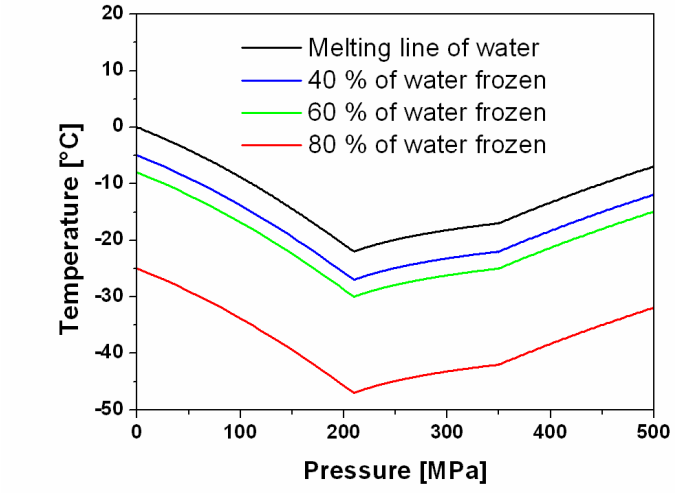

Figure 4.48 Estimation of the ice content of a liquid corresponding in composition to the intracellular liquid of a bacterial cell.

The *internal disintegration* mechanism can explain some observations that are contradictory to the *external disintegration*. During freezing in lab scale experiments, samples were quite small with about 1 ml and usually quite flat in pouches. This shows that it is likely that a lot of bacteria are not located within the ice due to a high ration of surface to sample size. If cells are not included in the ice matrix, they cannot be disintegrated by ice crystals. Körber (1988) examined the behavior of cells at an advancing ice front and showed quite complex behavior that sometimes leads to rapid inclusion of cells in the ice matrix between growing ice dendrites, but in other conditions cells are repelled and pushed forward by the ice front. This does not allow to conclude more on the location of bacterial cells, but it shows that if cell repulsion might be a factor even more cells are located at the edges of the sample. Sample sizes of 50 ml however showed quite the same inactivation results. This supports the idea of *external*

disintegration which does not require the immediate vicinity of ice crystals to bacteria to explain disintegration.

The *external disintegration* also explains the temperature dependency of inactivation among the microorganisms better. A look at Figure 4.36 (*P. fluorescens and S. cerevisiae*) shows the differing effect of treatment temperature on the inactivation at a glance. This behavior can be attributed to different permittivity for water of the cells as well as to differing water availability as cells with a low water permittivity would be more difficult to inactivate at lower temperatures while at higher temperature usually high pressure inactivation is dominating. Nevertheless cells with slow water influx should probably show more time dependency of inactivation. The sometimes noted effect of temperature dependency until one minute (e.g. *S. cerevisiae*) however can be explained by incomplete water influx during that time. It would also explain the lower inactivation at -60 °C well, because there is simply less thawed water to flow in the cell.

In contrary, the fact that variation of the pressure release rate did not show any effect, is not covered by the *external disintegration* theory, as fast pressure release is required in the assumptions. Slow pressure release would likely permit water to flow out of the cell again to maintain osmotic equilibrium with the environment. A possibility for explanation would be that the inactivation by different pressure release rates is obtained by either of the two theories at different rates.

As a last note with regard to temperature it is stressed that temperatures of -25 °C are not sufficient and are not explained by either of the mechanisms because they require a high amount of ice III already during expansion. Samples treated around -25 °C are likely thawed to a content that can be estimated in Figure 4.48 with pressure shift freezing of the thawed liquid occurring during expansion. Flow cytometry of pressure shift frozen lactic acid bacteria showed that cells are not disintegrated if just ice I is formed around them (Volkert, Luscher, Ananta & Knorr 2008). The formation of ice inside the cell of bacteria is however not likely at this temperature level. At this temperature, high pressure inactivation (pressure induced cold denaturation) is dominating. It is estimated that at least -30 °C should be maintained at the phase transition point to get an effect of ice III transition.

In summary, both proposed mechanism give reason to support them. It is likely that both mechanisms act on microorganisms and one of them dominates depending on the conditions and microorganisms. For the system of *L. innocua* in PBS at -45 °C, in which most of the experiments were carried out, it is assumed that internal disintegration is more important.

4.4 Effect of ice I – ice III phase transitions on pork meat

4.4.1 Texture

For evaluation of the quality of meat samples, meat stripes were cut longitudinal to the fibre of pork *longissimus dorsi*, packaged, frozen and treated at 340 MPa, -35 °C for one minute to obtain a phase transition of ice I to ice III in the meat.

After roasting of meat pieces, the texture was very difficult to evaluate instrumentally. With the standard method for meat texture studies, the Warner-Bratzler blade, no evaluable results were obtained. Instead a ball probe for compression tests was used. Results as shown in Figure 4.49 (left) were derived for samples derived from one carcass, but it was not possible to derive average values, as the variation among samples from different carcasses was higher than the effect of the treatments on the texture. In general, a slight difference in texture was noteable without instruments by sensory analysis. A test with ten untrained testers from the department revealed a precise classification of the treatments.

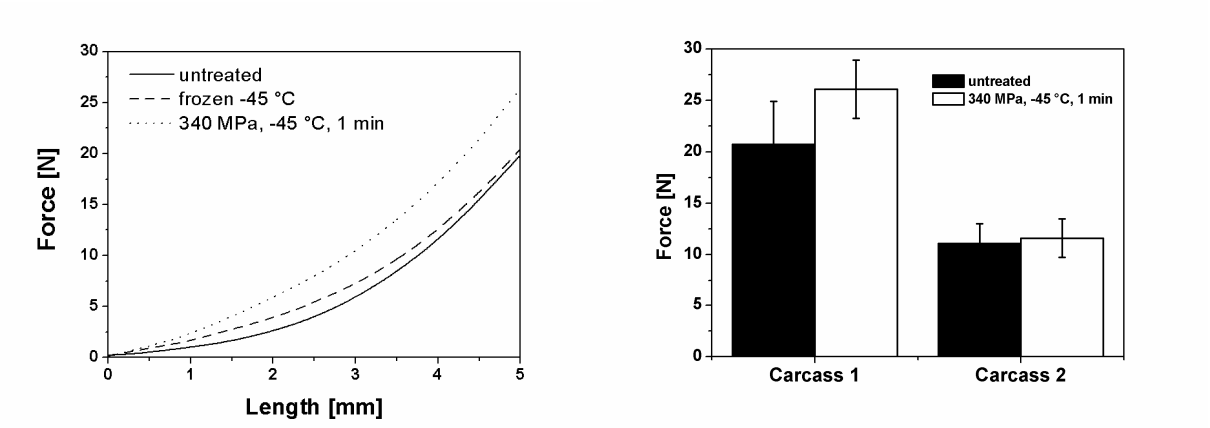

Figure 4.49 Left: pork meat texture of pork after freezing and after pressure treatment in the frozen state by ball probe compression test; right: maximum pressure of ball probe test after frozen storage at -18 °C of samples from two caracasses.

Figure 4.49 (right) shows the results of samples stored frozen at -18 °C for 14 days with and without pressure treatments. The influence of different carcasses can be easily noticed. It can be concluded, that there is a slight but notable hardening effect after roasting of pressure treatments in the frozen state including an ice III transition. This hardening can be ascribed to disintegration effects on the microstructure level which lead to loss of hydration of myosin fibers and subsequently to aggregation and hardening. This effect is however smaller than the variation among carcasses from different animals.

4.4.2 Color

The color of meat samples after thawing, but without roasting was evaluated. Obvious was a whitening effect, as it is commonly found in high pressure – low temperature conditions. The decrease in meat color was reflected by the decrease in the redness value a*, but not in the lightness value L*, which indicates a decrease in myoglobin. Samples after freezing and after pressure treatments in the frozen phase could not be differentiated by instrumental color evaluation, however, it was slightly visible. The whitening effect was prevalent throughout the whole diameter of the sample, which excludes pure surface thawing during pressurization at low temperature conditions. An additional effect of pressure treatments on myoglobin is possible, but the sample color was not very different from normal frozen samples.

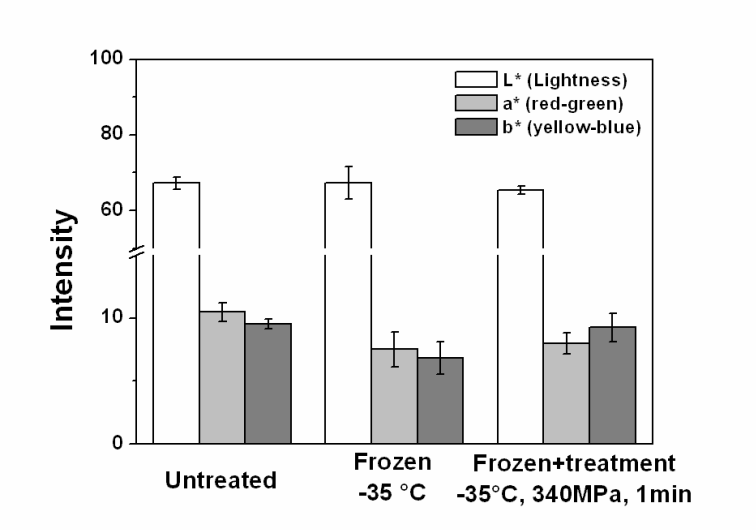

Figure 4.50 L*a*b* - color of pork meat samples after freezing and and frozen pressure treatment.

4.4.3 Drip loss

The evaluation of drip loss by weight loss after thawing and after roasting is shown in Table 4.11. Weight loss after thawing of samples pressure treated in the frozen state was slightly higher than after freezing only. The combined drip loss after roasting was however essentially unchanged in comparison to frozen samples, as less water was lost during roasting. Again a tremendous influence by examining meat from different carcasses was noted which would mask any effect of treatment if averages of samples were calculated. There is essentially no effect of storage during 14 days on the drip loss.

Table 4.11 Drip loss of pork meat after high pressure – low temperature treatments with and without storage

	Carcass number	Thawing drip loss [%]	Roasting drip loss [%]	Total drip loss [%]
Fresh	1	-	29 ± 2	29
Frozen -35 °C	1	6 ± 2	29 ± 2	34
Frozen -35 °C with treatment 340 MPa, 1 min	1	8 ± 3	26 ± 3	35
Frozen -35 °C, storage	1	5 ± 1	29 ± 1	33
Frozen -35 °C with treatment 340 MPa, 1 min, storage	1	8 ± 2	25 ± 2	33
Frozen -35 °C, storage	2	3 ± 1	18 ± 3	21
Frozen -35 °C with treatment 340 MPa, 1 min, storage	2	5 ± 1	19 ± 3	24

“Storage” denotes 14 days of at -18 °C. Values in triplicates.

4.4.4 Summary

The results of the quality of pork meat are supported by one examination from literature (Fernandez et al. 2007b). It was shown, that color in terms of redness value a* was slightly, though not significantly, decreased after pressure treatments at 650 MPa, -30 C°, 10 min in comparison to air blast frozen samples. Lightness values L* were unchanged. Drip loss and expressible moisture by centrifugation was not different from conventionally frozen samples, like shown in this study. They also did not derive differences in Warner-Bratzler shear force between samples treated at high pressure in the frozen state compared to air frozen samples, which is in accordance with the findings derived in this study that showed slight differences by a ball probe texture analysis, but not by Warner-Bratzler methodology.

In summary, it can be stated that the influence of ice I – ice III is not as detrimental as it would be expected from the disintegrative effect on microorganisms. Slight effects of hardening and increased drip loss after thawing were noted, that indicate disintegration and subsequent aggregation of myosin fibers. In comparison to freezing at ambient pressure the effect

was not very pronounced. The quality loss due to pressure treatments in the frozen state does not preclude the development of meat or fish applications.

A picture of pollock, pork meat and ground meat was taken after these treatments and is shown in the end to obtain a visual impression of foods treated in the ice III phase.

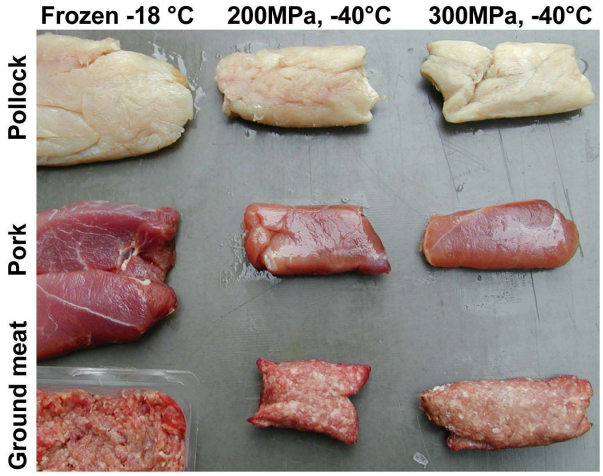

Figure 4.51 Thawed samples of pollock, pork and ground meat (beef and pork mix) after high pressure – low temperature treatments including a transition to ice III and back to ice I at 300 MPa. Treatment time was 1 min.

5 Conclusions

5.1 Summary

In the first part processing criteria for high pressure treatments in the frozen phase were defined. Freezing and thawing of sucrose and NaCl solutions was investigated leading to more precise insights in the phase transition behavior of high concentrated solutions under pressure, which are a model system for biological samples taking into account freeze concentration of the liquid during freezing. Nucleation and freezing point depression of different solute concentration were systematized and an equation was derived that makes the calculation of the melting pressure for sucrose solutions as a function of solute concentration and temperature in the ice I range possible. The results obtained were used to identify reproducible experimental conditions for high pressure treatments of high moisture frozen foods by avoiding partial thawing as much as possible.

In the second part the freeze damage of bacteria was examined with two exemplary species by flow cytometry. Mechanisms of inactivation and sublethal injury were identified and related to processing and storage conditions. The state of bacterial cells during freezing was determined which was necessary to interpret the inactivation during high pressure treatments of frozen food. Additionally, the results provide valuable possibilities to optimize processing and frozen storage of conventionally frozen food to achieve a more directed microbial reduction by freezing.

Very promising inactivation results were achieved when pressure treating frozen suspensions of microorganisms. These were however species dependent and varying with experimental conditions. Inactivation levels in buffer solutions ranged from 3 to 7 inactivation logs for all examined vegetative microorganisms. The minimum of 3 logs were obtained for *L. innocua* which is known as a psychrotroph organism. It was derived that the phase transition to ice III and back to ice I, which are going along with rapid changes of ice volume, were the cause of inactivation as cells were clearly disintegrated. Thus, high pressure was only used as a tool to trigger the transformation of ice. In consequence high pressure inactivation, as it is known at temperatures above zero, is only playing a minor role. Mechanisms of disintegration on a microstructural level were proposed and discussed. The general feasibility to inactivate microorganisms in pilot plant scale, in real food and by very short treatment times was demonstrated. It was furthermore shown that the treatment is leading to slight influences in meat quality, however, the changes are not detrimental.

5.2 Innovative potential

It was shown that the phase boundaries of solutions and consequently of complex foods cannot be derived by just shifting them to lower temperatures according to the melting point depression at ambient pressure. In combined experimental and theoretical approach it was shown that this assumption is misleading and first results for the real complex behavior were derived. A model that incorporates mechanist elements was derived which makes the freezing point calculation of sucrose solution in a wide range of pressure and solute concentrations possible. It shows that the ratio of liquid water, especially during pressure thawing processes is controllable and predictable in such systems. It was shown that freezing of water in highly concentrated viscous liquids is difficult and obtained very slowly at high pressure. The eutectic state of sodium chloride was shown under pressure. For the design of high pressure – low temperature food processes, the behavior of concentrated solutions as a model for cellular liquids is most intriguing.

For pressure induced phase transitions the mechanism of phase transition form ice I to ice III was evaluated, because no data was available at temperatures of such processes below -30 °C. Reproducible processing conditions are defined. The phase transition of ice II to ice III was shown, even though this is of limited applicability.

The freeze damage of bacteria was shown by flow cytometry, while little is apparently known about the cryoinjury of bacteria with modern microbiological methods, especially if no cryoprotectants are added. Flow cytometry was not applied to bacteria in the freeze injury field before. The results indicate that bacteria at -18 °C survive because no ice forms inside the cells. In contrast, at -40 °C, intracellular ice seems to form during storage which is however species dependent in rate of ice formation. Results with insight in intracellular ice formation in bacteria were not shown before. They can be used to define freezing conditions which inactivate bacteria in a directed way or more generally to give new insights in frozen food microbiology.

This study shows finally the effectiveness of high pressure treatments of frozen food as a completely new process for food preservation. It was demonstrated that microbial counts can be reduced and the main influence factors were identified. It is proposed to treat frozen food by high pressure at about 400 MPa in a temperature range from -30 °C to -45 °C to achieve a directed reduction in microbial counts. Short time treatments with one minute of pressure holding time are absolutely enough to achieve disintegration of microbial cells by ice III phase transitions. It is not necessary to apply higher pressure, because only very little addi-

tional effect is expected which makes clear that high pressure inactivation in ice is almost non-existent. More inactivation is possibly obtained if the treatment is repeated; however, the efficiency of subsequent pressure cycles is not as high as in the first one. This process was developed as a completely new possibility in food processing in the course of this study.

5.3 Outlook

Concerning the field of high pressure – low temperature processes, it is proposed to examine the state of water during processes, namely the ratio of frozen water under pressure in connection with ice types III, V and VI which is already done for ice I by finite element calculations in other research groups. The state of water governs the pressure influence on the desired or undesired modification of quality parameters like texture and protein denaturation, thus, it should therefore be better reflected in quality related studies than by just thinking in the two states of ice and liquid water. In future, it should be considered more to use ratios of water that is frozen and that is freezable. As a matter of fact, little is for example about water binding properties under pressure, especially in connection with high pressure ice modifications. Experimental techniques like differential scanning calorimetry (DSC) or nuclear magnetic resonance (NMR) under pressure should be used to understand the state of water better and to refine calculation approaches under pressure.

In the future, it is worth examining the treatment of frozen food by pressure with more food systems of different composition, as the main parameters of the treatment are essentially understood. Treatments should cover food with high freezable water content, like vegetables, gels, meat and fish, possibly also sherbets. The treatment is not useful for products with incorporated gases, like bakery products, due to pressure compression of gases, and also not for products with a high fat or sugar content, like ice cream, as there was no inactivation detectable. Influences on food quality like texture modifications, protein denaturation and drip loss have to be weighed up against the inactivation of foodborne microorganisms to conclude whether the treatment makes sense for food applications. The highest interest in reducing microorganisms in frozen food should exist in the production of raw unprocessed products, that cannot be pasteurized, blanched or heat treated before freezing in any other way, like frozen poultry, red meat, fish and seafood.

A scale-up of such treatments to industrial production is probably implemented relatively easy as it requires less pressure (400 MPa) than current food applications at temperatures above zero (500 to 700 MPa) and the limitation of the cost-intensive pressure dwell time is an intrinsic property of the process. It must be stated that real industrial scale vessels for high pressure

– low temperature treatments were not built yet, however, high pressure steels which are usable at low temperatures exist and the implementation of a cooling jacket to an industrial scale pressure vessel is in principle possible. Further research would be necessary in the field of pressure transmitting media that are suitable and cheap enough for food processing. Nevertheless, the development of an industrial process based on this study is feasible and promising, provided there is interest from the food freezing industry.

Curriculum vitae

Cornelius Martin Luscher
* 19.07.1976

Department of Food Biotechnology and
Food Process Engineering
Technische Universität Berlin
Königin – Luise – Straße 22
14195 Berlin, Germany
Phone: +49-30-314-71255
cornelius.luscher@tu-berlin.de

Heckerdamm 265b
13627 Berlin
cornelius_luscher@yahoo.de

Since 2002	PhD student and research associate
2002	M.Sc. (Diplom – Ingenieur)
1996 – 2002	Studies in Food Technology, Technische Universität Berlin
1995 – 1996	Community service in Stuttgart
1995	High school graduation (Abitur) in Stuttgart

Research interests

- Freezing and thawing under high pressure: influence on technical parameters, microbial inactivation and food quality parameters
- Pasteurization of frozen food by high pressure
- Influence of conventional freezing processes on microorganisms
- Fat crystallization by high pressure
- Processing effects on quality parameters of fruit and vegetable

Teaching activities (lab courses at pilot plant scale)

- Thermal process engineering in food processing (4^{th} year M.Sc. students)
- Fruit and vegetable processing (5^{th} year M.Sc. students)
- Food biotechnology (5^{th} year M.Sc. students)
- Fruit juice processing (2^{rd} year M.Sc. students)
- Project work: convenience products from potato (1^{st} year M.Sc. students)
- Supervision of 5 master theses

List of publications

Technical remark: my publications which are not part of this thesis are cited throughout the text like normal publications.

Scientific journals (peer reviewed)

M. Volkert, E. Ananta, C. Luscher & D. Knorr (2008) Effect of air freezing, spray freezing, and pressure shift freezing on membrane integrity and viability of Lactobacillus rhamnosus GG. *Journal of Food Engineering* accepted for publication.

C. Luscher, O. Schlüter & D. Knorr (2005) High pressure - low temperature processing of foods: Impact on cell membranes, texture, color and visual appearance of potato tissue. *Innovative Food Science and Emerging Technologies* 6(1): 59-71.

W. Kowalczyk, C. Hartmann, C. Luscher, M. Pohl, A. Delgado & D. Knorr (2005) Determination of thermophysical properties of foods under high hydrostatic pressure in combined experimental and theoretical approach. *Innovative Food Science and Emerging Technologies* 6(3): 318-326.

C. Luscher, A. Balasa, A. Fröhling, E. Ananta & D. Knorr (2004) Effect of high pressure induced ice I - ice III phase transitions on the inactivation of *Listeria innocua* in frozen suspension. *Applied and Environmental Microbiology* 70(7): 4021–4029.

C. Luscher & D. Knorr (2004) Bakterieninaktivierung in gefrorenen Lebensmitteln durch hochdruckinduzierte Eiskristall-Phasenübergänge**.** *Chemie Ingenieur Technik* 76(12): 1869-1872.

Conference Proceedings (with ISBN)

C. Luscher, J. Sunderhoff. G. Urrutia Benet & D. Knorr (2005) Pasteurisation of meat in frozen conditions by high pressure. In: *Innovations in Traditional Foods INTRADFOOD*. P. Fito & F. Toldra (Eds.) Elsevier, London. pp 1379-1382.

C. Luscher, O. Schlüter, A. Angersbach & D. Knorr (2002) Comparison of Structural Cell Membrane Changes Induced by Different High Pressure Processes at Low Temperatures. In: *Advances in High Pressure Bioscience and Biotechnology II.* R. Winter (Ed.) Springer, Berlin. pp 351-354.

Oral presentations

C. Luscher & D. Knorr (2005) Hochdruckbehandlung gefrorener Lebensmittel**.** *GDL - Kongress Lebensmitteltechnologie 2005 (Dresden, Germany).*

C. Luscher & D. Knorr (2004) Influence of high pressure treatments in the ice phases ice I and ice III on the viability of bacteria. *High Pressure Bioscience and Biotechnology HPBB-2004 (Rio de Janeiro, Brazil).*

C. Luscher & D. Knorr (2004) Application of high pressure to frozen aqueous systems. *Novel food-preservation technologies, Seminar of the SAFE Consortium (Brussels, Belgium).*

C. Luscher & D. Knorr (2004) Inaktivierung von Bakterien in gefrorenen Lebensmittelsystemen durch hydrostatischen Hochdruck unter Ausnutzung des Phasenübergangs Eis III - Eis I. *VDI – GVC Fachausschuss Lebensmittelverfahrenstechnik (Baden - Baden, Germany).*

C. Luscher & D. Knorr (2004) Hochdruck – Tieftemperatur – Verfahren. *Verband der Deutschend Fruchtsaftindustrie Professorentreff (Berlin, Germany).*

C. Luscher, O. Schlüter & D. Knorr (2001) Experimentelle Bestimmung und mathematische Beschreibung der Phasengrenzlinien von Lebensmitteln bei Gefrier- und Auftauprozessen unter hohem hydrostatischem Druck bis 450 MPa. *GDL - Kongress Lebensmitteltechnologie 2001 (Berlin, Germany).*

Posters

(with references to proceedings without ISBN)

C. Luscher, J.-K. Sunderhoff & D. Knorr (2005) Pasteurisation of meat in frozen conditions by high pressure. Proceedings see above. *EFFoST Conference Innovations in Traditional Foods INTRADFOOD (Valencia, Spain).*

C. Luscher, J.-K. Sunderhoff & D. Knorr (2005) Hochdruckbehandlung gefrorener Lebensmittel. *Diskussionstagung des Forschungskreises der Ernährungsindustrie FEI (Berlin, Germany).*

C. Luscher, A. Balasa, E. Ananta & D. Knorr (2004) High pressure processing for microbial inactivation in frozen food. *EFFoST Conference Food Innovations for an Expanding Europe FOODINNO (Warsaw, Poland).*

C. Luscher, E. Ananta & D. Knorr (2004) Application of high pressure processing to frozen food systems - Influence on microorganisms. *19th International ICFMH Symposium FOOD MICRO (Portoroz, Slovenia)*

O. Schlüter, C. Luscher, W.B. Herppich & D. Knorr (2004) Effects of multiple high pressure supported phase changes on potato tissue. *Postharvest Unlimited Downunder (Sydney, Australia).*

C. Luscher, O. Schlüter, G. Urrutia Benet, J. Kern & D. Knorr (2004) Pressure-supported freezing processes above 210 MPa and their impact on *Listeria innocua.* Proceedings pp. 598-603. *CIGR International Conference (Beijing, China).*

C. Luscher, A. Fröhling, A. Balasa & D. Knorr (2004) Inactivation of *Listeria innocua* and *E. coli* at high pressure and subzero temperature with consideration of the phase transitions of water. Proceedings on CD-Rom paper # 776. *ICEF 9 - International Congress on Engineering and Food (Montpellier, France).*

C. Luscher, A. Balasa & D. Knorr (2003) Inactivation of *Listeria innocua* at high pressures and low temperatures: Observations in the subzero temperature range (centigrade) considering the state of aggregations of water. *Joint IFT - EFFoST Workshop on Non - Thermal Food Preservation (Wageningen, The Netherlands).*

C. Luscher, O. Schlüter, A. Angersbach & D. Knorr (2002) Comparison of structural cell membrane changes induced by different high pressure processes at low temperatures. Proceedings see above. *High Pressure Bioscience and Biotechnology HPBB-2002 (Dortmund, Germany).*

O. Schlüter, C. Luscher & D. Knorr (2001) Liquid – solid phase boundaries of potato tissue at subzero (°C) temperatures and pressures up to 450 MPa. *European Conference on Advanced Technology for Safe and High Quality Foods EUROCAFT (Berlin, Germany).*

Publications of general interest

G.C. Holt, M. Henchion, C. Reynolds, B. Baviera, J. Calabrese, L. Contini, C. Cowan, T. Dowgielwicz, C. Luscher, A. Maraglino, R. Prugger & R. Tononi (2007) Research agenda for SMEs in electronic platforms for the European food industry. *Foresight* 9(3): 42-53.

D. Knorr, V. Heinz & C. Luscher (2007) Thermal Processing of Foods: Technological Aspects. In: *Thermal Processing of Food: Potential Health Benefits and Risks. Symposium of Deutsche Forschungsgemeinschaft.* G. Eisenbrand et al. (Eds.) Wiley-VCH, Weinheim. pp 17-25.

Literature

Besides the cited literature, this study includes the experimental results of the following master theses which were carried out in collaboration:

Balasa, Ana (2003) Results from 4.3.2, 4.3.3, 4.1.9

Fröhling, Antje (2004) Results from 4.3.3 to 4.3.7

Pohl, Marcel (2004) Results from 4.1.2, 4.1.3, 4.1.8

Sunderhoff, Jan (2005) Results from 4.3.4, 4.3.6, 4.4

Motahar, Ashkan (2006) additional experiments in 4.1.9

Acker, J. P. & L. E. McGann (2003). *Protective effect of intracellular ice during freezing?* Cryobiology 197-202.

Alberts, B. (1995). *Molekularbiologie der Zelle*. Weinheim, VCH.

Alizadeh, E., N. Chapleau, M. De Lamballerie & A. Le Bail (2007). *Effects of freezing and thawing processes on the quality of Atlantic salmon (Salmo salar) fillets.* Journal of Food Science 72(5): E279-E284.

Ananta, E., V. Heinz & D. Knorr (2004). *Assessment of high pressure induced damage on Lactobacillus rhamnosus GG by flow cytometry.* Food Microbiology 21: 567-577.

Angersbach, A., V. Heinz & D. Knorr (2002). *Evaluation of process-induced dimensional changes in the membrane structure of biological cells using impedance measurement.* Biotechnology Progress 18(3): 597-603.

Anon, M. C. & A. Calvelo (1980). *Freezing rate effects on the drip loss of frozen beef.* Meat Science 4(1): 1-14.

Babb, S. E. (1963a). *Parameters in the Simon equation realting pressure and melting temperature.* Reviews of Modern Physics 36(2): 400-413.

Babb, S. E. (1963b). *Some notes concerning Bridgman's manganin pressure scale.* In: High-pressure measurement - papers presented at the High-Pressure Measurement Symposium 1962. A. A. Giardini & E. C. Lloyd, Eds. New York City, ASME.

Baltes, W. (1989). *Lebensmittelchemie*. Berlin, Springer.

Bockisch, M. (1993). *Nahrungsfette und -öle*. Stuttgart, Ulmer.

Boonsupthip, W. & D. R. Heldman (2007). *Predicition of frozen food properties during freezing using product composition.* Journal of Food Science 72(5): 254-263.

Bridgman, P. W. (1912). *Water, in the liquid and five solid forms, under pressure.* Proceedings of the American Academy of Arts and Sciences 47: 441-558.

Bridgman, P. W. (1914). *The coagulation of albumen by pressure.* Journal of Biological Chemistry 19: 511-512.

Bubnik, Z. & P. Kadlec (1995). *Sucrose solubility.* In: Sucrose - Properties and applications. M. Mathlouthi & P. Reiser, Eds. Glasgow, Blackie Academic and Professional: 101-125.

Buchheim, W. & A. M. Abou El-Nour (1992). *Induction of milkfat crystallization in the emulsified state by high hydrostatic pressure.* Fat Science and Technology 94(10): 369-373.

Buckow, R., V. Heinz & D. Knorr (2007). *High pressure phase transition kinetics of maize starch.* Journal of Food Engineering 81(469-475).

Bundesgesetzblatt (2007). *Verordnung über tiefgefrorene Lebensmittel in der Fassung der Bekanntmachung vom 22.2 2007, geändert durch Art. 12 der Verordnung vom 8.8. 2007.* Bundesgesetzblatt I: 1816.

Calcott, P. H. & R. A. MacLeod (1974). *Survival of Escherichia coli from freeze-thaw damage: a theoretical and practical study.* Canadian Journal of Microbiology 20(671-681).

Chandrasekaran, S. K. & C. Judson King (1971). *Solid-liquid phase equilibria in multicomponent aqueous sugar solutions.* Journal of Food Science 36: 699-704.

Chaplin, M. (2007). *Water structure and science.* www.lsbu.ac.uk/water/: accessed 10/09/2007.

Cheftel, J. C. & J. Culioli (1997). *Effects of high pressure on meat: a review.* Meat Science 46(3): 211-236.

Cheftel, J. C., J. Levy & E. Dumay (2000). *Pressure-assisted freezing and thawing: Principles and potential applications.* Food Reviews International 16: 453-483.

Cheftel, J. C., M. Thiebaud & E. Dumay (2002). *Pressure-assisted freezing and thawing of foods: a review of recent studies.* High Pressure Research 22(3/4): 601-611.

Chen, C. S. (1986). *Effective molecular weight of aqueous solutions and liquid foods calculated fromt the freezing point depression.* Journal of Food Science 51(6): 1537-1539.

Chen, X. D. & P. Chen (1996). *Freezing of aqueous solution in a simple apparatus designed for measuring freezing point.* Food Research International 29(8): 723-729.

Chevalier, D., A. Le Bail, J. M. Chourot & P. Chantreau (1999). *High pressure thawing of fish (whiting): influence of the process parameters on drip losses.* Lebensmittel - Wissenschaft und Technologie 32(1): 25-31.

Chevalier, D., A. Le Bail & M. Ghoul (2001). *Evaluation of the ice ratio formed during quasi-adiabatic pressure shift freezing.* High Pressure Research 21: 227-235.

Chevalier, D., A. LeBail & M. Ghoul (2000). *Freezing and ice crystals formed in a cylindrical food model: part 2. Comparison between freezing at atmospheric pressure and pressure-shift freezing.* Journal of Food Engineering 46: 287-293.

Chevalier-Lucia, D., A. Le Bail, M. Ghoul & J. M. Chourot (2003). *High pressure calorimetry at sub-zero temperature: evaluation of the latent heat and frozen water ratio of gelatin gels.* Innovative Food Science and Emerging Technologies 4(4): 361-366.

Choukron, M. & O. Grasset (2007). *Thermodynamic model for water and high-pressure ices up to 2.2 GPa and down to the metastable domain.* The Journal of Chemical Physics 127: paper #124506.

Chourot, J. M., A. Le Bail & D. Chevalier (2000). *Phase diagram of aqueous solution at high pressure and low temperature.* High Pressure Research 19(191-199).

Christophersen, J. (1968). *Effect of freezing and thawing on the microbial population of foodstuff.* In: Low temperature biology of foodstuffs. J. Hawthorn, Ed. Oxford, Pergamon Press: 251-269.

Debye, P. & E. Hückel (1923). *Zur Theorie der Elektrolyte.* Physikalische Zeitschrift 24(9): 185-206.

Denys, S., O. Schlüter, M. E. Hendrickx & D. Knorr (2002). *Effects of high pressure on water-ice transitions in foods.* In: Ultra High Pressure Treatments of Foods. M. E. G. Hendrickx & D. Knorr, Eds. New York, Kluwer Academic/Plenum Publishers: 215-248.

Dumay, E., L. Picart, S. Regnault & M. Thiebaud (2006). *High pressure–low temperature processing of food proteins.* Biochimica et Biophysica Acta 1764(599-618).

Dumont, F., P. A. Marechal & P. Gervais (2003). *Influence of cooling rate on Saccharomyces cerevisiae destruction furing freezing: unexpected viability at ultra-rapid coolin rates.* Cryobiology 46(1): 33-42.

Dumont, F., P. A. Marechal & P. Gervais (2004). *Cell size and water permeability as determining factors for cell viability after freezing at different cooling rates.* Applied and Environmental Microbiology 70(1): 268-272.

Dumoulin, M., S. Ozawa & R. Hayashi (1998). *Textural properties of pressure-induced gels of food proteins obtained under different temperatures including subzero.* Journal of Food Science 63(1): 92-95.

Dunand, D. C., C. Schuh & D. L. Goldsby (2001). *Pressure-induced transformation plasticity of H_20 ice.* Physical Review Letters 86(4): 668-671.

Edebo, L. (1960). *A new press for the disruption of micro-organisms and other cells.* Journal of Biochemical and Microbiological Technology and Engineering 2(4): 453-479.

Edebo, L. & C.-G. Hedén (1960). *Disruption of frozen bacteria as a consequence of changes in the crystal structure of ice.* Journal of Biochemical and Microbiological Technology and Engineering 2(1): 113-120.

El-Kest, S. E. & E. H. Marth (1992). *Freezing of Listeria monocytogenes and other microorganisms: a review.* Journal of Food Protection 55(8): 639-648.

Evans, L. F. (1967). *Selective nucleation of the high-pressure ices.* Journal of Applied Physics 38: 4930-4932.

Fernandez, P. P., M. N. Martino, N. E. Zaritzky, B. Guignon & P. D. Sanz (2007a). *Effects of locust bean, xanthan and guar gums on the ice crystals of a sucrose solution frozen at high pressure.* Food Hydrocolloids 21(4): 507-515.

Fernandez, P. P., L. Otero, B. Guignon & P. D. Sanz (2006). *High-pressure shift freezing versus high-pressure assisted freezing: effects on the microstructure of a food model.* Food Hydrocolloids 20(4): 510-522.

Fernandez, P. P., G. Prestamo, L. Otero & P. D. Sanz (2006). *Assessment of cell damage in high-pressure-shift frozen broccoli: comparison with market samples.* European Food Research and Technology 224(1): 101-107.

Fernandez, P. P., P. D. Sanz, A. D. Molina-Garcia, L. Otero, B. Guignon & S. R. Vaudagna (2007b). *Conventional freezing plus high pressure–low temperature treatment: Physical properties, microbial quality and storage stability of beef meat.* Meat Science 77(4): 616-625.

Fernandez-Martin, F., L. Otero, M. T. Solas & P. D. Sanz (2000). *Protein denturation and structural damage during high-pressure-shift freezing of porcine and bovine muscle.* Journal of Food Science 65(6): 1002-1008.

Flanders, K. J. & C. W. Donnelly (1994). *Injury, resuscitation and detection of Listeria spp. from frozen environments.* Food Microbiology 11(473-480).

Först, P. (2001). *In-situ Untersuchungen der Viskosität fluider, komprimierter Lebensmitte-Modellsysteme*. Technische Universität München, Ph.D. thesis, accessible online.

Först, P., F. Werner & A. Delgado (2000). *The viscosity of water at high pressures - especially at subzero degrees centigade.* Rheologica Acta 39: 566-573.

Först, P., F. Werner & A. Delgado (2002). *On the pressure dependence of the viscosity of aqueous sugar solutions.* Rheologica Acta 41: 369-374.

Fuchigami, M., N. Ogawa & A. Teramoto (2002). *Trehalose and hydrostatic pressure effects on the structure and sensory properties of frozen tofu (soybean curd).* Innovative Food Science and Emerging Technologies 3(2): 139-147.

Fuchigami, M. & A. Teramoto (2003a). *Changes in temperature and structure of agar gel as affected by sucrose during high-pressure freezing.* Journal of Food Science 68(2): 528-533.

Fuchigami, M. & A. Teramoto (2003b). *Texture and structure of high-pressure-frozen gellan gum gel.* Food Hydrocolloids 17(6): 895-899.

Fuchigami, M., A. Teramoto & Y. Jibu (2006). *Texture and structure of pressure-shift-frozen agar gel with high visco-elasticity.* Food Hydrocolloids 20(2-3): 160-169.

Georgala, D. L. & A. Hurst (1963). *The survival of food poisoning bacteria in frozen foods.* Journal of Applied Bacteriology 26: 346-358.

Goff, H. D. (1992). *Low-temperature stability and the glassy state in frozen foods.* Food Research International 25(4): 317-325.

Gounot, A. M. (1991). *Bacterial life at low temperature: physiological aspects and biotechnological implications.* Journal of Applied Bacteriology 71(386-397).

Gribaudo, L. M. & A. C. Rubiolo (1992). *Phase equilibria in the water-sucrose-sodium chloride system.* International Journal of Food Science and Technology 27: 159-169.

Guignon, B., L. Otero, A. D. Molina-Garcia & P. D. Sanz (2005). *Liquid water-ice I phase diagrams under high pressure: sodium chloride and sucrose models for food systems.* Biotechnology Progress 21: 439-445.

Hartmann, C. & A. Delgado (2003). *Convective and diffusive transport effects in a high-pressure-induced inactivation process of packed food.* Journal of Food Engineering 59(1): 33-44.

Hartmann, C., J.-P. Schuhholz, P. Kitsubun, N. Chapleau, A. Le Bail & A. Delgado (2004). *Experimental and numerical analysis of the thermofluiddynamics in a high-pressure autoclave.* Innovative Food Science and Emerging Technologies 5: 399-411.

Hashizume, C., K. Kimura & R. Hayashi (1995). *Kinetic analysis of yeast inactivation by high pressure treatment at low temperatures.* Bioscience Biotechnology Biochemistry 59(8): 1455-1458.

Hashizume, C., K. Kimura & R. Hayashi (1996). *High pressure inactivation of yeast cells in saline and strawberry jam at low temperatures.* In: High pressure bioscience and biotechnology. R. Hayashi & C. Balny, Eds. Amsterdam, Elsevier.

Hayakawa, K., Y. Ueno, S. Kawamura, T. Kato & R. Hayashi (1998). *Microorganism inactivation using high-pressure generation in sealed vessels under sub-zero temperature.* Applied Microbiology and Biotechnology 50: 415-418.

Heinz, V. & D. Knorr (2002). *Effects of high pressure on spores.* In: Ultra high pressure treatments of foods. M. E. G. Hendrickx & D. Knorr, Eds. New York, Kluwer Academic/ Plenum Publishers: 77-114.

Heldman, D. R. (1974). Transactions of the ASAE 17: 63-66.

Heremans, K. (2002). *Effects of high pressure on biomaterials.* In: Ultra High Pressure Treatments of Foods. M. E. G. Hendrickx & D. Knorr, Eds. New York, Kluwer Academic/Plenum Publishers: 23-51.

Hogenboom, D. L., J. S. Kargel, G. J. Consolmagno, T. C. Holden, L. Lee & M. Buyyounouski (1997). *The ammonia-water system and the chemical differentiation of icy satellites.* Icarus 128: 171-180.

Horne, R. A. & D. S. Johnson (1967). *The effect of electrolyte addition on the viscosity of water under pressure.* Journal of Physical Chemistry 71(4): 1147-1149.

Iglev, H., M. Schmeisser, K. Simeonidis, A. Thaller & A. Laubereau (2006). *Ultrafast superheating and melting of bulk ice.* Nature 439: 183-186.

IIR (1972). *Recommendations for the processing and handling of frozen foods*. Paris, International Institute of Refrigeration.

IIR (1998). *Listeria Monocytogenes in refrigerated foods.* In: 2nd Informatory Note on Refrigeration and Food- Paris, International Institute of Refrigeration.

Indrawati, A. M. Van Loey, L. R. Ludikhuyze & M. E. Hendrickx (2000). *Kinetics of pressure inactivation at subzero and elevated temperatures of lipoxygenase in crude green bean (Phaseolus vulgaris L.) extract.* Biotechnology Progress 16: 109-115.

Indrawati, A. M. Van Loey, L. R. Ludikhuyze & M. E. Hendrickx (2001). *Pressure-temperature inactivation of lipoxygenase in green peas (Pisum sativum): a kinetic study.* Journal of Food Science 66(5): 686-693.

Indrawati, I., L. R. Ludikhuyze, A. M. Van Loey & M. E. Hendrickx (2000). *Lipoxygenase inactivation in green beans (Phaseolus vulgaris L.) due to high pressure treatment at subzero and elevated temperatures.* Journal of Agricultural and Food Chemistry 48: 1850-1859.

Indrawati, I., A. van Loey, S. Denys & M. Hendrickx (1998). *Enzyme sensitivity towards high pressure at low temperature.* Food Biotechnology 12(3): 263-277.

Ingram, M. (1951). *The effect of cold on microorganisms in relation to food.* Proceedings of the Society of Applied Bacteriology 14: 243.

Jay, J. M. (1996). *Modern food microbiology*. New York, Chapman & Hall.

Kanda, T., K. Kitagawa & K. Fujinuma (1993). *Behavior of ice under pressure.* In: High Pressure Bioscience and Food Science. R. Hayashi, Ed. Kyoto, San-Ei Publishing Company: 24-26.

Kanda, Y., M. Aoki & T. Kosugi (1992). *Freezing of tofu (soybean curd) by pressure-shift freezing and its structure.* Nippon Shokuhin Gakkaishi 39(7): 608-614.

Kanno, H. & C. A. Angel (1977). *Homogenous nucleation and glass formation of aqueous alkali halide solutions at high pressure.* Journal of Physical Chemistry 81(26): 2639-2643.

Kanno, H., R. J. Speedy & C. A. Angell (1975). *Supercooling of water to -92°C under pressure.* Science 189: 880-881.

Kapranov, S. V., M. Pehl, C. Hartmann, A. Baars & A. Delgado (2003). *On the influence of high pressure on edible oils.* In: Advances in high pressure bioscience and biotechnology II. R. Winter, Ed. Berlin, Springer.

Karlsson, J. O. M., E. G. Cravalho & M. Toner (1993). *Intracellular ice formation: causes and consequences.* Cryo-Letters 14: 323.

Kaufmann, D. W. (1960). *Sodium chloride*. London, Chapman & Hall.

Kinsho, T., Y. Ueno, R. Hayashi, C. Hashizume & K. Kimura (2002). *Sub-zero temperature inactivation of carboxypeptidase Y under high hydrostatic pressure.* Europeand Journal of Biochemistry 269: 4666–4674.

Knorr, D., O. Schlüter & V. Heinz (1998). *Impact of high hydrostatic pressure on phase transitions of foods.* Food Technology 52(9): 42-45.

Kolakowski, P., E. Dumay & J.-C. Cheftel (2001). *Effects of high pressure and low temperature on β-lactoglobulin unfolding and aggregation.* Food Hydrocolloids 15: 215-232.

Köpke, U. (2002). *Zusammensetzung der psychrotrophen Hackfleischmikroflora "industrieller" Herstellung mit mikroökologischer und hygienischer Bewertung ihrer Hauptkomponenten*. Freie Unviversität Berlin, Ph.D. thesis, accessible online.

Körber, C. (1988). *Phenomena at the advancing ice-liquid interface: solutes, particles and biological cells.* Quarterly Review of Biophysics 21(2): 229-298.

Kowalczyk, W., C. Hartmann & A. Delgado (2004). *Modelling and numerical simulation of convection driven high pressure induced phase changes.* International Journal of Heat and Mass Transfer 47: 1079-1089.

Kowalczyk, W., C. Hartmann, C. Luscher, M. Pohl, A. Delgado & D. Knorr (2005). *Determination of thermophysical properties of foods under high hydrostatic pressure in combined experimental and theoretical approach.* Innovative Food Science and Emerging Technologies 6(3): 318-326.

Kunugi, S. & N. Tanaka (2002). *Cold denaturation of proteins under high pressure.* Biochimica et Biophysica Acta 1595(1/2): 329-344.

Le Bail, A., L. Boillereaux, A. Davenel, M. Hayert, T. Lucas & J. Y. Monteau (2003). *Phase transition in foods: effect of pressure and methods to assess or control phase transition.* Innovative Food Science and Emerging Technologies 4(1): 15-24.

Le Bail, A., D. Chevalier, D. M. Mussa & M. Ghoul (2002). *High pressure freezing and thawing of foods: a review.* International Journal of Refrigeration 25: 504-513.

Le Bail, A., M. Hayert, M. H. Rigenbach & E. Gruss (2002). *High pressure calorimetry: application to selected lipids.* Poster presentation at the conference "High pressure bioscience and biotechnology 2002", Dortmund.

Leliwa-Kopystynski, J., M. Maruyama & T. Nakajima (2002). *The water-ammonia phase diagram up to 300 MPa: application to icy satellites.* Icarus 159: 518-528.

Levy, J., E. Dumay, E. Kolodziejczyk & J. C. Cheftel (1999). *Freezing kinetics of a model oil-in-water emulsion under high pressure or by pressure release. Impact on ice crystals and oil droplets.* Lebensmittel-Wissenschaft und -Technologie 32: 396-405.

Lille, M. & K. Autio (2007). *Microstructure of high-pressure vs. atmospheric frozen starch gels.* Innovative Food Science and Emerging Technologies 8(1): 117-126.

Lobban, C., J. L. Finney & W. F. Kuhs (2000). *The structure and ordering of ices III and V.* Journal of Chemical Physics 112(16): 7169-7180.

Loehe, J. R. & M. D. Donohue (1997). *Recent advances in modeling thermodynamic properties of aqueous strong electrolyte systems - review.* AIChE Journal 43(1): 180-195.

Luscher, C. (2001). *Untersuchung hochdruckunterstützter Phasenübergänge in pflanzlichem Gewebe (Kartoffel) unter Berücksichtigung metastabiler Zustände*. Technische Universität Berlin, Studienarbeit (Minor thesis).

Luscher, C., O. Schlüter & D. Knorr (2005). *High pressure - low temperature processing of foods: Impact on cell membranes, texture, color and visual appearance of potato tissue.* Innovative Food Science and Emerging Technologies 6(1): 59-71.

MacDougall, D. B. (1982). *Changes in the colour and opacity of meat.* Food Chemistry 9(1-2): 75-88.

Mackie, I. E. (1993). *The effects of freezing on flesh proteins.* Food Reviews International 9(4): 575-610.

Magnusson, K. E. (1977a). *The continuation of the phase-boundary between ice I and liquid into the region of ice III and II and its relation to freeze-pressing of biological material.* Cryobiology 14: 68-77.

Magnusson, K. E. (1977b). *A physical description of freeze-pressing of biological material with the X-Press.* Cryobiology 14: 78-86.

Magnusson, K. E. & L. Edebo (1974). *Estimation of disruption in freeze-pressed Saccharomyces cerevisiae by an electronic particle counter.* Biotechnology and Bioengineering 16: 1273-1282.

Magnusson, K. E. & L. Edebo (1976a). *Influence of cell concentration, temperature, and press performance on flow characteristics and disintegration in the freeze-pressing of Saccharomyces cerevisiae with the X-press.* Biotechnology and Bioengineering 18: 865-883.

Magnusson, K. E. & L. Edebo (1976b). *Influence of salts and gelatin in disintegration of Saccharomyces cerevisiae by freeze-pressing.* Biotechnology and Bioengineering 18: 449-463.

Magnusson, K. E. & L. Edebo (1976c). *Large scale disintegration of microorganisms by freeze-pressing.* Biotechnology and Bioengineering 18: 865-883.

Malinowska-Panczyk, E., I. Kolodziejska, E. Dunajski, M. Rompa & S. Cwalina (2004). *Effect of high pressure and sub-zero temperature on some gram-neagtive bacteria.* Polish Journal of Food and Nutrition Sciences 13/54(3): 279-283.

Margules, M. (1895). Sitzungsberichte der Mathematisch-Naturwissenschaftlichen Classe der Kaiserlichen Akademie der Wissenschaften Wien / 2a 104: 1243.

Marion, G. M., J. S. Kargel, D. C. Catling & S. D. Jakubowski (2005). *Effects of pressure on aqueous chemical equilibria at subzero temperatures with applications to Europa.* Geochimica et Geophysica Acta 69(2): 259-274.

Mazur, P. (1961). *Manifestations of injury in yeast cells exposed to subzero temperatures.* Journal of Bacteriology 82: 662-672.

Mazur, P. (1963). *Kinetics of water loss from cells at subzero temperatures and the likelihood of intracellular freezing.*

Mazur, P. (1966a). *Physical and chemical basis of injury in single-celled microorganisms subjected to freezing and thawing.* In: Cryobiology. H. T. Meryman, Ed. New York, Academic Press.

Mazur, P. (1966b). *Theoretical and experimental effects of cooling and warming velocity on the survival of frozen and thawed cells.* Cryobiology 2(4): 181-192.

Mazur, P. (2004). *Principles of cryobiology.* In: Life in the frozen state. B. J. Fuller, N. Lane & E. E. Benson, Eds. Boca Raton, CRC Press: 3-65.

Mazur, P., S. Seki, I. L. Pinn, F. W. Kleinhans & K. Edashige (2005). *Extra- and intracellular ice formation in mouse oocytes.* Cryobiology 51(1): 29-53.

McFarlan, R. F. (1936). *The structure of ice III.* Journal of Chemical Physics 4: 253-259.

Miles, C. A. (1991). *The thermophysical properties of frozen foods.* In: Food freezing: today and tomorrow. W. B. Bald, Ed. London, Springer-Verlag: 45-65.

Molina-Garcia, A. D., L. Otero, M. N. Martino, N. E. Zaritzky, J. Arabas, J. Szczepek & P. D. Sanz (2004). *Ice VI freezing of meat: supercooling and ultrastructural studies.* Meat Science 66(3): 709-718.

Moussa, M., J. M. Perrier-Cornet & P. Gervais (2006). *Synergistic and antagonistic effects of combined subzero temperature and high pressure on inactivation of Escherichia coli.*

Muldrew, K., J. P. Acker, J. A. W. Elliott & L. E. McGann (2004). *The water to ice transition: implications for living cells.* In: Life in the frozen state. B. J. Fuller, N. Lane & E. E. Benson, Eds. Boca Raton, CRC Press.

Ngapo, T. M., I. H. Babare, J. Reynolds & R. F. Mawson (1999). *Freezing and thawing rate effects on drip loss from samples of pork.* Meat Science 53: 149-153.

Nordell, B. (1990). *Measurement of P-T coexistence curve for ice-water mixture.* Cold Regions Science and Technology 19(1): 83-88.

Otero, L., A. Ousegui, G. Urrutia Benet, C. de Elvira, M. Havet, A. Le Bail & P. D. Sanz (2007). *Modelling industrial scale high-pressure-low-temperature processes.* Journal of Food Engineering 83(2): 136-141.

Otero, L. & P. D. Sanz (2000). *High-pressure shift freezing. Part 1. Amount of ice instantaneously formed in the process.* Biotechnology Progress 16: 1030-1036.

Otero, L. & P. D. Sanz (2003). *High pressure-assisted and high pressure-induced thawing: two different processes.* Journal of Food Science 68(8): 2523-2528.

Otero, L. & P. D. Sanz (2006). *High-pressure-shift freezing: Main factors implied in the phase transition time.* Journal of Food Engineering 72(4): 354-363.

Özmutlu, Ö., C. Hartmann & A. Delgado (2006). *Momentum and energy transfer during phase change of water under high hydrostatic pressure.* Innovative Food Science and Emerging Technologies 7(3): 161-168.

Perrier-Cornet, J. M., S. Tapin, S. Gaeta & P. Gervais (2005). *High-pressure inactivation of Saccharomyces cerevisiae and Lactobacillus plantarum at subzero temperatures.* Journal of Biotechnology 115: 405-412.

Perrier-Cornet, J. M., S. Tapin & P. Gervais (2002). *High pressure inactivation of yeast and spheroplasts at subzero temperature.* In: Advances in High Pressure Bioscience and Biotechnology II. R. Winter, Ed. Heidelberg, Springer.

Perrin, M., M. Bemer & C. Delamare (2003). *Fatal Case of Listeria innocua Bacteremia.* Journal of Clinical Microbiology 41(11): 5308-5309.

Pham, Q. T. (1996). *Prediction of calorimetric properties and freezing time of foods from composition data.* Journal of Food Engineering 30: 95-107.

Pham, Q. T. & J. Willix (1989). *Thermal conductivity of fesh lamb meat, offals and fat in the range -40 to +30 °C: measurements and correlations.* Journal of Food Science 54(3): 508-515.

Picart, L., E. Dumay, J.-P. Guiraud & J. C. Cheftel (2005). *Combined high pressure-sub-zero temperature processing of smoked salmon mince: phase transition phenomena and inactivation of Listeria innocua.* Journal of Food Engineering 68(1): 43-56.

Picart, L., E. Dumay, J.-P. Guiraud & J.-C. Cheftel (2004). *Microbial inactivation by pressure-shift freezing: effects on smoked salmon mince inoculated with Pseudomonas fluorescens, Micrococcus luteus and Listeria innocua.* Lebensmittel - Wissenschaft und Technologie 37: 227-238.

Pongsawatmanit, R. & O. Miyakawi (1993). *Measurement of the temperature-dependent ice fraction in frozen foods.* Bioscience, Biotechnology, Biochemistry 57(10): 1650-1654.

Prestamo, G., L. Palomares & P. Sanz (2005). *Frozen foods treated by pressure shift freezing: proteins and enzymes.* Journal of Food Science 70(1): S22-S27.

Rall, W. F., P. Mazur & J. J. McGrath (1983). *Depression of the ice-nucleation temperature of rapidly cooled mouse embryos by glycerol and dimethyl sulfoxide.* Biophysical Journal 41(1): 1-12.

Ranken, M. D. (2000). *Handbook of meat product technology*. Oxford, Blackwell Science.

Reid, D. S. (1990). *Optimizing the quality of frozen foods.* Food Technology 44(7): 78.

Reid, D. S. (1993). *Basic physical phenomena in the freezing and thawing of plant and animal tissue.* In: Frozen food technology. C. P. Mallett, Ed. Glasgow, Blackie Academic & Professional: 1-19.

Riiner, Ü. (1970). *Investigation of the polymorphism of fats and oils by temperature programmed X-ray diffraction.* Lebensmittel - Wissenschaft und Technologie 3(6): 101-106.

Robert-Koch-Institut (2003). Epidemologisches Bulletin(46).

Rouillé, J., A. Le Bail, H. S. Ramaswamy & L. Leclerc (2002). *High pressure thawing of fish and shellfish.* Journal of Food Engineering 53(1): 83-88.

Sahagian, M. E. & H. D. Goff (1996). *Fundamental aspects of the freezing process.* In: Freezing effects on food quality. L. E. Jeremiah, Ed. New York, Marcel Dekker: 1-50.

Salzmann, C. G., I. Kohl, T. Loerting, E. Mayer & A. Hallbrucker (2003). *Pure ices IV and XII from high-density amorphous ice.* Canadian Journal of Physics 81: 25-32.

Salzmann, C. G., P. G. Radaelli, A. Hallbrucker, E. Mayer & J. L. Finney (2006). *The preparation and structure of hydrogen ordered phases of ice.* Science 31: 1758-1761.

Sanz, P. D. & L. Otero (2000). *High-pressure shift freezing. Part 2. Modeling of freezing times for a finite cylindical model.* Biotechnology Progress 16: 1037-1043.

Schlegel, H. G. (1992). *Allgemeine Mikrobiologie*. Stuttgart, Georg Thieme Verlag.

Schlüter, O. (2003). *Impact of High Pressure -Low Temperature Processes on Cellular Materials Related to Foods*. Technische Universität Berlin, Ph.D. thesis, urn:nbn:de:kobv:83-opus-6647, http://opus.kobv.de/tuberlin, also Fortschritt-Berichte VDI, Series 3, Number 802.

Schlüter, O., G. Urrutia Benet, V. Heinz & D. Knorr (2004). *Metastable States of Water and Ice during Pressure-Supported Freezing of Potato Tissue.* Biotechnology Progress 20(3): 799 -810.

Schubring, R., C. Meyer, O. Schlüter, S. Boguslawski & D. Knorr (2003). *Impact of high pressure assisted thawing on the quality of fillets from various fish species.* Innovative Food Science and Emerging Technologies 4(3): 257-267.

Scully, D. B. (1974). *Thermodynamics and rheology of the Hughes press.* Biotechnology and Bioengineering 16(5): 675-687.

Serra, X., N. Grebol, M. D. Guardia, L. Guerrero, P. Gou, P. Masoliver, M. Gassiot, C. Sarraga, J. M. Monfort & J. Arnau (2007a). *High pressure applied to frozen ham at different process stages. 2. Effect on the sensory attributes and on the colour characteristics of dry-cured ham.* Meat Science 75(1): 21-28.

Serra, X., C. Sarraga, N. Grebol, M. D. Guardia, L. Guerrero, P. Gou, P. Masoliver, M. Gassiot, J. M. Monfort & J. Arnau (2007b). *High pressure applied to frozen ham at different process stages. 1. Effect on the final physicochemical parameters and on the antioxidant and proteolytic enzyme activities of dry-cured ham.* Meat Science 75(1): 12-20.

Sharma, A., J. H. Scott, G. D. Cody, M. L. Fogel, R. M. Hazen, R. J. Hemley & W. T. Huntress (2002). *Microbial activity at gigapascal pressures.* Science 295: 1514-1516.

Shen, T., G. Urrutia Benet, S. Brul & D. Knorr (2005). *Influence of high-pressure-low-temperature treatment on the inactivation of Bacillus subtilis cells.* Innovative Food Science and Emerging Technologies 6(3): 271-278.

Simon, F. & G. Glatzel (1929). *Bemerkungen zur Schmelzdruckkurve.* Zeitschrift für Anorganische und Allgemeine Chemie 178: 309-316.

Simpson, R. K. & A. Gilmour (1997). *The effect of high hydrostatic pressure on the activity of intracellular enzymes of Listeria monocytogenes.* Letters in Applied Microbiology 25: 48-53.

Smeller, L. (2002). *Pressure-temperature phase diagrams of biomolecules.* Biochimica et Biophysica Acta 1595: 11-29.

Smelt, J. P., J. C. Hellemons & M. Patterson (2002). *Effects of high pressure on vegetative microorganisms.* In: Ultra High Pressure Treatments of Foods. M. E. G. Hendrickx & D. Knorr, Eds. New York, Kluwer Academic/Plenum Publishers: 55-76.

Spieß, W. E. L. (1981). *Der Einfluß der Gefriergeschwindigkeit auf die Qualität tiefgefrorener Lebensmittel.* ZFL 32(4): 136-139.

Steponkus, P. L. (1984). *Role of the plasma membrane in freezing injury and cold acclimation.* Annual Review of Plant Physiology 35(543-584).

Takahashi, K. (1992). *Sterilisation of microorganisms by hydrostatic pressure at low temperature.* In: High Pressure and Biotechnology. C. Balny, R. Hayashi, K. Heremans & P. Masson, Eds. Montrouge, Colloques INSERM / John Libbey Eurotext: 303-307.

Takai, R., T. T. Kozhima & T. Suzuki (1991). *Low temperature thawing by using high pressure.* Proceedings of the XVII International Congress of Refrigeration, Montreal, Canada 4: 1951-1955.

Tammann, G. (1900). *Über die Grenzen des festen Zustandes IV.* Annalen der Physik 2(4): 1-31.

Tay, A., T. H. Shellhammer, A. E. Yousef & G. W. Chism (2003). *Pressure death and tailing behavior of Listeria monocytogenes strains having different barotolerances.* Journal of Food Protection 66(11): 2057-2061.

Thiebaud, M., E. Dumay & J. C. Cheftel (2002). *Pressure-shift freezing of o/w emulsions: influence of fructose and sodium alginate on undercooling, nucleation, freezing kinetics and ice crystal size distribution.* Food Hydrocolloids 16(6): 527-545.

Tironi, V., A. Le Bail & M. De Lamballerie (2007). *Effects of pressure-shift freezing and pressure-assisted thawing on sea bass (Dicentrarchus labrax) quality.* Journal of Food Science 72(7): C381-387.

Ulmer, H. M., H. Herberhold, S. Fahsel, M. G. Gaenzle, R. Winter & R. F. Vogel (2002). *Effects of pressure-induced membrane phase transitions on inactivation of HorA, an ATP-dependent multidrug resistance transporter, in Lactobacillus plantarum.* Applied and Environmental Microbiology 68(3): 1088-1095.

Urrutia Benet, G. (2006). *High-pressure low-temperature processing of foods: impact of metastable phases on process and quality parameters*. Technische Universität Berlin, Ph.D. thesis, urn:nbn:de:kobv:83-opus-11912, http://opus.kobv.de/tuberlin.

Urrutia Benet, G., T. Balogh, J. Schneider & D. Knorr (2007). *Metastable phases during high-pressure–low-temperature processing of potatoes and their impact on quality-related parameters.* Journal of Food Engineering 78(2): 375-389.

Urrutia Benet, G., N. Chapleau, M. Lille, A. Le Bail, K. Autio & D. Knorr (2006). *Quality related aspects of high pressure low temperature processed whole potatoes.* Innovative Food Science and Emerging Technologies 7(1): 32-39.

Urrutia Benet, G., O. Schlüter & D. Knorr (2004). *High pressure–low temperature processing. Suggested definitions and terminology.* Innovative Food Science and Emerging Technologies 5(4): 413-427.

Van Buggenhout, S., M. Lille, I. Messagie, A. Van Loey, K. Autio & M. Hendrickx (2006a). *Impact of pretreatment and freezing conditions on the microstructure of frozen carrots: quantification and relation to texture loss.* European Food Research and Technology 222: 543-553.

Van Buggenhout, S., I. Messagie, V. Maes, T. Duvetter, A. Van Loey & M. Hendrickx (2006b). *Minimizing texture loss of frozen strawberries: effect of infusion with pect-inmethylesterase and calcium combined with different freezing conditions and effect of subsequent storage/thawing conditions.* European Food Research and Technology 223(3): 395-404.

Van Buggenhout, S., I. Messagie, I. Van der Plancken & M. E. Hendrickx (2006c). *Influence of high-pressure–low-temperature treatments on fruit and vegetable quality related enzymes.* European Food Research and Technology 223(4): 475-485.

Van Buggenhout, S., I. Messagie, A. Van Loey & M. Hendrickx (2005). *Influence of low-temperature blanching combined with high-pressure shift freezing on the texture of frozen carrots.* Journal of Food Science 70(4): S304-S308.

Volkert, M., C. Luscher, E. Ananta & D. Knorr (2007). *Effect of air freezing, spray freezing, and pressure shift freezing on membrane integrity and viability of Lactobacillus rhamnosus GG.* Journal of Food Engineering: accepted for publication.

Wagner, W., A. Saul & A. Pruß (1994). *International equations for the pressure along the melting and along the sublimation curve of ordinary water substance.* Journal of Physical and Chemical Reference Data 23: 515-527.

Wemekamp-Kamphuis, H. H., A. K. Karatzas, J. A. Wouters & T. Abee (2002). *Enhanced levels of cold shock proteins in Listeria monocytogenes LO28 upon exposure to low temperature and high hydrostatic pressure.* Applied and Environmental Microbiology 68(2): 456-463.

Wilson, P. W., A. F. Heneghan & A. D. J. Haymet (2003). *Ice nucleation in nature: supercooling point (SCP) measurements and the role of heterogeneous nucleation.* Cryobiology 46: 88-98.

Wilton, I. & G. Wode (1963). *Quick and simple method for studying crystallization behavior of fats.* Journal of the American Oil Chemists Society 40: 707-711.

Winter, R. & C. Czelik (2000). *Pressure effects on the structure of lyotropic lipid mesophases and model biomembrane systems.* Zeitschrift für Kristallographie 215: 454-474.

Wirths, W. (1985). *Lebensmittel in ernährungsphysiologischer Bedeutung*. Paderborn, Uni-Taschenbücher.

Yasuda, A. & K. Mochizuki (1992). *The behavior of trigycerides under high presure : the high pressure can stably crystallize cocoa butter in chocolate.* In: High pressure and biotechnology. C. Balny, R. Hayashi, K. Heremans & P. Mason, Eds. London, Colloque INSERM/John Libbey: 255-259.

Yayanos, A. A. (2002). *Are cells viable at gigapascal pressure? Technical comment.* Science 297: 295a.

Yokoyama, C., Y. Tamura & Y. Nishiyama (1998). *Crystal growth rates of tricaprin and trilaurin under high pressures.* Journal of Crystal Growth 191: 827-833.

Young, F. E. & F. T. Jones (1949). *Sucrose hydrates - The sucrose-water phase diagram.* Journal of Physical and Colloid Chemistry 53: 1334-1350.

Yuste, J., R. Pla, E. Beltran & M. Mor-Mur (2002). *High pressure processing at subzero temperature: effect on spoilage microbiota of poultry.* High Pressure Research 22(3/4): 673-676.

Zachariassen, K. E. & E. Kristiansen (2000). *Ice nucleation and antinucleation in nature.* Cryobiology 41: 257.

Zhu, S., A. Le Bail, H. S. Ramaswamy & N. Chapleau (2004). *Characterization of ice crystals in pork muscle formed by pressure-shift freezing as compared to classical freezing methods.* Journal of Food Science 69(4): FEP190-FEP194.

Zhu, S., H. S. Ramaswamy & A. Le Bail (2005). *High-pressure calorimetric evaluation of ice crystal ratio formed by rapid depressurization during pressure-shift freezing of water and pork muscle.* Food Research International 38(2): 193-201.

Zhu, S., H. S. Ramaswamy & A. Le Bail (2006). *Calorimetry and pressure-shift freezing of different food products.* Food Science and Technology International 12(3): 205-214.